NANOPARTICLE DELIVERY OF SIRNA FOR CANCER THERAPY

Yunching Chen

A dissertation submitted to the faculty of the University of North Carolina at Chapel Hill in partial fulfillment of the requirements for the degree of Doctor of Philosophy in the Eshelman School of Pharmacy.

Chapel Hill
2010

Approved by,

Rudy Juliano, Ph.D., Professor, School of pharmacy, UNC at Chapel Hill

Moo J. Cho, Ph.D., Professor, School of Pharmacy, UNC at Chapel Hill

Leaf Huang, Ph.D., Professor, School of Pharmacy, UNC at Chapel Hill

Xiao Xiao, Ph.D., Professor, School of Pharmacy, UNC at Chapel Hill

Bruce Sullenger, Ph.D., Professor, School of Medicine, Duke

ABSTRACT

Yunching Chen: Nanoparticle Delivery of siRNA for Cancer Therapy
(Under the direction of Leaf Huang, Ph.D.)

We have developed lipid-polycation-DNA (LPD) nanoparticles containing DOTAP and targeted with polyethylene glycol (PEG) tethered with a targeting ligand such as anisamide (AA) to specifically deliver siRNA to cancer cells. Two novel non-glycerol based cationic lipids which contain both a guanidinium and a lysine or an arginine residue as the cationic headgroup are synthesized to replace DOTAP and form nanoparticles. DSGLA, which contains a lysine residue, down-regulated pERK more efficiently in H460 cells than DOTAP. DSAA, which contains an arginine residue, induced reactive oxygen species (ROS), triggered apoptosis and down-regulated anti-apoptotic protein Bcl-2 in B16F10 melanoma cells. A significant improvement in tumor growth inhibition was observed after dosing with targeted nanoparticles containing DSGLA or DSAA.

We further designed a LPD nanoparticle modification with NGR (aspargine–glycine–arginine) peptide, targeting aminopeptidase N (CD13) expressed in the tumor cells or tumor vascular endothelium. The targeted nanoparticles efficiently delivered c-myc siRNA into the cytoplasm of HT-1080 xenograft tumor and effectively suppressed c-myc expression and triggered cellular apoptosis in the tumor, resulting in a partial tumor growth inhibition. When doxorubicin (Dox) and siRNA were co-formulated in the multi-functional nanoparticles, an enhanced therapeutic effect was observed.

Furthermore, we explored the application of the multi-functional nanoparticles in multi-drug resistant cells which are new targets for cancer therapy. In this study, we have used a multi-functional anionic LPD (LPD-II) nanoparticle for efficient systemic co-delivery of siRNA against c-myc and Dox, into P-gp-positive NCI/ADR-RES tumors in a xenograft model. c-Myc siRNA delivered by the targeted nanoparticles significantly down-regulated both c-myc and P-gp expressions in the tumor, caused enhanced Dox uptake and sensitized tumor cells to the co-delivered Dox. Three daily intravenous injections of c-myc siRNA and Dox co-formulated in the targeted nanoparticles showed a significant improvement in tumor growth inhibition.

We have further developed a LPH (liposome-polycation-hyaluronic acid) nanoparticle formulation modified with tumor specific scFv (single chain variable fragment) for systemic delivery of small interfering RNA (siRNA) and microRNA (miRNA) into lung metastasis of murine B16F10 melanoma. When miR-34a and therapeutic siRNAs were co-formulated in C4-targeted nanoparticles, an enhanced anti-cancer effect was observed.

ACKNOWLEDGEMENTS

I would like thank my academic advisor, Dr. Leaf Huang, for his guidance and support on my research. I also thank my committee members, Drs. Cho, Juliano, Sullenger and Xiao for their suggestions on my dissertation project. The kind assistance from the Huang lab during my graduate research and study is acknowledged. I also appreciate the supports from my friends and family.

Drs. Jinzi J. Wu, Xiaodong Zhu, Xiaoju Zhang, Bin Liu, Joyeeta Sen, Surendar Reddy Bathula, Jun Li, Wei-Yun Sheng and Miss Qi Yang and Raffaella Fittipaldi are acknowledged for their help on this project. J.S. and S.B. synthesized the DSPE-PEG-anisamide, DSGLA and DSAA. J.L. obtained the TEM picture shown in **Figure 5.1**.

TABLE OF CONTENTS

LIST OF FIGURES

1.0 INTRODUCTION AND LITERATURE REVIEW

RNA interference (RNAi) was first discovered in the plant in the late 1980s (1). RNAi, serving as an anti-viral mechanism (2), is a unique regulatory system that uses small double stranded RNA (dsRNA) molecules to degrade the target mRNA in a homology-dependent manner (3). Small interfering RNA (siRNA) of 21-23 bp in length is produced from longer dsRNA which is cleaved by Dicer, a dsRNA-specific endonuclease (4-6). Dicer is a complex which includes TAR-RNA binding protein (TRBP). Dicer and siRNA form RNA-induced silencing complex (RISC). Argonaute 2, the core component of RISC, cleaves the target mRNA between bases 10 and 11 relative to the 5′ end of the antisense strand. The cleaved mRNA fragments are released from RISC and degraded.

RNAi technology has recently been developed as a potential therapeutic agent. Comparing with antisense oligonucleotides, siRNAs are more resistant to nuclease degradation and show prolonged therapeutic effect (6, 7). Properly delivered RNAi works in both cell lines and various primary cells (8). It is broadly, yet specifically, applicable to any target gene with which the sequence is known. The promise that siRNA can specifically down-regulate ‘‘undruggable’’ gene products brings hope to the “incurable” diseases and usher in a new era of pharmaceutical (9). This chapter summarizes on different signaling pathways inhibited by siRNA and the advantage made in the usage of targeted siRNA delivery system.

1.1 SIRNA FOR CANCER TREATMENT

1.1.1 Inhibition of angiogenesis

Angiogenesis is a main factor which regulates tumor growth, invasion, and metastasis. The vascular endothelial growth factor (VEGF) family has been reported as a key mediator of these processes [10]. VEGF, a glycoprotein, can activate the signaling pathway to enhance endothelial cell growth, differentiation and migration and protect the pre-existing vasculature from death. As shown in **Figure 1.1**, activation of VEGFR-1 or VEGFR-2 can lead to cell survival, proliferation or migration via several different pathways. First, Ras pathway is activated to stimulate cell proliferation and survival via the mitogen-activated protein-kinase cascade (MAPK). Secondly, VEGF can also phosphorylate phospholipase C (PLC-γ), which activates protein kinase C and triggers the MAPK pathway (10). Third, AKT pathway is phosphorylated through VEGFR activation in a PI3K-dependent manner. Finally, focal adhesion kinase (FAK) activation is mediated via the C-terminal tail of VEGFR-2 and is required for cell migration (11, 12).

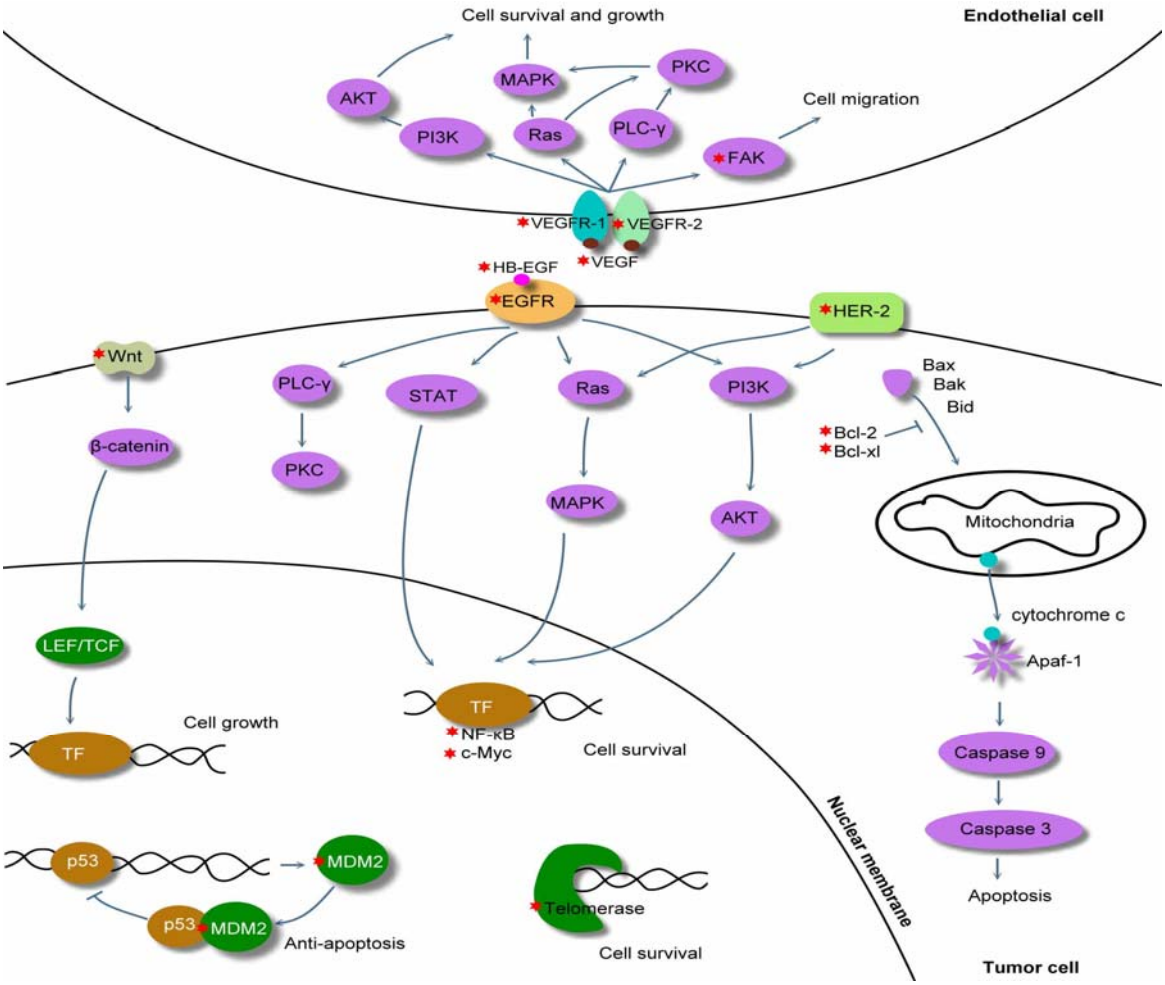

Figure 1.1 Cellular signaling in tumor and endothelial cells. Target genes to which siRNA has been used for down-regulation are identified with a red star.

siRNA which down-regulates VEGF expression inhibits tumor growth in HeLa cells, ovarian carcinoma or melanoma cells *in vitro*, as well as in a PtdCho-3 xenograft model (13). Blocking VEGF receptor expression is another way to inhibit angiogenesis. It has been shown in endothelial cells of different tumor models that siRNAs down-regulating VEGFR-1 and VEGFR-2 could block angiogenesis. Combination of anti-VEGF and anti-VEGFR siRNA improves therapeutic effect (14-16).

1.1.2 Inhibition of tumor survival and induction of apoptosis

siRNAs targeting oncogenes that are involved in survival or anti-apoptosis show great therapeutic potential for cancer therapy (17). Wnt pathway plays an important role in carcinogenesis. Wnt signaling is transduced through Wnt receptors to the beta-catenin-Tcf pathway, the c-Jun-N-terminal kinase (JNK) pathway or the Ca^{2+}-releasing pathway. Wnt/beta-catenin signaling pathway is highly activated and results in beta-catenin accumulation in a variety of human cancer. Anti-Wnt-1 siRNA induced apoptosis in MCF-7 breast cancer cell line (18). siRNAs blocking Wnt pathway have also been used to target cancerous stem cells in non-small cell lung cancer (NSCLC) which has limited response to single-agent chemotherapy (19). These results suggest that siRNA inhibiting Wnt pathway may serve as a potential anti-cancer agent.

NF-κB, a transcription factor which regulates various genes involved in different pathological states, has been related to oncogenesis and serves an important role on cell survival and anti-apoptosis in response to chemotherapy. siRNA is currently used to inhibit the function of NF-κB pathway. Combination of p65 siRNA and CPT-11, a topoisomerase I inhibitor, significantly delayed tumor growth and reduced tumor size (20). These studies demonstrate siRNA targeting NF-κB can not only enhance apoptosis but also increase sensitivity to radiation or chemotherapy in tumor cells (20, 21).

siRNA targeting heparin binding-epidermal growth factor-like growth factor (HB-EGF), a ligand of epidermal growth factor receptor (EGFR), can inhibit each step involved in peritoneal dissemination in human ovarian cancer *in vitro* and *in vivo* [21]. EGFR, which is over-expressed in a variety of tumors, is related to tumor proliferation, anti-apoptosis,

enhanced metastasis and drug resistance (22, 23). As shown in **Figure 1.1,** activation of EGFR results in homo/hetero-dimerization of the receptor, phosphorylation of specific tyrosine kinases which trigger several signal pathways. For example, PLC γ binds directly to the receptor and activates PKC. The transcription factors, STAT, enters into the nucleus to activate the expression of target genes. Ras/Raf/MAPK pathway and PI3K/AKT pathway are both triggered by EGFR signaling and lead to transcription activation of target genes related with cell proliferation, anti-apoptosis, invasion, and metastasis (24). siRNA against EGFR could trigger cell death and inhibit tumor growth in NCI-H460 xenograft tumor and the complete tumor growth inhibition lasted for 1 week when combined with cisplatin (25).

Many cancer cells over-express HER-2/neu which inhibits apoptosis and promotes cell growth. HER-2/neu over-expression activates Ras/MAPK pathway which helps cell survival and growth (26). Zhou et al. (27) demonstrated that activation of *HER-2/neu* activated AKT, which phosphorylated MDM2, could enhance MDM2-mediated ubiquitination and degradation of p53. Loss of p53, a key molecule in regulating cell growth and apoptosis, makes the cancer cells resistance to DNA-damaging agents. Her-2 siRNA formulated in nanoparticles significantly inhibited Her-2 protein expression and suppressed tumor growth *in vitro* and *in vivo* (28).

Telomerase, an enzyme maintaining cancer cell immortality and promoting malignant transformation, is abundant in most malignant cells but expressed only at low levels in normal somatic cells. Wang et al. (29) evaluated the ability of siRNA targeting a human telomerase reverse transcriptase component (hTERT) to inhibit telomerase activity in human cancer cells. In their research, tumor-specific siRNA expression system targeting hTERT driven by the survivin promoter could inhibit the growth and increase the radiosensitivity of

human cervical carcinoma cells (HeLa). Shen et al. (30) demonstrated that siRNA targeting hTERT inhibited telomerase activity, HCT116 cell growth *in vitro* and tumorigenicity *in vivo*. They further showed the depletion of hTERT also repressed cell adhesion, migration, and invasion by down-regulating the expression of adhesion- and motility-related proteins such as c-Met and integrins. Taken together, hTERT siRNA may offer a new potential gene therapy strategy for cancer.

p53, a transcription factor, maintains the normal cell cycle and keeps the genome integrity through apoptosis induction in response to DNA damage. p53 is negatively regulated by MDM2. Down-regulation of MDM2 by siRNA results in increasing p53 which is able to regulate its target genes (31). Loss-of-function p53 gene mutations results in a decreased ability of the cancer cells to undergo apoptosis. Martinez et al. (32) showed that highly sequence-specific siRNA could suppress the expression of mutated p53 and restored the wild-type p53 in cells expressing both forms, thereby promoting apoptosis of the treated tumor cells, reducing the cancer formation and inhibiting the development of malignant process.

Bcl-2 which is over-expressed in many cancer cells such as gastric cancer has a strong anti-apoptotic effect. Both Bcl-2 and Bcl-XL, which belong to anti-apoptotic Bcl-2 family, counteract the activity of pro-apoptotic molecules such as Bid, Bax and Bak and thus can suppress pro-apoptotic signaling in the mitochondria. When apoptotic signaling is triggered in the mitochondria, cytochrome c escapes from the mitochondrial intermembrane space to the cytosol and forms apoptosomes with Apaf-1 and dATP. After apoptosome formation, caspase-9 cleaves pro-caspase-3 into the active form caspase-3 and leads to cell death (33). Hao et al. (34) reported that siRNAs inhibiting Bcl-2 expression decreased

telomerase activity (by about 80 %), promoted apoptosis and delayed the growth of human gastric cancer cells. Therefore, knockdown of Bcl-2, an important factor in carcinogenesis, may provide an efficient therapeutic approach for treating cancer.

1.1.3. Enhancing the chemo-sensitivity

The occurrence of drug resistance is a main impediment to the success of cancer chemotherapy. Cancer cells develop different ways to be resistant to chemotherapy drugs of malignant tumors. Over-expression or activation of anti-apoptotic molecules such as Bcl-2 proteins achieves imbalanced apoptosis regulation and drug resistance (35, 36). Oncogenes which activate cell survival signaling also play the roles to develop drug resistance. For example, a calcium-dependent protein crosslinking enzyme, tissue transglutaminase 2 promoting fibronectin-mediated cell attachment and cell growth contributes to the occurrence of the drug-resistant phenotype (37). Furthermore, increased drug-metabolizing enzymes can trigger drug resistance through enhanced detoxification of the chemotherapy drugs (38). Over-expression of drug transporter proteins, such as P-glycoprotein (P-gp) plays a key role to regulate drug resistance. P-gp is directly related to the drug resistance to vinca alkaloids (vinblastine, vincristine), anthracyclins (adriamycin, daunorubicin), etoposide and paclitaxel. For enhancing the therapeutic effect of these chemotherapeutic agents, siRNAs were designed to inhibit MDR1 expression and convert the tumor back to the drug-sensitive state [29,30].

Furthermore, it has been shown that combination of siRNAs targeting various oncogenes and angiogenic factors mediated greater anti-tumor effect. In order to achieve siRNA combination approach, Chen et al. (39) have constructed multiple shRNA expression vectors that simultaneously targeted VEGF, hTERT and Bcl-xl. The reduction in VEGF,

hTERT and Bcl-xl expression significantly repressed tumor growth in human laryngeal squamous carcinoma (Hep-2) *in vivo*. Li et al. (40) showed that selective delivery of siRNA targeting c-myc, MDM2 and VEGF by LPD nanoparticles significantly reduced the lung metastasis of B16F10 melanoma cells *in vivo*. These studies suggest that siRNA targeting multiple genes in human cancers could prove to be valuable in preventing cancer cell proliferation and metastasis and should be considered as a novel approach for cancer therapy.

Co-delivery of a chemotherapy drug and siRNAs as suppressors of drug resistance is an efficient strategy to treat cancer. For example, mesoporous silica nanoparticles can be modified to carry Dox inside the pores. The Dox-loaded mesoporous silica nanoparticles modified with generation 2 (G2) amine-terminated polyamidoamine (PAMAM) dendrimers can bind with siRNA. The bi-functional MSNs which co-delivered Dox and Bcl-2 siRNA achieved enhanced apoptosis in multidrug-resistant A2780/AD human ovarian cancer cells (41).

1.1.4 Inhibition of metastasis

The thrombin receptor [protease-activated receptor-1 (PAR-1)] is up-regulated in malignant metastatic melanoma cell lines and in patients with metastatic tumor. Down-regulation of PAR-1 with lentiviral short hairpin RNA significantly inhibited both tumor growth and metastasis of metastatic melanoma cell lines *in vivo*. PAR-1 Silencing also decreased the expression of vascular endothelial growth factor, interleukin-8, and matrix metalloproteinase-2 which are involved in the invasion and angiogenesis. Therefore, PAR-1 can serve as a therapeutic target for inhibition of the melanoma cell growth and metastasis by suppression of the angiogenic and invasive factors (42).

In summary, siRNA shows great potential in many different anti-cancer strategies. However, there are serious obstacles that need to be overcome before it becomes a powerful new class of drug: difficulties with delivery, bio-stability, pharmacokinetics, and the off-target effect, just to name a few. The half life of the naked siRNA is less than an hour in human plasma, and the circulating siRNA is rapidly cleared by the kidneys because of their relatively small size. Recently, adverse off-target activity due to cross-reactivity between RNAi pathways was identified as potential cause of toxicity (43). It is unwise to systemically administer naked siRNA as a therapeutic agent. Thus, use of a delivery system and/or chemical modification is developed to protect siRNA from degradation and to enhance its stability in serum.

1.2 NON-VIRAL VECTORS FOR SIRNA DELIVERY

Effective strategy to deliver siRNA systematically into solid or metastatic tumor should fulfill at least five requirements – protection of siRNA from degradation and rapid clearance, prolonged circulation time after administration, efficient uptake of siRNA by the tumor, cellular uptake of siRNA, and endosomal release of siRNA into the cytoplasm (44). Some viral vectors can effectively deliver their genomes into the tumor cells and express short hairpin RNA (shRNA) for gene silencing (45). But none of the viral vectors can efficiently accumulate in the tumor after systemic administration. Their strong immunogenicity and other safety issues are also concerns (46).

It is of great importance to prevent instability and inactivation of siRNA in the human blood and avoid the side effect such as off-target effect of siRNA, the interferon response, or the activation of Toll-like receptors. This might be accomplished by several different strategies: chemical modification of siRNA, inhibition of RNAse family enzymes that

degrade siRNA in the blood circulation and use of siRNA carriers such as cationic liposomes and polymers [37,38]. These non-viral vectors are commonly used.

1.2.1 polycationic polymer based polyplexes

Systemic delivery of siRNA to tumor cells continues to be a major hurdle. Several synthetic cationic polymers and oligopeptides have been designed as systemic, nonviral delivery vectors for polynucleotides. The drawback of the carrier system is the positively charged complex nonspecifically interacts with anionic plasma proteins or other blood components, such as heparan sulfate and hyaluronic acid, resulting in the inactivation of the vector and undesired toxicity.

Therefore, using a water-soluble polymer, such as poly (ethylene glycol) (PEG) and polysaccharides, to modify the polymer/siRNA complex have been a major strategy to decrease such non-specific interactions, and thereby prolong the blood circulation time. Sato et al. (47) studied a cationic comb-type copolymer (CCC) consisting of a polycation backbone and side chains of water-soluble polymer and found that the dense brush of the water-soluble side chain polymer enhanced interpolyelectrolyte complex between the polycation backbone and siRNA. Furthermore, the CCC/siRNA complex exhibited a protective effect against nuclease activity and produced prolonged circulation time of siRNA in mouse.

Bartlett and Davis [40] developed cyclodextrin-containing polycations (CDP) nanoparticles for siRNA delivery. Inclusion complex formed between adamantane (AD)-containing molecule and the β-cyclodextrin allowed the attachment of poly (ethylene glycol) (AD-PEG) for steric stabilization and a targeting ligand (AD-PEG-transferrin) for target specific delivery of the siRNA. The nanoparticles protected siRNA from nuclease

degradation, prevented aggregation at physiological salt concentrations and avoided complement fixation. CDP vector may serve as a tool for targeted siRNA delivery.

For developing a safe and serum stable carrier system that can rapidly release siRNA from endosome, calcium phosphate (CaP) is incorporated into the formulation. The siRNA-entrapped CaP nanoparticles made with poly(ethylene glycol)-block-poly(methacrylic acid) (PEG-PMA) was designed by Kakizawa et al. (48). PMA nanoparticles undergo a conformational transition at pH 4–6, which is similar to the endosomal pH. The formulation can protect the entrapped siRNA from degradation until it arrives at the acidic endosome, where the siRNA escapes the nanoparticles and enters into the cytoplasm. They demonstrated a highly efficient transfection activity of siRNA using nano-sized calcium phosphate crystals with appreciable serum stability.

Polyethyleneimine (PEI) is a synthetic polymer which contains many cationic charges and a protonable amino group in every third position [42]. PEI condenses DNA and delivers it into mammalian cells *in vitro* and *in vivo*. It is also known to exhibit a "proton sponge effect" due to its strong buffering capacity at mildly acidic pH in the endosome and lysosome to facilitate the escape of DNA into the cytoplasm (49). More recently, PEI was used to deliver siRNA, but the siRNA has to be polymerized into greater lengths to increase its interaction with PEI (50). Werth et al. (51) also demonstrated that the non-covalent complexation of siRNA and a commercially available polymer, Jet-PEI, led to enhanced siRNA stabilization and delivery efficacy. They also showed that lyophilized PEI/siRNA complex retained the activity and the stability to serve as a ready-to-use reagent for specific and efficient silencing of genes.

Inorganic particles such as gold nanoparticles modified with polymers served as safe and effective carriers of siRNA. siRNA was conjugated to the gold nanoparticles modified with the hydrophilic polymer poly(ethylene glycol) (PEG) via biodegradable disulfide linkages. The gold nanoparticles coated with a library of end-modified poly(beta-amino ester)s (PBAEs) showed efficient siRNA delivery *in vitro* (52). Polyethyleneimine (PEI)-capped gold nanoparticles (AuNPs) were recently developed to efficiently and safely deliver siRNA. PEI served as both the reductant and stabilizer to generate PEI-capped AuNPs and interact with siRNA. siRNA against an oncogene polo-like kinase 1 (PLK1) delivered by PEI-capped AuNPs/siRNA showed stronger gene silencing effect and induced more apoptosis in MDA-MB-435s cells than siRNA delivered by PEI alone. Without the unwanted toxicity, PEI-capped AuNPs appear to be suitable carriers for siRNA therapy (53)

Chitosan, a cationic polymer, has also been used to delivery siRNA. Morten et al. developed the easy-to-use freeze-dried chitosan/siRNA complex capable of efficient knockdown of target gene *in vitro* with an extended storage period. These systems provide the advantage for RNAi based high throughput screening, surface mediated siRNA delivery for implants as well as storage of siRNA therapeutics (54).

The Dynamic Polyconjugate technology is recently developed by Rozema et al. (55). A membrane-active polymer is designed to reversibly mask its activity until it reaches the acidic environment of the endosome. It also possesses the features of prolonged circulation time, reduced toxicity and targeted delivery to the hepatocytes *in vivo* after i.v. administration. They demonstrated that siRNA formulated in the dynamic polyconjugate could effectively silence either apolipoprotein B (apoB) or peroxisome proliferator-activated receptor alpha (PPARa) in the mouse liver.

1.2.2 Lipid based lipoplex and liposomes

Lipid based lipoplex and liposomes have been applied for the delivery of siRNA to provide an improved pharmacokinetic property and a decreased toxicity profile. Liposomes are composed of a single or multiple lipid bilayers and an aqueous core. Usually, a cargo is entrapped in the aqueous core of the liposomes. In contrast, a typical feature of lipoplex is a heterogeneous association of cationic lipid and nucleic acid (56). Generally, liposomes are more stable than lipoplex in biological fluid.

Zimmermann et al. [48] developed a liposomal formulation, i.e., stable nucleic acid lipid particles (SNALP), for systemic delivery of siRNA in non-rodent species. siRNA against apoB formulated in SNALP could silence the disease target apoB in the liver 48 h after administration in cynomolgus monkey. Twenty four hours after the treatment, apoB protein, serum cholesterol and low-density lipoprotein levels were significantly reduced and the therapeutic effect lasted for 11 days. Their studies demonstrated that liposomal formulation of siRNA could be an efficient strategy for silencing hepatocyte genes.

To avoid the drawback of cationic lipid such as immunogenicity and instability in the serum, neutral liposomal delivery systems have also been developed for siRNA delivery. Halder et al. (57) successfully delivered siRNA against FAK into human ovarian tumor in nude mice by neutral liposome 1,2-dioleoyl-sn-glycero-3-phosphatidylcholine (DOPC). The siRNA formulation inhibited FAK expression for up to 4 days in tumor tissue and reduced mean tumor weight by 44% to 72% in three different human ovarian cell lines (HeyA8, A2780-CP20, and SKOV3ip1). This group also reported recently that siRNA targeting IL-8 incorporated into neutral liposomes (siRNA-DOPCs) reduced the mean tumor weight by 32% and 52% in the HeyA8 and SKOV3ip1 mouse models and also decreased microvessel

density of these tumors (58). Since the liposomes did not contain charges, it is unclear how siRNA could be efficiently encapsulated in the liposomes.

To prolong the circulation time of liposomes, Morrissey et al. [51] reported a sustained circulation in the blood of a formulation of chemically modified siRNA employing polyethylene glycol (PEG)-modified liposomes. They demonstrated that siRNA against HBV encapsulated by the modified liposomes could be delivered to the mouse liver and reduced the HBV DNA titer *in vivo*. Ueno et al. [52] have developed the LPD which showed enhanced stability and increased transfection efficiency. Li and Huang (59) modified the LPD formulation for siRNA delivery. The tumor-targeted nanoparticles LPD-PEG-anisamide (LPD-PEG-AA) increased the tumor uptake of siRNA and the associated gene-silencing effect, resulting in an inhibition of tumor growth *in vitro* and *in vivo*.

Efficient endosomal release of siRNA into the cytoplasm can significantly improve siRNA delivery. pH-dependent (PD) liposomes have been designed for endosomal release of siRNA (60). A polycationic block, either poly [2-(dimethylamino)ethyl methacrylate] (31 or 62 DMA repeat units) or polylysine (21 K repeat units), serves as an anchor for PEG. 1,2-dioleoyl-3-dimethylammonium-propane (DAP), a titratable lipid, was added into the liposomes to enhance the net cationic character at the acidic condition, resulting in polymer release and membrane fusion in the endosomes. Auguste et al. demonstrated that the polymer release from PD liposomes increased siRNA-mediated gene silencing effect.

Wrapsome (WS) is developed by using both polymer and liposome as siRNA carriers. It is composed of a core containing siRNA and a cationic lipofection complex and an envelope containing a neutral lipid bilayer and hydrophilic polymers. WS prolonged the blood circulation of siRNA and efficiently delivered siRNA into the tumor site. siRNA

against KLF5 which plays a role in tumor angiogenesis delivered by WS reduced angiogenesis and exhibited significant antitumor effect (61).

1.3 NON-VIRAL TARGETED SIRNA DELIVERY TO TUMOR

For cancer therapy, an effective delivery system is designed to specifically deliver functional siRNA into the target tumor cells and reach an effective intracellular concentration. A suitable targeting ligand is usually added into the carrier to achieve tumor specific siRNA delivery. The following is a review of different targeting ligands used for delivery.

1.3.1 Peptides

The RGD peptide has been used to target siRNA to integrins over-expressed in the tumor neovasculature. Schiffelers et al. [55] attached siRNA against VEGF receptor to PEGylated PEI with an RGD peptide as a targeting ligand. They showed suppression of angiogenesis, reduction of tumor growth in the murine neuroblastoma N2A xenograft tumor. De Wolf (62) further designed nanoparticles assembled upon complexation of siRNA with cationic liposome (DOTAP/DOPE) and RGD-PEG-PEI, a PEGylated polymer that carries RGD. They showed that both the circulation kinetics and the overall tumor accumulation of the siRNA complex were similar to non-complexed siRNA. However, the intratumoral distribution of siRNA was improved by the carriers. The benefits from using the targeted carrier were attributed to the specific transport towards the tumor mediated by the RGD ligand.

Peptide carriers have been developed that have proved effective for siRNA delivery. Leng et al. (63) demonstrated that the highly branched polymers composed of histidine and lysine were effective carriers of siRNA. Furthermore, RGD containing peptide carriers

showed more siRNA silencing activity in an endothelial cell line (SVR-bag4) than the carriers without RGD peptide. Thus, RGD peptide can be used as a targeting ligand for siRNA delivery into the tumor neovasculature and enhance the therapeutic effect.

A tumor-homing peptide (F3) was found to target the cell-surface nucleolin (64). It binds to the surface of the tumor cells and is internalized by the tumor cells when administered systemically as a free peptide [59]. Derfus et al. (65) used a PEGlyated quantum dot (QD) core as a scaffold conjugated with both siRNA and tumor-homing peptide (F3) on the particle surface. siRNA attached to the particle by a disulfide cross-linker showed a greater silencing effect than that attached by a nonreducible thioether linkage. Delivery of the enhanced green fluorescence protein (EGFP) siRNA by F3/siRNA-QD complex to EGFP-transfected HeLa cells led to significant knockdown of the EGFP signal. By replacing EGFP siRNA with other therapeutic siRNAs, the targeted complex may be useful to treat cancer.

1.3.2 Small molecular weight ligands

Yoshizawa et al. (28) developed a folate-linked nanoparticle (NP-F) for tumor-targeted siRNA delivery. NP-F was composed of cholesteryl-3-beta-carboxyamidoethylene-N-hydroxyethylamine (OH-Chol), Tween 80 and folate-poly(ethylene glycol)-distearoyl-phosphatidylethanolamine conjugate (f-PEG(2000)-DSPE). NP-F could delivery higher amounts of siRNA into the cytoplasm than the non-targeted nanoparticles in human nasopharyngeal KB cells, which over-expressed the folate receptor (FR). Her-2 siRNA formulated by NP-F significantly and selectively suppressed Her-2 protein expression and inhibited tumor growth *in vitro* and *in vivo*. These results provided optimism for tumor-targeted siRNA therapy.

Tenascin-C is an extracellular matrix glycoprotein highly expressed in a range of tumors, but not in normal tissues. Shao et al. (66) developed a liposomal carrier system, using sulfatide as a targeting ligand which binds with tenascin-C. The targeted liposomes bound specifically with the tenascin-C expressing glioma cells. After binding to the extracellular matrix, the sulfatide-containing liposomes were internalized via both caveolae/lipid raft- and clathrin-dependent pathways and the cargoes in the liposomes were released into the cytoplasm. Such targeted, lipid-based intracellular delivery shows promise for effective siRNA mediated cancer therapy in the future.

Li and Huang (59) have developed a tumor-targeted LPD formulation for siRNA delivery. (**Figure 1.2**). This formulation included anisamide (AA), which binds with the sigma receptor over-expressed in NCI-H460 lung cancer cells. The tumor-targeted nanoparticles LPD-PEG-anisamide increased the siRNA delivery efficiency and the gene-silencing effect *in vitro*. siRNA against survivin formulated by LPD-PEG-AA induced 90% of apoptosis and sensitized the cells to cisplatin *in vitro*. Four hours after IV injection of LPD-PEG-AA into a xenograft model, 70-80% of the injected siRNA/g accumulated in the tumor, approximately 10%/g was detected in the liver and approximately 20%/g recovered in the lung (25). siRNA against the epidermal growth factor receptor (EGFR) delivered by LPD-PEG-AA significantly silenced EGFR in the tumor, induced approximately 15% tumor cell apoptosis and completely inhibited tumor growth for 1 week when combined with cisplatin. They also selectively delivered a mixture of siRNA against MDM2, c-myc, and VEGF co-formulated in LPD-PEG-AA into a lung metastasis model of B16F10, sigma receptor–expressing murine melanoma cells (40). siRNAs delivered by targeted nanoparticle caused simultaneous silencing of each of the oncogenes in the metastatic nodules. Two

consecutive IV injections of siRNA formulated in the LPD-PEG-AA significantly reduced the lung metastasis (~70–80%) and significantly prolonged the mean survival time of the animals by 30% as compared to the untreated controls. A lipid coated calcium phosphate nanoparticle (LCP) was recently developed for improvement of siRNA silencing effect by

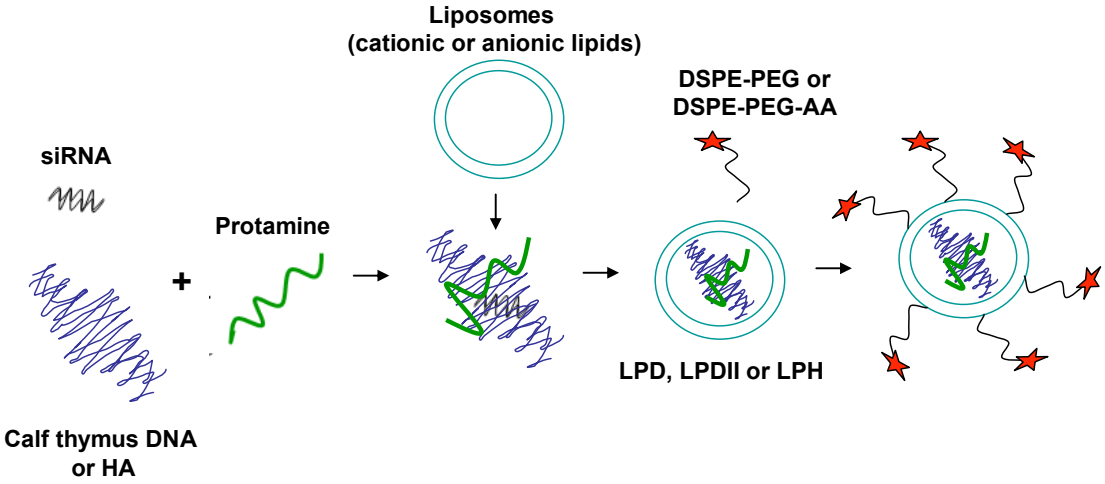

Figure 1.2 Illustration of preparation of LPD or LPH nanoparticles containing siRNA

enhanced siRNA release from the endosome (67). LCP contains a core which is composed a biodegradable nano-sized calcium phosphate precipitate and siRNA. After entering the cells, siRNA was released from LCP into the cytoplasm at acidic pH in the endosome. Luciferase siRNA delivered by the targeted LCP suppressed about 70% and 50% of luciferase activity of the solid tumors in a xenograft model. These studies indicate that surface-modified LPD and LCP may serve as a potent vector for RNAi-based tumor therapy.

1.3.3 Antibodies and Proteins

The development of a systemically administered, tumor-specific immunoliposome nanocomplex with high transfection efficiency could serve as a carrier for siRNA delivery and be utilized as effective anticancer clinical modalities when formulated with a therapeutic siRNA.

A receptor-specific monoclonal antibody delivery system and avidin-biotin technology were used to deliver siRNA into brain tumor across the blood-brain barrier (68). The siRNA was mono-biotinylated on either terminus of the sense strand, in parallel with the production of a conjugate of the targeting antibody and streptavidin. Intravenous administration of the transferrin receptor antibody attached siRNA caused 69-81% suppression in luciferase gene expression in the intracranial brain cancer (C6 or RG-2) model *in vivo*. This study showed a therapeutic potential for brain cancer gene therapy.

Pirollo et al. (69) have developed an anti-transferrin receptor (TfR) single-chain antibody fragment-directed nanoimmunoliposome to deliver siRNA to both primary tumor and metastatic disease. A pH-sensitive histidine-lysine peptide and a modified hybrid (DNA-RNA) anti-HER-2 siRNA molecule were used to enhance the efficiency of this complex. The nanoimmunoliposome anti-HER-2 siRNA complex could silence the target gene and its downstream pathway components *in vivo*, sensitize the tumor cells to chemotherapeutic agent, and inhibit tumor growth in a pancreatic cancer model.

A polymer, OEI-HD (beta-propionamide-cross-linked oligoethylenimine) conjugated with transferrin were used for siRNA delivery into the mouse Neuro2a neuroblastoma cells *in vitro* and *in vivo* (70). siRNA against the Ras-related nuclear protein Ran delivered by transferrin-conjugated OEI-HD (three intravenous applications at 3-day interval) resulted in >80% reduced Ran protein expression, apoptosis, and a reduced tumor growth in a xenograft Neuro2A tumor models without unspecific toxicity. Bartlett et al. (71) used positron emission tomography (PET) and bioluminescence imaging to quantify the *in vivo* biodistribution and function of siRNA formulated in cyclodextrin-containing polycation nanoparticles. Both non-targeted and transferrin-targeted siRNA nanoparticles showed similar biodistribution and

tumor localization through the enhanced permeability and retention (EPR) effect [66]. However, the transferrin-targeted siRNA nanoparticles decreased luciferase activity in the tumor more than the nontargeted nanoparticles. Their results demonstrated that the function of the targeting ligand is to enhance the cellular uptake in tumor cells rather than tumor localization. Li et al. (25, 59) have reached the same conclusion in their work using the anisamide ligand.

1.3.4. Aptamers

Aptamer is a nucleic acid molecule selected for high affinity binding with a protein target (72). McNamara et al. (73) have developed an aptamer-siRNA chimeric RNA capable of specific binding and delivery of therapeutic siRNAs into the target cells. The aptamer portion of the chimera had the ability to bind with PSMA, a cell-surface receptor over-expressed in prostate cancer cells and tumor vascular endothelium, but not the normal cells. siRNA delivered by aptamer-siRNA chimera were internalized and processed by Dicer, resulting in repression of the target protein and cell death. siRNA against a survival gene delivered by aptamer-siRNA chimera also specifically inhibited tumor growth and mediated tumor regression in a xenograft model of the prostate cancer. The formulation did not contain an endosome release mechanism. So, how the chimera could escape the endosomes is not clear.

1.4 CONCLUSION

Various targeted siRNA delivery systems described above serve as a promising approach for the development of safer and effective therapeutics for cancer. However, the following issues are to be dealt with before a full-scale development effort is embarked.

1.4.1 Safety

One of the important features of a good delivery system is its lack of nonspecific immune stimulation. For example, transferrin-conjugated OEI-HD did not induce acute toxicity or significant changes in the host body weight, hematology parameters, or liver enzymes (AST, ALT, or AP). siRNA formulated by LPD-PEG-AA caused a low level of toxicity based on the serum level of liver enzymes and body weight monitoring during the treatment. The carrier itself only showed little immunotoxicity (IMT). To improve the safety of siRNA delivery, Chono et al. (74) have developed a nanoparticle formulation [liposomes-protamine-hyaluronic acid nanoparticles (LPH-NP)] for systemically delivering siRNA into the tumor. siRNA formulated in the targeted LPH-NP showed similar gene silencing effect as LPD-PEG-AA, but the targeted LPH-NP showed very little immunotoxicity in a wide dose range (0.15 - 1.2 mg siRNA/kg) compared with LPD-NP (liposome-protamine-DNA nanoparticles) which had a much narrower therapeutic window (0.15-0.45 mg/kg)(**Figure 1.2**).

1.4.2 Efficacy

As an effective therapeutics for oncology applications, siRNA formulated in nanoparticles can accumulate in the tumor through the EPR effect independent of the targeting ligand. However, targeting ligand attached to the nanoparticles can enhance the cellular uptake of siRNA and lead to enhanced potency compared to the non-targeted formulation. Receptor mediated endocytosis of the targeted nanoparticles is considered a key feature for effective siRNA delivery. An ideal receptor targeted by the nanoparticles should have several properties, such as over-expression on the tumor cells rather than the normal

cells, homogeneous distribution on all tumor cells, accessibility from the blood circulation and rapid internalization of carried cargo after binding to the target cells.

Internalization often occurs through the receptor-mediated endocytosis. For example, when the pH sensitive folate-targeted nanoparticles bind with the folate receptor, the nanoparticles are internalized into the endosomes. As the pH in the endosome decreases, the formulated siRNA is released from the endosome into the cytoplasm. At the same time, the folate receptor released from the endosome returns to the cell membrane and starts another round of internalization through binding with new folate-targeted nanoparticles (75). A RGD-oligolysine containing cationic liposome showed the ability to deliver plasmid DNA through endocytosis. The vector complex internalizes into the early endosomes within 5 min, and then enters into the late endosomes and the lysosomes (76). Since the vector internalization and trafficking is important for siRNA delivery, a better understanding of these processes should help design improved carriers.

Gene therapy is a potential way for the treatment of cancer. Major limitations of siRNA therapy such as low stability and poor cellular uptake need to be overcome by using a suitable vector. An ideal carrier system for tumor targeted siRNA delivery should form neutrally charged and nano-scale particle size to achieve a high EPR effect. Additional component such as PEG should be added into the nanoparticles to maintain prolonged circulation. A suitable targeting ligand facilitates the binding to the tumor cells and the internalization of the nanoparticles into the endosomes. The ability to release the cargo from the endosome to the cytoplasm such as the proton sponge effect is another key feature for improving siRNA delivery. Fortunately, siRNA does not need to penetrate into the nucleus, which is a significant barrier for DNA. In conclusion, siRNA has an excellent potential to

become a class of novel cancer therapeutics. A suitable carrier that can delivery siRNA into the tumor tissue and achieve the therapeutic effect is the most important issue facing the field. In particular, targeted nanoparticles offer the potential to improve the pharmacokinetics of siRNA, while providing clinical applications for diagnostic imaging and cancer therapy.

1.5 AIMS AND OBJECTIVES OF THIS DISSERTATION PROJECT

The Huang lab has designed LPD nanoparticles which can efficiently delivery of siRNA to the solid and metastasis tumor and silence the target gene. However, the current formulation only induced partial apoptosis and growth inhibition. We hypothesize that this was due to alternative pathways of proliferation in the cancer cell. This project is to further enhance the activity and expand the therapeutic applications of LPD nanoparticles via the following strategies. **First** is to design novel cationic lipids that can enhance the therapeutic activity of the LPD nanoparticles for efficient tumor killing in a xenograft model. **Second** is to expand the application of the LPD nanoparticles to treat different tumor models or target tumor vasculature by designing a peptide-targeted LPD nanoparticle. **Third** is to design and test a combination therapy using multi-functional LPD nanoparticle formulations that contain both siRNA and a chemotherapy drug to induce synergistic tumor cell apoptosis and overcome drug resistance.

1.6 ORGANIZATION OF DISSERTATION

The framework for this project is presented in the following Chapters. A novel lipid containing a lysine residue that delivers siRNA in lung cancer cells is presented in Chapter 2. Chapter 3 describes another novel lipid containing an arginine residue delivers siRNA to the murine melanoma lung cancer cells. Chapter 4 presents a nanoparticle formulation targeted with tumor specific peptide ligand co-delivers c-myc siRNA and Dox for anticancer

therapy. A multi-functional nanoparticle formulation, i.e., LPD-II, delivering both siRNA and Dox to overcome drug resistance in cancer is described in Chapter 5. A nanoparticle formulation modified with scFv that co-delivered siRNA and miRNA into B16F10 lung metastases is presented in Chapter 6. Discussions, conclusions and directions for future research are presented in Chapter 7.

2.0 NOVEL CATIONIC LIPID THAT DELIVERS SIRNA AND ENHANCES THERAPEUTIC EFFECT IN LUNG CANCER CELLS

We have developed LPD nanoparticles containing 1,2-dioleoyl-3-trimethylammonium-propane (DOTAP) and targeted with polyethylene glycol (PEG) tethered with anisamide (AA) to specifically deliver siRNA to H460 human lung carcinoma cells which express the sigma receptor. A novel non-glycerol based cationic lipid which contains both a guanidinium and a lysine residue as the cationic headgroup, i.e., DSGLA, down-regulated pERK more efficiently in H460 cells than DOTAP. As demonstrated by using fluorescently labeled siRNA, LPD-PEG-AA prepared with DSGLA efficiently delivered siRNA to the cytoplasm of the H460 cells. Although the siRNA delivered by LPD-PEG-AA containing either DOTAP or DSGLA could effectively silence EGFR expression, a synergistic cell killing effect in promoting cellular apoptosis was only observed with DSGLA. The fluorescently labeled siRNA was efficiently delivered into the cytoplasm of H460 xenograft tumor by the LPD-PEG-AA containing either DOTAP or DSGLA 4 h after intravenous injection. Three daily injections (0.6 mg/kg) of siRNA formulated in the LPD-PEG-AA containing either DOTAP or DSGLA could effectively silence the epidermal growth factor receptor (EGFR) in the tumor, but the formulation containing DSGLA could induce more cellular apoptosis. A significant improvement in tumor growth inhibition was observed after dosing with LPD-PEG-AA containing DSGLA. Thus, DSGLA served as both

a formulation component as well as a therapeutic agent which synergistically enhanced the activity of siRNA.

2.1 INTRODUCTION

Non-small cell lung cancer (NSCLC) is the most common lung cancer which is the most common cancer and the major cause of death throughout the world according to the World Health Organization (WHO) cancer report (77). Because of their propensity to metastasize early and develop resistance to a wide range of anticancer drugs, the prognosis of lung cancer patients has had limited improvement and innovative strategies that effectively treat lung cancer are urgently needed.

Recently, new approaches such as immunotherapy, targeted agents and gene therapy are developed for cancer therapy. Success of gene therapy critically depends on the safety and efficacy of the transfection vector used in delivering the therapeutic gene (78, 79). Small interfering RNA (siRNA) that can induce sequence-specific gene silencing has been developed as a potential cancer therapy agent (80-82). Cancer growth inhibition was observed after siRNA mediated knockdown of the over-expressed oncogenes such as EGFR that are essential to NSCLC proliferation (25). Cationic liposomes as well as viral vectors have been shown to be powerful tools to deliver siRNA (83).

To enhance gene transfection effect, various cationic liposomes have been synthesized to deliver plasmid DNA, antisense or siRNA to the cytoplasm or nucleus (84-88). A cationic lipid generally contains two parts - a cationic headgroup and a hydrophobic moiety such as hydrocarbon chains (89-91). One of the critical factors that influences nucleic acid delivery is the composition of the cationic headgroup (92). For example, a spacer between the headgroup of cholesterol-based gemini lipids increases the serum compatibility

of the lipoplex (93, 94). Spermine or spermidine containing headgroup has the ability to condense nucleic acid. Kim et al. demonstrated that a lysine headgroup can enhance gene expression efficiency and decrease cytotoxicity (95). Obata et al. reported that cationic lipids bearing lysine or arginine as a cationic headgroup showed higher gene transfection activity, more serum compatible, and lower cytotoxicity compared with Lipofectamine2000 (92). Furthermore, cationic transfection amphiphiles containing guanidinium functionality, which mimics the arginyl residues in DNA binding protein such as histones and protamine, were first reported by Vigneron et al. (96). The guanidinium group remains protonated over a much wider range of pH than other basic groups due to its high pKa value. It also forms characteristic parallel zwitterionic hydrogen bonds N-H+…O- with phosphate ions. The guanidinium groups are also capable of forming hydrogen bonds with nucleic acid bases, thus further enhancing the capacity to deliver plasmid DNA or siRNA.

Our lab has developed LPD nanoparticles which are composed of cationic liposomes and polycation-condensed DNA to deliver plasmid DNA or siRNA (25, 97, 98). We have demonstrated that siRNA can be formulated in LPD and causes gene silencing activity in the treated cells. The LPD formulation contained a commercially available cationic lipid DOTAP. However, DOTAP activates ERK in the dendritic cells (99). ERK is a member of the mitogen activated protein kinase (MAPK) family, activation of which could lead to an anti-apoptosis effect.

In order to combat this potential problem in cancer therapy and improve siRNA delivery efficacy, we developed a novel non-glycerol based cationic lipid DSGLA which contains both guanidinium and lysine residues as a cationic headgroup. We substituted the DOTAP with DSGLA to form LPD nanoparticles for siRNA delivery *in vitro* and *in vivo*.

Here we report the studies of formulating EGFR siRNA in LPD prepared with DSGLA. We have shown enhanced cellular uptake of siRNA, pronounced down-regulation of the target gene, increased apoptosis of the tumor cells and improved antitumor activity of the novel formulation as compared with the formulation containing DOTAP.

2.2 MATERIALS AND METHODS

2.2.1 Materials

DOTAP and cholesterol were purchased from Avanti Polar Lipids, Inc. (Alabaster, AL). Protamine sulfate (fraction X from salmon) and calf thymus DNA (for hybridization, phenol-chloroform extracted and ethanol precipitated) were from Sigma-Aldrich (St. Louis, MO). The EGFR and control siRNA sequences are adopted from the previous studies (25). Synthetic 19-nt RNAs with 3' dTdT overhangs on both sequences were purchased from Dharmacon (Lafayette, CO). The sequence of EGFR siRNA was 5'-AACACAGTGGAGCGAATTCCT-3' and high-purity control siRNA with sequence 5'-AATTCTCCGAACGTGTCACGT-3' was also synthesized in Dharmacon. For quantitative studies, cy3 was conjugated to 5' sense sequence. 5' cy3 labeled siRNA sequence was also obtained from Dharmacon. NCI-H460 human lung cancer cells were obtained from American Type Culture Collection. Cells were maintained in RPMI-1640 medium supplemented with 10% fetal bovine serum (Invitrogen, Carlsbad, CA), 100 U/ml penicillin, and 100 μg/ml streptomycin (Invitrogen, Carlsbad, CA).

2.2.2 Experimental animals

Female athymic nude mice of age 6–8 weeks were purchased from Charles River Laboratories (Wilmington, MA). All work performed on animals was in accordance with and permitted by the University of North Carolina Institutional Animal Care and Use committee.

2.2.3 Synthesis of DSGLA

Detailed synthetic procedures, spectral and purity data delineated in another manuscript (Bathula et al., unpublished).

2.3.4 Preparation of Liposomes.

A cationic lipid and cholesterol in 1:1 mole ratio were dissolved in a mixture of chloroform in a 5 ml glass vial. The solvent was removed with a thin flow of moisture-free nitrogen gas, and the dried lipid film was then kept under high vacuum for 8 h. An amount of 5 mL of sterile deionized water was added to the vacuum-dried lipid film, and the mixture was allowed to swell overnight. The vial was then vortexed for 2-3 min at room temperature and sonicated in a bath type sonicator for 5 min followed by extrusion (Hamilton Co., Reno, NV, USA) through 400, 200 and 100 nm membrane filters and was stored at 4°C before use. The resulting clear aqueous liposomes were used in forming LPD.

2.3.5 Preparation of PEGylated LPD Formulations.

LPD were prepared as previously described with slight modifications (100). Briefly, small unilamellar liposomes consisting of DOTAP (or DSGLA) and cholesterol (1:1 molar ratio) were prepared by thin film hydration followed by membrane extrusion. The total lipid concentration of the liposome was fixed at 10 mM. LPD was composed of DOTAP (or DSGLA) /cholesterol liposome, protamine, and the mixture of siRNA and calf thymus DNA (1:1 weight ratio). To prepare LPD, 6 μL of protamine (2 mg/mL), 47 μL of deionized water, and 8 μL of a mixture of siRNA and calf thymus DNA (2 mg/mL) were mixed in a 1.5 mL tube. The complex was allowed to stand at room temperature for 10 min before the addition of 40 µL of DOTAP (or DSGLA)/cholesterol liposome (total lipid concentration = 10 mM). LPD nanoparticles were kept at room temperature for another 10 min before further

application. PEGylated LPD formulations were prepared by the postinsertion method (101, 102). Briefly, 100 μL of preformed LPD was mixed with 0.63-16 μL of DSPE-PEG or DSPE-PEG-AA (20 mg/mL) and then incubated at 50-60 ℃ for 10 min. The resulting formulations were allowed to cool to room temperature before use. The particle size of LPD and PEGylated LPD was measured by using a Coulter N4 Plus particle sizer (Beckman Coulter, San Francisco, CA). Particle sizes were reported as the mean ± standard deviation. For size exclusion chromatography, either 10 mol% NBD-cholesterol labeled liposomes containing DSGLA or DOTAP or 10 mol% DSPE-PEG_{2000}-CF labeled DSPE-PEG_{2000} was used for the preparation of the PEGylated LPD. Ten µl of the samples was loaded onto a phosphate buffered saline (PBS) pre-equilibrated Sepharose CL 2B column (1 × 10 cm). Column was eluted with PBS. The eluted fractions (200-500 µl) were collected, diluted 1:1 in ethanol and detected for fluorescence intensity with a plate reader (λex: 485 nm, λem: 535 nm) (PLATE CHAMELEON Multilabel Detection Platform, Bioscan Inc., Washington, DC).

2.3.6 Analysis of ROS in H460 cells

H460 cells (1×10^6 per well) were seeded into 12-well plates. Cells were treated with 10 µM DSGLA or DOTAP liposomes in serum containing medium at 37 ℃ for 30 min. Then cells were incubated with 20 mM 2′,7′-dichlorodihydrofluorescein diacetate (DCFH-DA) (Sigma-Aldrich) in serum containing medium for 30 min at 37 °C. Cells were quickly washed and immediately analyzed by flow cytometry.

2.3.7 Cellular Uptake and Quantification Study.

H460 cells (10^5 per well) were seeded in 12-well plates (Corning Inc., Corning, NY) 12 h before experiments. Cells were treated with different formulations at a concentration of 100 nM for cy3 labeled siRNA in serum containing medium at 37 °C for 4 h. Cells were

washed twice with PBS. Cells were fixed with 3.8% paraformaldehyde in PBS at room temperature for 10 min, mounted onto a glass slide, and imaged by a Leica SP2 confocal microscope. Cy3 positive cells were detected and quantified by flow cytometry (Becton-Dickinson, Heidelberg, Germany). Results were processed using the Cellquest software (Becton-Dickinson).

2.3.8 Assessment of Apoptosis by TUNEL Staining

TUNEL assay was conducted using a TACS^{TM} TdT Kit (R&D Systems, Minneapolis, MN). H460 cells (5×10^4 per well) were seeded into 24-well plates. Cells were treated with different formulations at a concentration of 500 nM for siRNA in serum containing medium at 37 ° C for 72 h. Cells were washed once with PBS, and then fixed in 4% buffered paraformaldehyde–PBS (pH 7.4) for 30 minutes at room temperature. Endogenous peroxidase was inactivated with 0.3% H_2O_2 methanol for 15 minutes at room temperature. The plates were then rinsed with PBS, and after processing with Permeabilization Buffer, labeling Buffer containing terminal deoxynucleotidyl transferase and fluorescein isothiocyanate–deoxyuridine 5-triphosphate was added to the plate. The plate was incubated in a humid atmosphere at 37°C for 60 minutes. The reaction was terminated by stop solution and developed with DAB according to manufacturer's instructions. Samples were imaged using a Nikon Microphot SA microscope. The number of apoptosis cells within the rectangular area of 300 cells was counted on three or four areas for each treatment.

2.3.9 Western blot analysis

Cells were lysed in lysis buffer for 20 min on ice and the soluble extract was recovered by centrifugation. Extracts were separated on a 10% acrylamide gel and transferred to a PVDF membrane. Membranes were blocked for 1 h in 5% skim milk and

then incubated for 1 h with monoclonal antibodies directed against pERK (Santa Cruz Biotechnology, Inc.) or polyclonal antibodies against EGFR (BD Transduction Labs), ERK 2 and actin (Santa Cruz Biotechnology, Inc.) for standardization. Membranes were washed in PBST (PBS, 0.1% Tween-20) and then incubated for 1 h with appropriate secondary antibodies. Membranes were again washed and then developed by an enhanced chemiluminescence system according to the manufacturer's instructions (PerkinElmer).

For in vitro p-ERK inhibition study, H460 cells were seeded in 12-well plates (1×10^5 per well) for 24 h. Cells were treated with different lipids at the concentration of 10μM and were collected after 1 h, 24 h and 48 h for measuring p-ERK expression. For *in vitro* EGFR gene silencing study, H460 cells were seeded in 6-well plates (2×10^5 per well) for 24 h. Cells were treated with siRNA-containing different formulations (250 nM siRNA) and were collected after 72 h for measuring EGFR protein expression. For *in vivo* EGFR gene silencing and pERK inhibition study, tumor-bearing mice were given IV injections of siRNA with different formulations at the dose of 0.6 mg siRNA/kg. One day after the third injection, the mice were killed and the tumors were collected for western blot analysis.

2.3.10 Immunofluorescence microscopy

H460 cells were washed, fixed with methanol/acetone (1:1), and permeabilized with triton X100 (1%). Cells were incubated with rabbit polyclonal anti-Apoptosis-Inducing-Factor (AIF) (Santa Cruz Biotechnology, Inc.) (1:100) for 1 h. After washed with PBS, the fluorescently labeled secondary antibody was added and incubated for 1 h. Nuclei were counterstained with Vectashield® mounting solution (Vector Laboratories, Inc., Burlingame, CA) containing DAPI.

2.3.11 Tissue distribution and siRNA uptake

Mice with tumor size around 1 cm^2 were intravenously injected with cy3 labeled siRNA in different formulations (1.2 mg/kg or 1.8 nmole siRNA per injection). Four hours later, mice were killed and tissues were collected, fixed in 10% formalin and embedded in paraffin. Tissues were sectioned (7 μm thick) and imaged using a Leica SP2 confocal microscope.

2.3.12 Tumor growth inhibition study.

H460 xenograft tumor-bearing mice (size 9–16 mm^2) were intravenously injected with siRNA-containing formulations at the dose of 0.6 mg/kg (one injection per day for 3 days). Tumor growth in the treated mice was monitored after treatment.

2.3.13 Statistical analysis.

All statistical analyses were performed by student *t*-test. Data were considered statistically significant when *p* value was less than 0.05.

2.4 RESULTS

2.4.1 Preparation and characterization of the nanoparticle - containing the novel cationic lipid

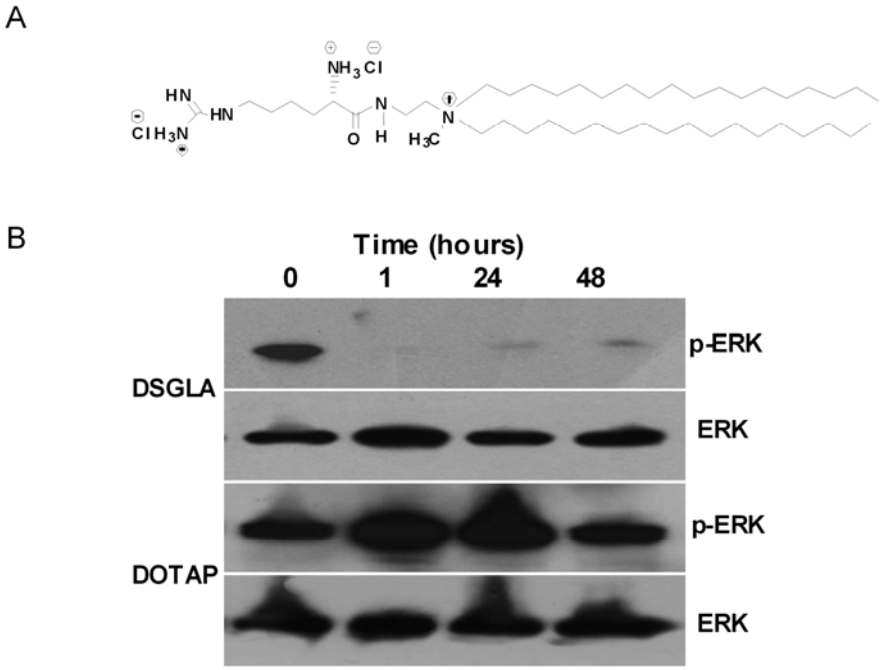

Figure 2.1 The structure of DSGLA and pERK inhibition induced by lipids. (A) The structure of DSGLA. (B) pERK and ERK expression in H460 cells after incubation with 10 μM DSGLA and DOTAP for various times.

We have developed a LPD nanoparticle formulation which is targeted with AA and contains the cationic lipid DOTAP to specifically deliver siRNA to H460 human lung carcinoma cells which express the sigma receptor. Our novel non-glycerol based cationic lipid (DSGLA) (**Fig. 2.1A**) could be readily used to formulate siRNA in LPD-PEG or LPD-

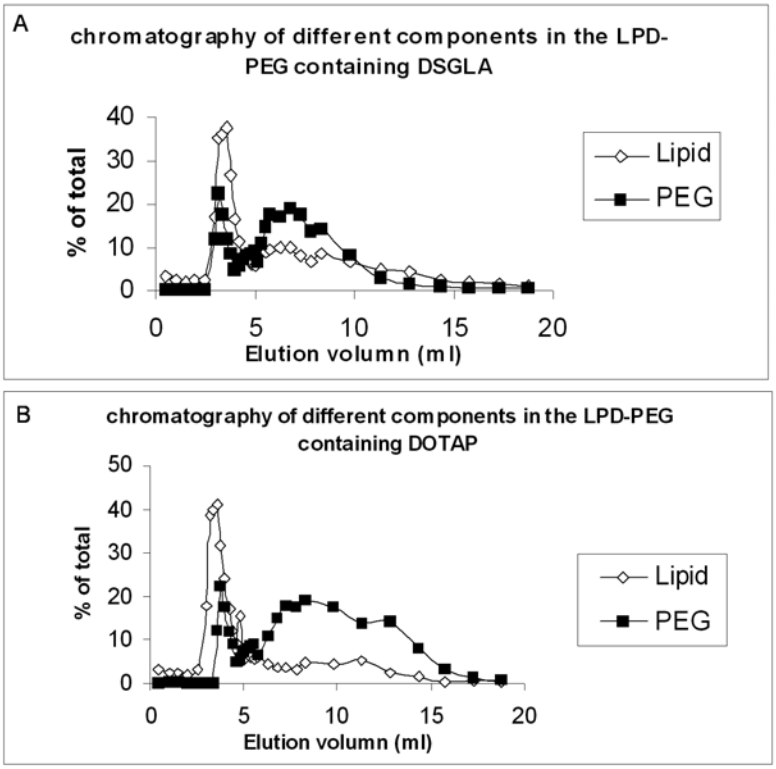

Figure 2.2 Sepharose CL 2B size exclusion chromatography of different nanoparticle samples. Separation of different components in the PEGylated LPD containing DSGLA (A) or DOTAP (B) is shown. Lipid was labeled with NBD-cholesterol. DSPE-PEG was labeled with DSPE-PEG-carboxyfluorescein. Ten µl of the samples was loaded onto a PBS pre-equilibrated Sepharose CL 2B column (1 × 10 cm). Column was eluted with PBS.

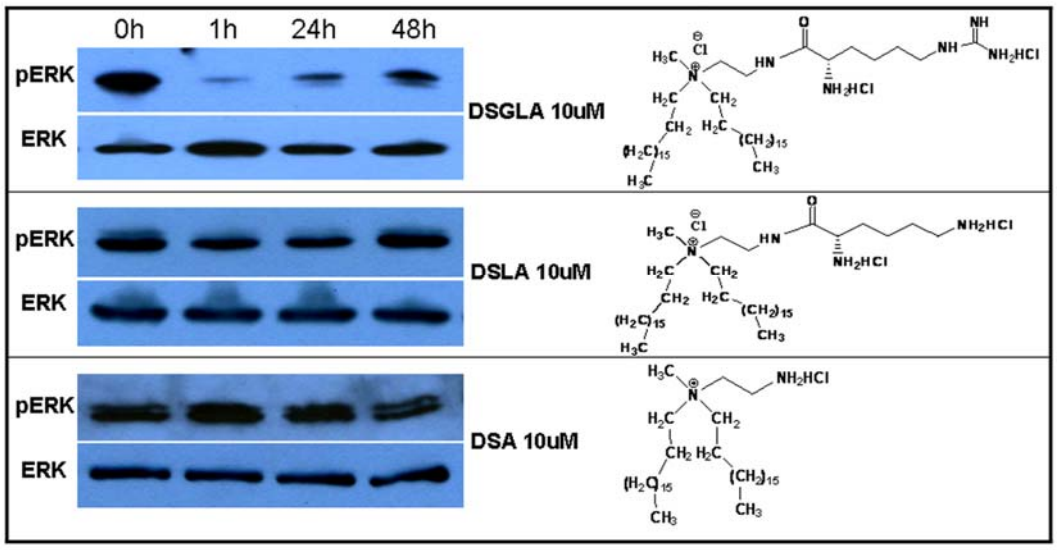

Figure 2.3 pERK and ERK expression in H460 cells after incubation with 10 μM DSGLA, DSLA (analog of DSGLA without the guanidinium group) and DSA (analog of DSGLA without the lysine and the guanidine residues) for various times.

PEG-AA nanoparticles, similar to the original DOTAP lipid. The particle size of the nanoparticles is around 100 nm and the zeta potential is 25 mV. To further characterize the new formulation, we used 10 mol% NBD-cholesterol labeled liposomes or 10 mol% DSPE-PEG_{2000}-carboxyfluorescein (DSPE-PEG_{2000}-CF) labeled DSPE-PEG_{2000} to make PEGylated LPD and the final formulation was separated by using a Sepharose CL 2B column. As shown in **figure 2.2**, two major particle populations were observed in the DSPE-PEG_{2000}-CF or NBD-cholesterol labeled LPD. **Figure 2.2** indicates that the nanoparticles containing DOTAP eluted in the first peak was composed of 47.3 % of total lipids and 23.4 % of the input DSPE-PEG_{2000}. The nanoparticles containing DSGLA eluted in the first peak was composed of 40.6 % of total lipids and 21.2 % of the input DSPE-PEG_{2000}. Based on our calculation, 11.4 mol% of the outer leaflet of the lipid bilayer containing DSGLA was modified with DSPE-PEG_{2000} and 10.8 mol% of the one containing DSGLA was modified with DSPE-PEG_{2000}. The ratio of PEGylation to LPD containing DOTAP was similar to

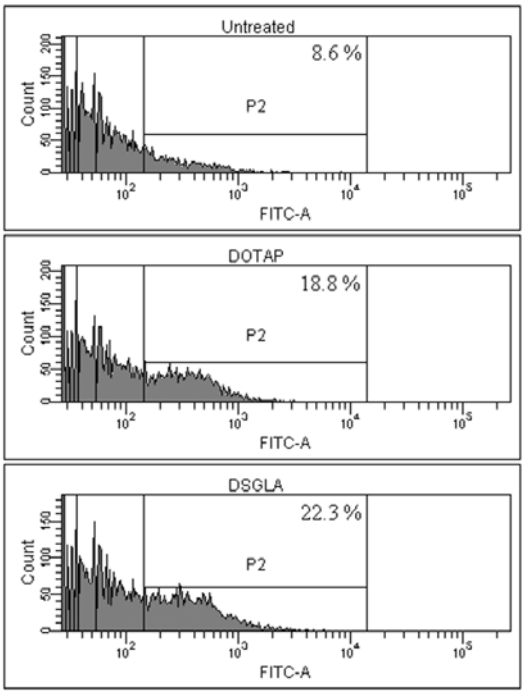

Figure 2.4 ROS generation by DSGLA or DOTAP in H460 cells. Cells were incubated with 20 mM DCFH-DA after treatment of different lipids to evaluate ROS induction. The ROS content of cells was analyzed by flow cytometry.

those containing DSGLA. The particle size and zeta potential of the PEGylated LPD containing either DSGLA or DOTAP collected from the first peak was around 160 nm and 3 mV, respectively.

2.4.2 Inhibition of ERK1/2 activation by novel lipid treatment

We first studied the activation of ERK in the H460 cells. The phosphorylation of ERK is often associated with the anti-apoptosis phenotype (103, 104). H460 cells were treated with DOTAP or DSGLA liposomes for different time periods, and ERK 1/2 phosphorylation which leads to the activation of the MAP kinase activity was measured by western blot analysis. As shown in **Fig. 2.1B**, 10μM DSGLA could decrease ERK1/2 activation. Total ERK1/2 expression remained unperturbed under all conditions. The lipids without guanidine group did not cause the inhibition of ERK1/2 activation (**Fig. 2.3**).

However, DOTAP increased ERK1/2 activation, an effect which is consistent with our previous findings (99). Besides, we also found that DSGLA could more efficiently induce reactive oxygen species (ROS) in H460 cells than DOTAP (**Fig. 2.4**). Interestingly, there was no statistically significant difference between the cytotoxicity of DSGLA and DOTAP based

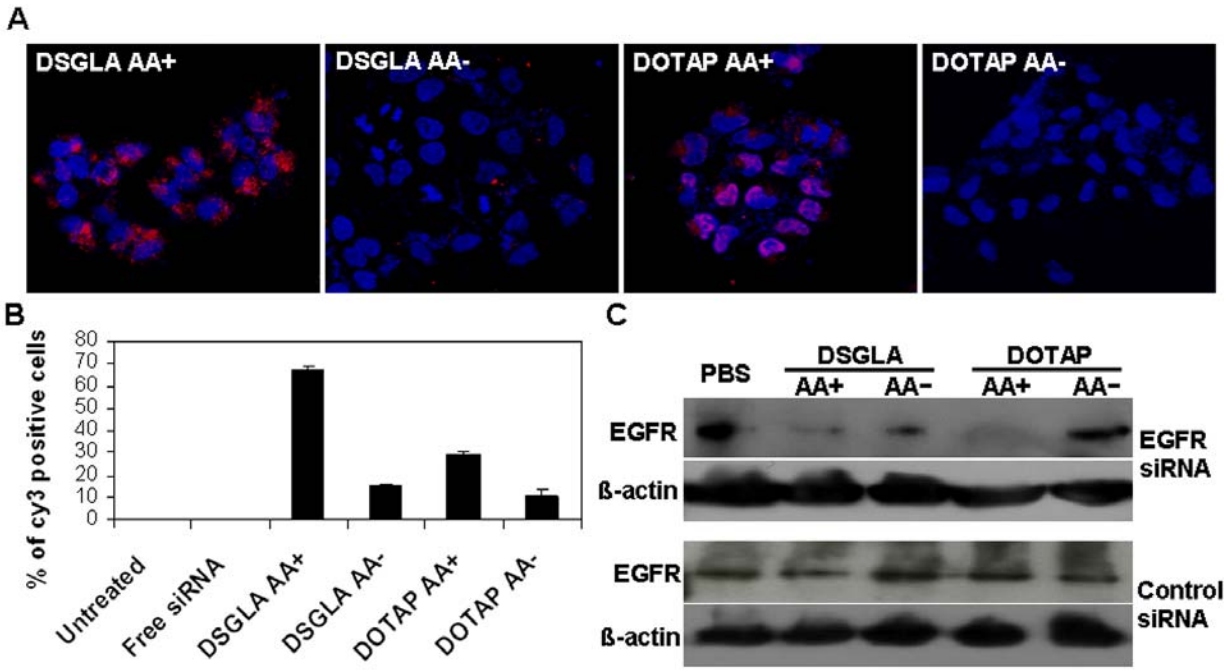

Figure 2.5 Cellular uptake of siRNA and EGFR expression inhibited by siRNA formulation in H460 cells *in vitro*. Fluorescence photographs of cultured H460 cells after treatment with sense strand 5'-cy3 labeled siRNA against an irrelevant target in LPD-PEG or LPD-PEG-AA with DSGLA or DOTAP as the cationic lipid for 4 h (A). Quantitative measurement of mean fluorescence intensity (MFI) of cy3 siRNA uptake by flow cytometry. Data = mean ± SD, n = 3 (B). (C) Western blot analysis of EGFR and β-actin in H460 cells treated with LPD-PEG with formulations containing anisamide ligand (AA+) or without (AA-). Formulations were prepared with either DOTAP or DSGLA.

A

on MTT assays and flow cytometry with propidium iodide (PI) staining (Bathula et al., unpublished). DSGLA alone is as safe as DOTAP. These observations suggest that inhibition of the ERK pathway by DSGLA may not induce cell death but can present a synergistic pro-apoptosis effect when combined with other treatment.

2.4.3 cellular uptake of siRNA *in vitro*

To achieve targeted delivery of siRNA in cancer gene therapy, we post-inserted PEGylated lipids onto our LPD formulation to increase the serum stability (98). In addition, we also tethered anisamide, a compound specifically binding to the sigma receptor, to the distal end of PEG as a targeting ligand (105). As shown in **Fig. 2.5A**, confocal microscopy

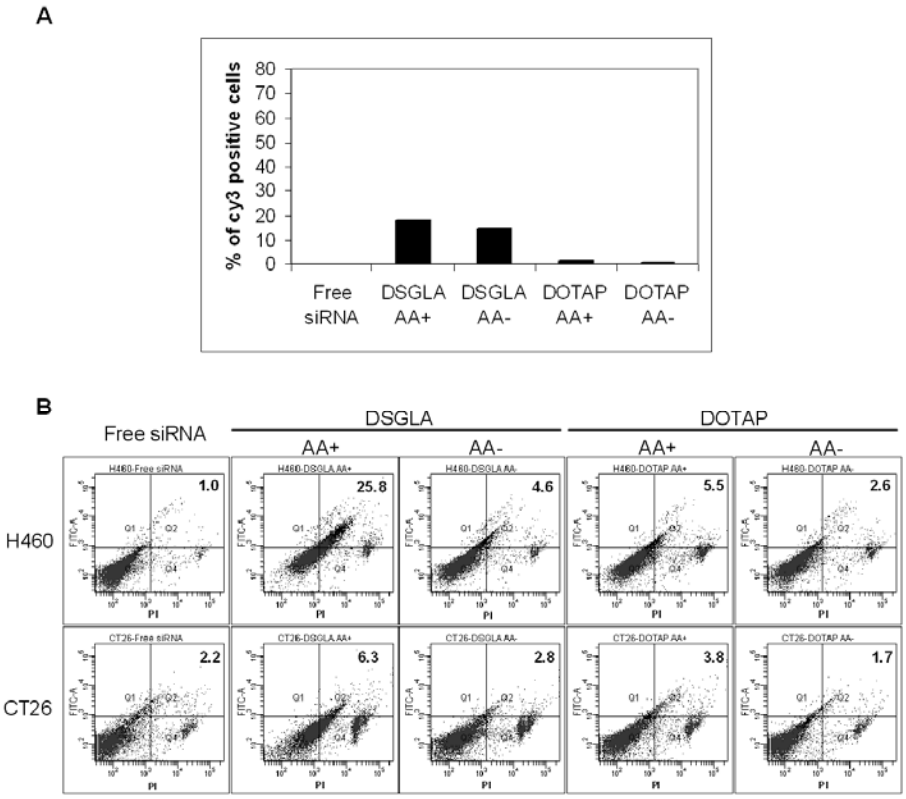

Figure 2.6 Intracellular uptake of siRNA and synergistic apoptosis induction in sigma receptor-positive H460 cells and in receptor-negative CT26 cells *in vitro*. (A), cells were treated with different formulations containing cy3-labeled siRNA for 4 h and analyzed for fluorescence by flow cytometry. (B), cells were treated with different formulations (250 nM siRNA) for 3 days and were then stained with annexin V-FITC (Y axis) and PI (X axis), and analyzed by flow cytometry. Both are apoptosis markers.

showed that the uptake to the cellular cytoplasm of H460 cells, which express sigma receptor (Li et al, 2008), of the fluorescently labeled siRNA formulated with LPD prepared with DSGLA was much greater than that prepared with DOTAP. Furthermore, for both lipids, the fluorescence signal in the cells treated with LPD-PEG-AA was much stronger than that of

cells treated with LPD-PEG. Quantitatively (**Fig. 2.5B**), the fluorescently labelled siRNA uptake by LPD-PEG-AA containing DSGLA was about two-fold higher than that of LPD-PEG-AA containing DOTAP as measured by flow cytometry. **Fig. 2.5B** also showed that ligand conjugation increased the delivery efficiency of PEGylated LPD prepared with DSGLA by 3-fold. Thus, the results indicate that the LPD-PEG-AA prepared with DSGLA could efficiently deliver siRNA to the tumor cells and the delivery was highly ligand dependent. The targeted LPD (AA+) did not show different siRNA uptake compared to non-targeted LPD (AA-) in the sigma receptor negative cell line CT26 (**Fig. 2.6**), suggesting that the cellular uptake of siRNA is related to sigma receptor expression.

2.4.4 Inhibition of EGFR expression in H460 cells

To further demonstrate the biological activity of the nanoparticle formulation, siRNA against EGFR was delivered by LPD formulations containing either DSGLA or DOTAP. The siRNA silencing effect on EGFR levels was determined by western blot analysis. We compared different formulations in the presence or the absence of AA targeting ligand. Free anti-EGFR siRNA had little effect due to the poor cellular uptake of this negatively charged oligonucleotide (data not shown). Cultured H460 cells were treated with anti-EGFR siRNA-containing LPD-PEG-AA prepared with DSGLA or DOTAP, and EGFR protein expression was measured after 72 h (**Fig. 2.5C**). LPD-PEG-AA formulations with either DSGLA or DOTAP knocked down EGFR expression with H460 cells in approximately equal efficiency. However, anti-EGFR siRNA in LPD-PEG (AA-) prepared with either DSGLA or DOTAP could only slightly down-regulate EGFR (**Fig. 2.5C**). Control siRNA did not show any silencing activity with any formulations. The data indicates that the siRNA could effectively suppress EGFR expression and the silencing activity was formulation dependent.

2.4.5 Synergistic apoptosis induction *in vitro*

The effect of the combination of anti-EGFR siRNA and DSGLA on cancer cell killing effect was further studied. To determine whether depletion of EGFR could promote tumor cell death, TUNEL assays were performed at 72 h after treatment with either anti-

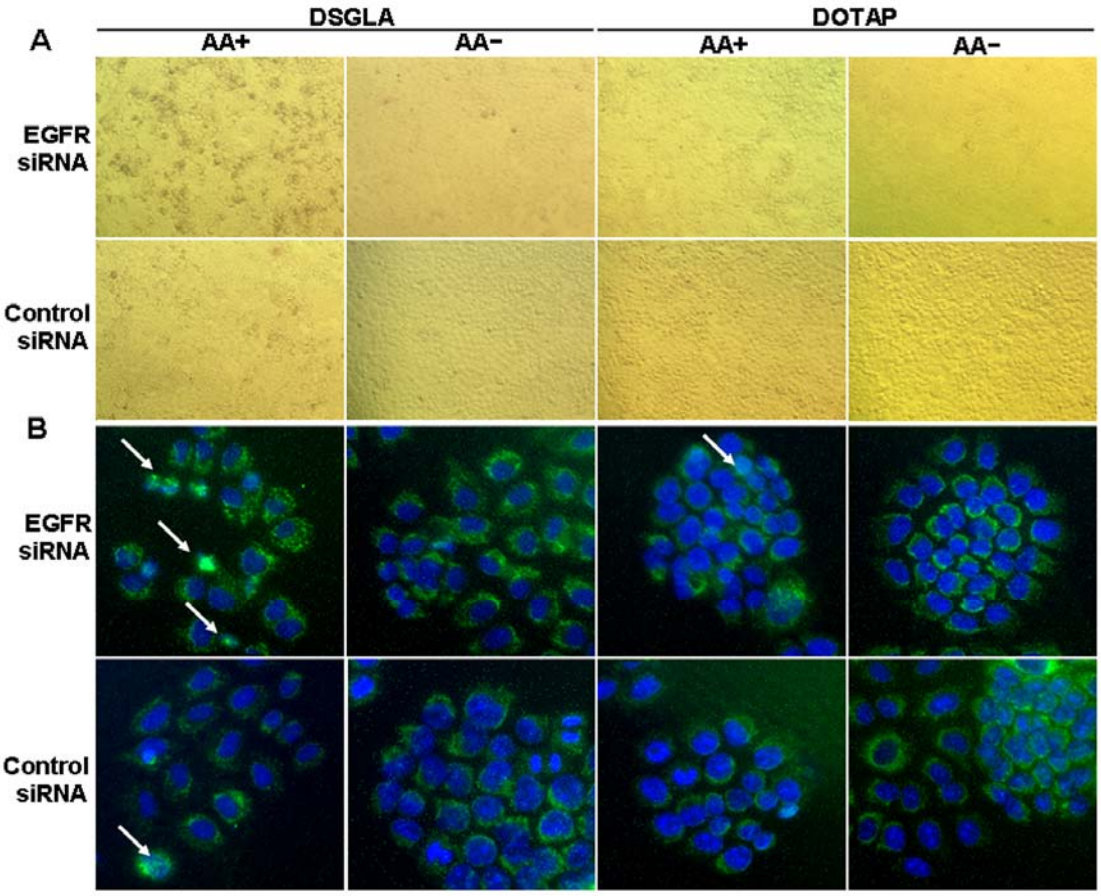

Figure 2.7 Apoptosis induced by siRNA formulation *in vitro*. Cells treated with different formulations for 72 h and analyzed for TUNEL staining (A), or AIF distribution (B). Cells with nuclear AIF are shown by arrows. Formulations contained anisamide ligand (AA+) or without (AA-). Formulations were prepared with either DOTAP or DSGLA.

EGFR or control siRNA formulations. **Fig. 2.7A** indicates that about 15 ± 3 % of H460 cells treated with EGFR siRNA-containing LPD-PEG-AA prepared with DSGLA underwent apoptosis. This value was higher than the ones treated with EGFR siRNA-containing LPD-

PEG prepared with DSGLA, EGFR siRNA-containing LPD-PEG-AA prepared with DOTAP, or control siRNA-containing LPD-PEG-AA prepared with DSGLA (**Fig. 2.7A**). It was also observed that about 4 ± 1 % of H460 cells treated with EGFR siRNA-containing LPD-PEG-AA prepared with DOTAP underwent apoptosis, compared to less than 1% in the control siRNA and EGFR siRNA-containing LPD-PEG (**Fig. 2.7A**). In addition, about 2.5 % of H460 cells treated with control siRNA-containing LPD-PEG-AA prepared with DSGLA underwent apoptosis as opposed to less than 1% in the control siRNA-containing LPD-PEG (**Fig. 2.7A**). Thus, the data indicate that cytotoxic effect mediated by LPD nanoparticles was siRNA sequence specific, targeting ligands specific and formulation lipid dependent. Thus, a synergistic effect between siRNA against EGFR and DSGLA, but not DOTAP, in promoting cellular apoptosis was observed and the synergy was well controlled by AA.

Redistribution of cytochrome C and apoptosis inducing factor (AIF) is an early event in the cellular apoptotic process (106, 107). To further evaluate the enhancement of H460 lung cancer cell death by the combination of EGFR siRNA and DSGLA, we examined the involvement of AIF by immunofluorescence microscopy (**Fig. 2.7B**). Immunofluorescence detection of AIF in untreated control cells normally yields a punctate cytoplasmic staining pattern with some preference for the perinuclear area as a typical pattern for mitochondrial localization (108-110). Cells treated with EGFR siRNA-containing LPD-PEG-AA that were prepared with DSGLA showed an increased translocation of AIF from the cytoplasm into the nucleus (**Fig. 2.7B**). No significant translocation was observed in other treatment groups. The results indicate that combined treatment with EGFR siRNA formulated with DSGLA interacted synergistically to promote cell death in H460, and that the synergistic effect was controlled by the targeting ligands.

To confirm that the selective synergistic cellular killing effect of the targeted nanoparticles, H460 cells were stained with annexin V-FITC and PI and analyzed by flow

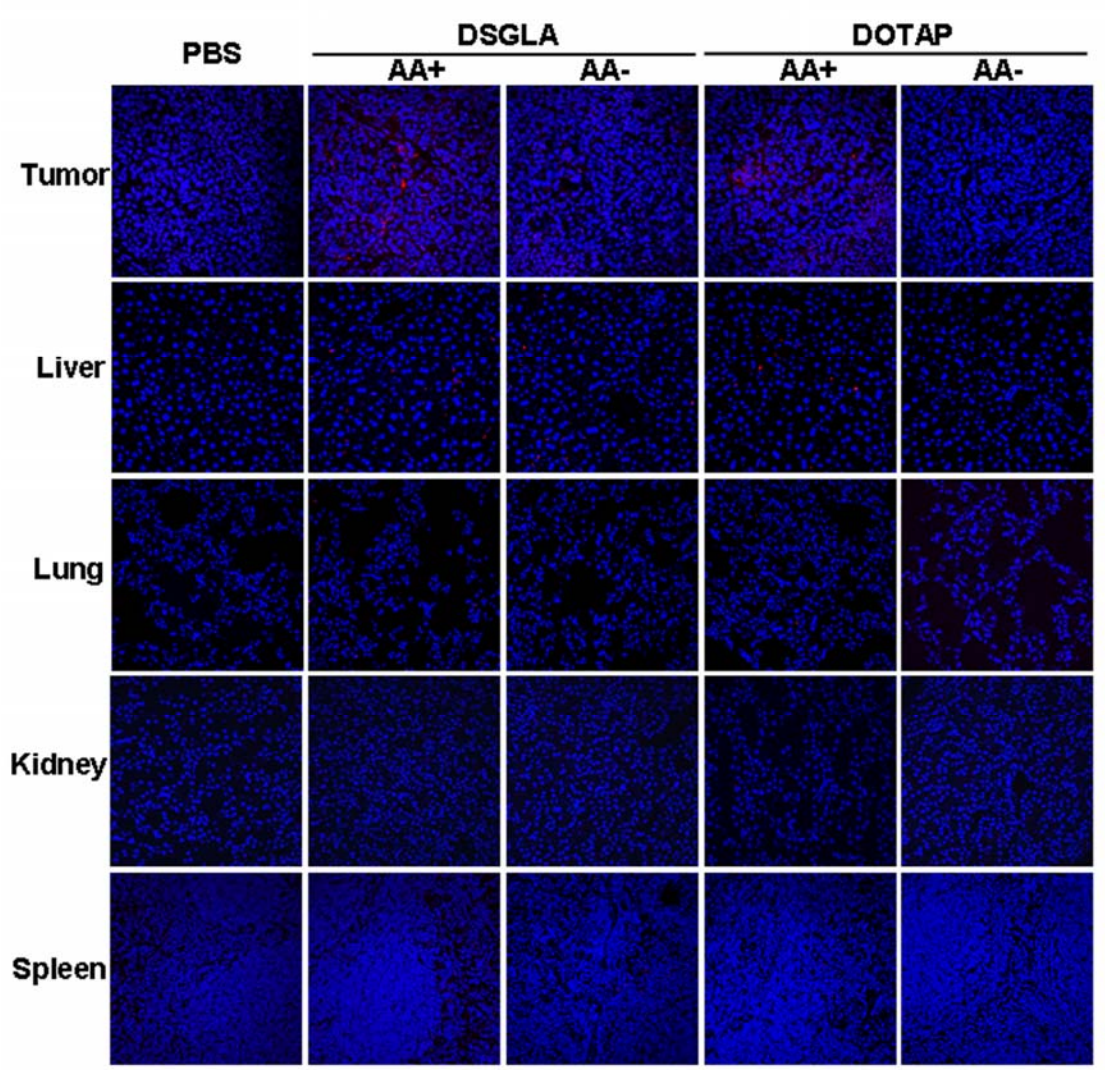

Figure 2.8 Tissue distribution and cellular uptake of siRNA in different formulations. Fluorescence signal of cy3 labeled siRNA in different tissues observed by confocal microscopy.

cytometry for apoptosis. As shown in **Fig. 2.6**, a ligand and lipid-dependent induction of apoptosis was observed. It indicates that about 25 % of H460 cells treated with EGFR siRNA-containing LPD-PEG-AA prepared with DSGLA underwent apoptosis. The sigma receptor negative CT26 cells were also assessed by an annexin V-FITC and PI binding assay. As shown in **Fig. 2.6**, the treatment of EGFR siRNA-containing LPD-PEG-AA prepared

with DSGLA induces a low level of apoptosis (6.3 %) in CT26 cells compared with the similar rate of apoptosis induced by other formulations. It indicates that the synergistic cellular killing effect of DSGLA AA+ containing EGFR siRNA is sigma receptor specific.

2.4.6 Tissue distribution and intracellular uptake of siRNA

We further studied the cy3-siRNA distribution and bioavailability in major tissues in

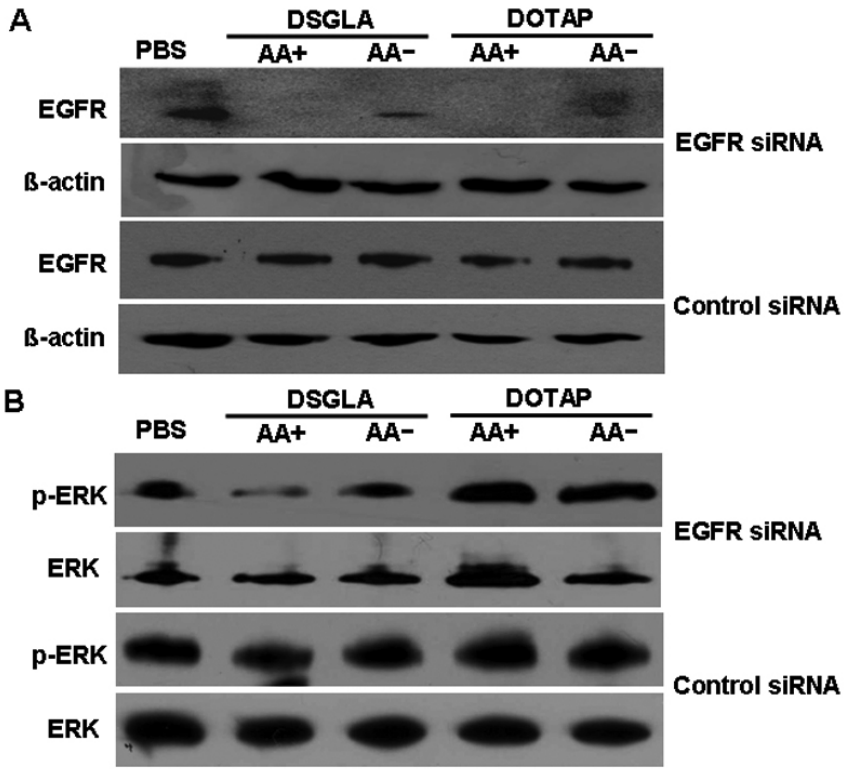

Figure 2.9 EGFR and p-ERK expression in H460 xenograft tumor. Western blot analysis of EGFR (A) and p-ERK (B) in the H460 xenograft tumor after treatment with different formulations.

the H460 xenograft model 4 hours after intravenous (i.v.) injections using confocal microscopy. As shown in **Fig. 2.8**, the intracellular fluorescence signals were hardly detected in the tumor tissues collected from the mice treated with LPD-PEG prepared with DSGLA and DOTAP. The LPD-PEG-AA prepared with DSGLA or DOTAP showed strong cytosolic delivery of cy3 siRNA in the tumor tissue, while other tissues showed lower uptake of siRNA. The distribution of cy3 siRNA in the tumor was heterogeneous. These results

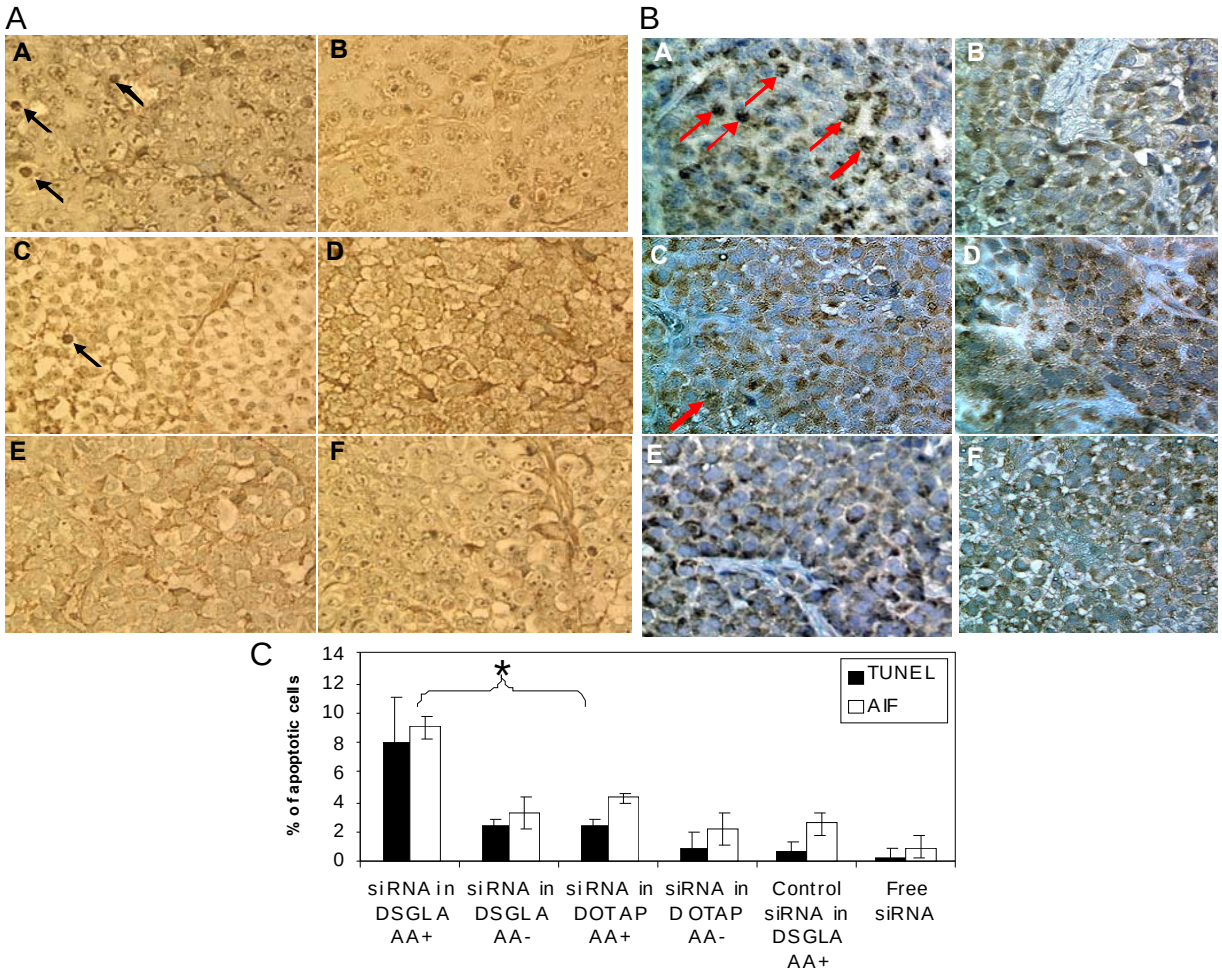

Figure 2.10 Synergistic apoptosis induction in H460 xenograft tumor. TUNEL staining (positive cells indicated by dark arrows) (A) and AIF expression and localization (cells with nuclear AIF indicated by red arrows) (B) in H460 tumor cells after treated with EGFR siRNA with different formulations *in vivo*. (C) Quantitative analysis of TUNEL positive staining and nuclear translocation of AIF in the tumors treated with different formulations. a, EGFR siRNA in DSGLA AA+; b, EGFR siRNA in DSGLA AA-; c, EGFR siRNA in DOTAP AA+; d, EGFR siRNA in DOTAP AA-; e, Control siRNA in DSGLA AA+; f, Free siRNA. Data = mean ± SD, n = 3-4. *indicates $P < 0.05$.

indicate that the LPD-PEG-AA prepared with the novel DSGLA can efficiently deliver siRNA to the tumor tissue and that the intracellular delivery is highly ligand dependent.

2.4.7 EGFR gene silencing, inhibition of ERK1/2 activation and apoptosis induction

To examine the biological activities of siRNA *in vivo*, EGFR levels in the xenograft tumor were detected by western blotting (**Fig. 2.9A**). EGFR in H460 tumor was silenced by EGFR siRNA in LPD-PEG-AA prepared with DSGLA and DOTAP. The EGFR siRNA-

containing LPD-PEG prepared with DSGLA and DOTAP showed only a partial effect, whereas the control siRNA showed no effect. The inhibition of ERK1/2 activation was only observed with LPD-PEG-AA prepared using DSGLA (**Fig. 2.9B**). We also stained for apoptotic markers in the H460 tumor (**Fig. 2.10**). **Fig. 2.10C** indicates that about 8 % of H460 cells treated with EGFR siRNA-containing LPD-PEG-AA prepared with DSGLA underwent apoptosis detected by TUNEL staining. This value was higher than that of tumors treated with EGFR siRNA-containing LPD-PEG prepared with DSGLA, EGFR siRNA-

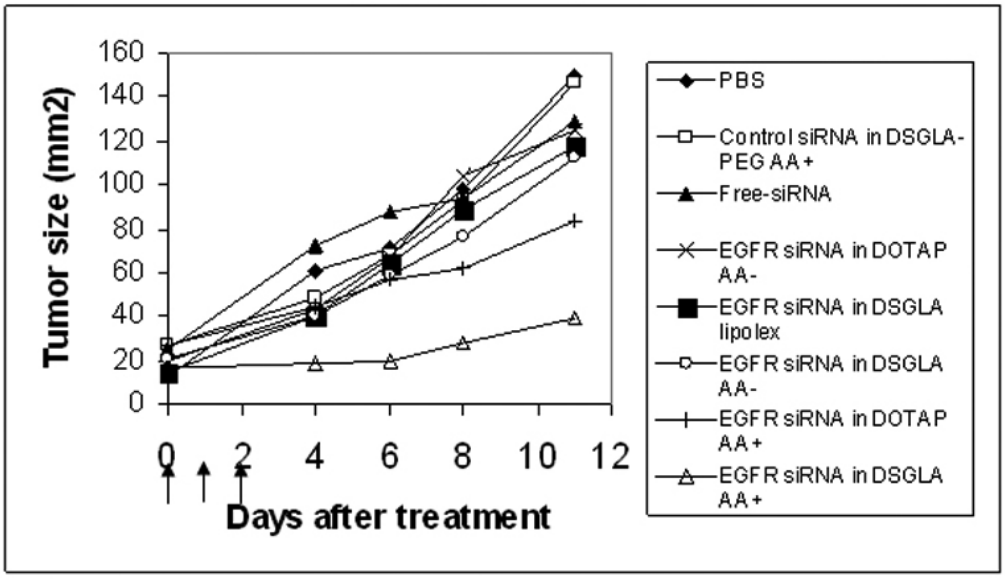

Figure 2.11 H460 xenograft tumor growth inhibition by siRNA in different formulations. Solid arrows indicate the intravenous administrations of siRNA (0.6 mg/kg). Data = mean, *n* = 5–7. SD of the data points is not shown for clarity.

containing LPD-PEG-AA prepared with DOTAP, or control siRNA-containing LPD-PEG-AA prepared with DSGLA (**Figs. 2.10A and 2.10C**). To further evaluate the enhancement of killing effect in the H460 tumor by the combination of EGFR siRNA and DSGLA, we examined the involvement of AIF in cellular apoptosis (**Fig. 2.10B**). Cells treated with EGFR siRNA-containing LPD-PEG-AA prepared with DSGLA showed an increased translocation of AIF from the cytoplasm into the nucleus (**Figs. 2.10B and 2.10C**). No significant

translocation was observed in other treatment groups. The results indicate that combined treatment with EGFR siRNA formulated with DSGLA interacted synergistically to promote cell death in the H460 tumor and that the synergy effect was ligand dependent.

2.4.8 Tumor growth inhibition

Three injections of EGFR siRNA in LPD-PEG-AA containing DOTAP showed a partial inhibition of tumor growth ($P < 0.01$ on day 11) similar to that of siRNA in LPD-PEG containing DSGLA (on day 8) (**Fig. 2.11**). A significant improvement in tumor growth inhibition was observed when treated with combination of siRNA and DSGLA (LPD-PEG-AA containing DSGLA) ($P < 0.001$ on day 6). Other control treatments had no or much lower therapeutic effects.

2.5 DISCUSSION

In this study, our objective was to develop a novel cationic lipid that could avoid the possible anti-apoptotic effect of DOTAP, yet could still deliver siRNA with high efficiency. We have synthesized a lysine based cationic lipid containing a guanidine group and tested its ability to form LPD. Our studies demonstrate that siRNA formulated in LPD prepared with DSGLA showed enhanced cellular uptake, gene silencing activity and synergistic therapeutic activity with EGFR siRNA in H460 tumor cells *in vitro* and *in vivo*. This synergistic therapeutic effect is AA ligand dependent which is targeted to the sigma receptor over-expressed in many human cancer cells (111, 112).

The strategy that we used to achieve tumor targeted delivery is based on the enhanced permeability and retention (EPR) effect (113, 114). Although the normal cells also express the sigma receptor (115), they are not accessible by the blood borne nanoparticles. Sigma

receptor-targeting ligands such as AA play the major role to increase the intracellular uptake of the nanoparticles but do not enhance tumor localization (116).

Obata et al. reported that cationic lipids bearing lysine or arginine as a cationic headgroup showed higher plasmid transfection efficacy and are more serum compatible than Lipofectamine 2000 (92). In our studies, we have demonstrated that DSGLA containing LPD showed higher cellular uptake of siRNA in H460 cells *in vitro* than DOTAP, although the enhanced siRNA uptake was not observed *in vivo*. We suggest that the enhanced siRNA uptake may be related to the guanidine containing headgroup and this hypothesis will be further evaluated. DSGLA also showed its own biological activity to down-regulate pERK (**Fig. 2.1B**) but the lipids without guanidine group did not cause this effect (**Fig. 2.3**). Clearly, the guanidine group plays an important role in determining the biological characteristics of the lipids.

We have found that DSGLA promoted apoptosis induced by EGFR siRNA synergistically. The mechanisms for promoting apoptosis of H460 cells induced by DSGLA could be complicated. A guanidine group, which easily accepts an electron, may generate a superoxide forming a hydroxyl radical (117). We also found that DSGLA can more efficiently induce reactive oxygen species (ROS) in H460 cells than DOTAP (**Fig. 2.4**) (118). It may involve different pathways in cancer cell killing. For example, in this study, inhibition of p-ERK, essential for cell survival, could be just one of the mechanisms (119). ROS mediates apoptosis in many different cell types. It plays an important role as a second messenger in many signaling pathways such as Akt, TNF and MAPK pathways (120). It also regulates the expression or stability of pro- or anti- apoptosis protein such as Bcl-2, the key enzyme suppressing apoptosis (121). ROS may also cause membrane and DNA damage,

which enhances poly(ADP-ribose) polymerase-1 (PARP-1) activation and triggers AIF translocation from mitochondria to the nucleus (122, 123). The extent of the ROS regulation of signaling pathways is not fully understood. We will study further to understand the network of signaling pathways influenced by DSGLA. The information may provide new therapeutic targets for cancer therapy.

Cancer cells develop multiple mechanisms to ensure proliferation, metastasis and survival (124, 125). Inhibiting a resistance or survival pathway is often an effective way to enhance the toxicity of a chemotherapeutic drug (126, 127). It is often necessary to target multiple pathways to efficiently reduce the growth of cancer cells (128). For this purpose, we studied the effect of combined treatment of human lung cancer cells with siRNA targeting EGFR and DSGLA.

Our data (**Figs. 2.10**) indicate that DSGLA significantly enhanced the killing effect of EGFR silencing in a formulation dependent manner both *in vitro* and *in vivo,* although the lipid itself is not cytotoxic (Bathula et al., unpublished). The synergistic pERK inactivation of EGFR siRNA delivered by LPD-PEG-AA containing DSGLA was demonstrated in a xenograft model of H460 cells (**Fig. 2.9**). However, DSGLA without the cooperation of EGFR siRNA (control siRNA delivered by LPD-PEG-AA containing DSGLA) or EGFR siRNA without the cooperation of DSGLA (EGFR siRNA delivered by LPD-PEG-AA containing DOTAP) did not show pERK inactivation (**Fig. 2.9B**). EGFR promotes cell proliferation by both the Raf/MEK/ERK and the PI3K/PDK1/Akt pathways (129). Thus, inhibition of pathways other than Raf/MEK/ERK, which is already effectively inhibited by DSGLA, by EGFR siRNA should bring enhanced apoptosis in cells treated with both agents

(**Fig. 2.10**). The synergistic therapeutic effect of LPD-PEG-AA containing DSGLA was also demonstrated in a xenograft model of H460 cells (**Fig. 2.11**).

In conclusion, we have described a target specific nanoparticle formulation that contains both siRNA and DSGLA, a new cationic lipid, and plays both roles of a delivery component and a therapeutic agent. As far as we know, this is the first demonstration of such approach and it may serve as a safe and effective anti-cancer drug.

3.0 TARGETED NANOPARTICLES DELIVER SIRNA TO MURINE MELANOMA

Melanoma is a severe skin cancer often leading to deaths. To examine the potential of siRNA therapy for melanoma, we have developed anisamide-targeted nanoparticles that can systemically deliver siRNA into the cytoplasm of B16F10 murine melanoma cells which express the sigma receptor. A c-myc siRNA delivered by the targeted nanoparticles effectively suppressed c-myc expression in the tumor and partially inhibited tumor growth. More significant tumor growth inhibition was observed with nanoparticles composed of DSAA, a guanidinium containing cationic lipid, than with a commonly used cationic lipid, DOTAP. Three daily injections of c-myc siRNA (1.2 mg/kg) formulated in the targeted nanoparticles containing DSAA could impair tumor growth, and the ED_{50} of c-myc siRNA was about 0.55 mg/kg. The targeted DSAA nanoparticles containing c-myc siRNA sensitized B16F10 cells to paclitaxel (Taxol®), resulting in a complete inhibition of tumor growth for 1 week. The enhanced anti-melanoma activity is probably related to the fact that DSAA, but not DOTAP, induced reactive oxygen species, triggered apoptosis and down-regulated anti-apoptotic protein Bcl-2 in B16F10 melanoma cells. Thus, the targeted nanoparticles containing c-myc siRNA may serve as an effective therapeutic agent for melanoma.

3.1 INTRODUCTION

Melanoma is the most serious type of skin cancer in the world, accounting for about 80% of deaths. Most patients develop metastasis with the five-year survival rate being only

14% (130). Currently, improved therapeutic options such as chemotherapy and immunotherapy are increasing but the therapeutic outcome is still limited due to the resistance of melanoma cells to these agents (131-133). Most therapeutic agents trigger anti-cancer effects by induction of apoptosis or generation of ROS (reactive oxygen species) (133, 134). However, the best response rate produced by a single-agent chemotherapy or biochemotherapy for melanoma is only 16% (132, 135). There is still plenty of room for improvement in the treatment strategy (136).

Over-expression of c-myc has been found in more than half of human cancers (137). Over two thousand myc-responsive genes have been identified. They are involved in cell cycle control, proliferation, cell death, cell adhesion, biosynthesis of ribosomal and transfer RNAs, protein synthesis and metabolism (138). In melanoma, c-myc expression is essential for nucleotide metabolism and proliferation of tumor cells (139). Over-expression of c-myc during progression of melanoma continuously suppresses oncogene-induced senescence in the cells (140). In this study, we explored the possibility of siRNA against c-myc as a therapy for subcutaneous malignant melanoma in a syngeneic murine model (40, 141).

siRNA therapy is a novel strategy for effective cancer treatment with reduced toxicity commonly found with conventional cytotoxic drugs (142). Combination therapy using siRNA and one or more chemotherapy drugs may be beneficial in decreasing the required dose of the drug and improving the therapeutic effect. Down-regulation of the epithelial growth factor receptor sensitizes small cell lung carcinoma to cisplatin, resulting in a significantly improved growth inhibition (25). siRNA against SLUG, which is required for melanoma cell survival and metastasis progression, enhances the efficacy of cisplatin and fotemustine (143). Similarly, a combination of siRNAs against MDM2, c-myc and VEGF

showed a synergistic tumor growth inhibition effect in the B16-F10 melanoma lung metastasis model (40).

To increase the stability of siRNA in the blood and promote selective uptake of siRNA into the tumor cells, we have developed targeted LPD nanoparticles containing cationic liposomes which are efficient in delivering siRNA to several different solid tumors in mouse models (25, 40). Here we show that a nanoparticle formulation targeted with anisamide, which binds with the sigma 1 receptor of the melanoma cells, is effective in delivering siRNA to B16F10 melanoma in a murine syngeneic model. Furthermore, a cationic lipid DSAA, which contains an arginine residue as the head group, was particularly suitable as a formulation lipid. Our study indicates that c-myc siRNA, delivered by DSAA-containing nanoparticles, may affect different signaling pathways and sensitize the melanoma cells to chemotherapeutic agents such as paclitaxel. The nanoparticle formulation showed minimal immunotoxicity in normal mice.

3.2 MATERIALS AND METHODS

3.2.1 Materials

DOTAP (1,2-dioleoyl-3-trimethylammonium-propane) and cholesterol were purchased from Avanti Polar Lipids, Inc. (Alabaster, AL). Protamine sulfate and calf thymus DNA were from Sigma-Aldrich (St. Louis, MO). Paclitaxel (Taxol.®.) was purchased from Bristol-Myers Squibb Company. Synthetic 19-nt RNAs with 3' dTdT overhangs on both sequences were purchased from Dharmacon (Lafayette, CO). For quantitative studies, cy3 was conjugated to 5' sense sequence. 5'-cy3 labeled siRNA sequence was also obtained from Dharmacon. The sequence of mouse c-myc siRNA was 5'-GAACAUCAUCAUCCAGGAC-3' and control siRNA with sequence 5'-AATTCTCCGAACGTGTCACGT-3' was obtained

from Dharmacon. DSPE-PEG_{2000}-anisamide was synthesized in our laboratory using the methods described earlier (105).

3.2.2 Cell culture

Murine melanoma B16F10 (sigma receptor positive (40)) cells were used in this study. The cells were purchased from American Type Culture Collection and stably transduced with GL3 firefly luciferase gene by using a retroviral vector produced in Dr. Pilar Blancafort's laboratory at the University of North Carolina at Chapel Hill. The cells were maintained in Dulbecco's modified Eagle's medium (Invitrogen, Carlsbad, CA) supplemented with 10% fetal bovine serum (Invitrogen, Carlsbad, CA), 100 U/ml penicillin, and 100 µg/ml streptomycin (Invitrogen).

3.2.3 Experimental animals

Female C57BL/6 mice of age 6–8 week were purchased from National Cancer Institute (Frederick, MD). All work performed on animals was in accordance with and approved by the IACUC committee at UNC.

3.2.4 Synthesis of DSAA

DSAA [*N*,*N*-Distearyl-*N*-methyl-*N*-2-(*N*'-arginyl) aminoethyl ammonium chloride]: DSAA is a non glycerol based cationic lipid that contains guanidine head group. It was synthesized in five steps. N-alkylation by n-octadecyl bromide and subsequent Boc deprotection of mono-Boc protected ethylene diamine yielded mixed primary tertiary amine N^1,N^1-dioctadecylethane-1,2-diamine. Tri Boc protected arginine conjugation to the primary amine group by the conventional EDCI and quaternization of the tertiary amine group using methyl iodide on the above obtained product gave tri Boc protected DSAA. To obtain final product DSAA, [(N-(2-(Arginyl)ethyl)-N-methyl-N, N-di octadecyl amonium chloride) Boc

group deprotection with TFA and chloride ion exchange with Amberlyst A 27(Cl^-)ion exchange resin was carried out. The resulting compound was characterized by using ^1H NMR spectra and LSIMS. Detailed synthetic procedures, spectral and purity data will be delineated elsewhere (Bathula et al., unpublished).

3.2.5 Analysis of ROS in B16F10 cells

B16F10 cells (10^6 per well) were seeded into each well of 12-well plates. Cells were incubated with 20 mM 2′,7′-dichlorodihydrofluorescein diacetate (DCFH-DA) (Sigma-Aldrich) in serum containing medium for 30 min at 37 °C. Then, cells were treated with DSAA or DOTAP liposomes at various doses in serum containing medium at 37 ℃ for 1 h. Cells were quickly washed and immediately analyzed by flow cytometry.

3.2.6 Preparation of PEGylated LPD Formulations

LPD were prepared according to the previously method with slight modifications (100). Briefly, cationic liposomes composed of DOTAP or DSAA and cholesterol (1:1 molar ratio) were prepared by thin film hydration followed by membrane extrusion to reduce the particle size. To prepare LPD, 18 μL of protamine (2 mg/mL), 140 μL of deionized water, and 24 μL of a mixture of siRNA and calf thymus DNA (2 mg/mL) were mixed and kept at room temperature for 10 min before adding 120 µL of cationic liposome (10mM). After 10 min at room temperature, LPD was mixed with 37.8 μL of DSPE-PEG-AA or DSPE-PEG (10 mg/mL) and incubated at 50-60 ºC for 10 min.

3.2.7 Cellular Uptake Study

B16F10 cells were seeded in 12-well plates (Corning Inc., Corning, NY) 12 h before experiments. Cells were treated with different formulations at a concentration of 250 nM for

5'-cy3-labeled siRNA in serum containing medium at 37 °C for 4 h. Cells were washed twice with PBS, counterstained with DAPI and imaged by using a Leica SP2 confocal microscope.

3.2.8 Western blot analysis

For *in vivo* study, B16F10 tumor bearing mice (tumor size around 1 cm^2) were i.v. injected via the tail vein with siRNA in different formulations (1.2 mg siRNA/kg) with one injection per day for 3 consecutive days. The day after the third injection, mice were killed and tumor samples were collected. Extracted protein (40 μg) from the tumor was separated on a 10% acrylamide gel and transferred to a PVDF membrane. Membranes were blocked for 1 h in 5% skim milk and then incubated for 12 h with polyclonal antibodies directed against c-myc (Santa Cruz Biotechnology, Inc.) and actin (Santa Cruz Biotechnology, Inc.) for standardization. Membranes were washed in PBST (PBS, 0.1% Tween-20) and then incubated for 1 h with appropriate secondary antibodies. Membranes were again washed and then developed by an enhanced chemiluminescence system according to the manufacturer's instructions (PerkinElmer).

For in vitro Bcl-2 down-regulation study, B16F10 cells were seeded in 12-well plates (1×10^5 per well) for 24 h. Cells were treated with different lipids at the concentration of 50 μM and were collected after 24 h and 48 h for measuring Bcl-2 expression by Western blot analysis as described above.

3.2.9 Tumor uptake study

Mice with tumor size of ~1 cm^2 were i.v. injected with cy3-labeled siRNA (1.2 mg/kg) and NBD-labeled cholesterol (Avanti Polar Lipids) in different formulations. Four h later, mice were killed and tissues were collected, fixed in 10% formalin and embedded in paraffin.

Tumor tissues were sectioned (7 ¼ μm thick) and imaged using a Leica SP2 confocal microscope.

3.2.10 Tissue biodistribution study

Mice with tumor size of ~1 cm^2 were i.v. injected with NBD- cholesterol in different formulations. Four hours later, mice were killed and tissues were collected and homogenized in lysis buffer and incubated at room temperature for 30 min. The supernatant was collected after centrifugation at 14,000 rpm for 10 min and 50 μl supernatant was transferred to a black 96-well plate (Corning, Corning, NY). The fluorescence intensity of the sample was measured by a plate reader (Bioscan, Washington, DC) at excitation wavelength 485 nm and emission wavelength 535 nm. Lipid concentration in each sample was calculated from a standard curve.

3.2.11 Tumor growth inhibition study

B16F10 tumor bearing mice (size 16–25 mm^2) were i.v. injected with different formulations containing siRNA (1.2 mg/kg) once per day for 3 days. Tumor size in the treated mice was measured at different days after the treatment.

3.2.12 Analysis of serum cytokine levels

C57BL/6 mice were i.v. injected with siRNA against c-myc formulated in formulations at the dose of 1.2 mg siRNA/kg (1.2 mg DNA /kg for DSAA AA+ without siRNA). Four h after the injections, blood samples were collected from the tail artery and allowed to stand on ice for 2 h for coagulation. Serum was obtained by centrifuging the clotted blood at 16,000 rpm for 20 min. Cytokine levels were determined by using ELISA kits for IL6 and IL12 (BD Biosciences, San Diego, CA).

3.2.13 Statistical analysis

All statistical analyses were performed by student *t*-test. Data were considered statistically significant when *p* value was less than 0.05.

3.3 RESULTS

3.3.1 Cellular uptake of siRNA in B16F10 melanoma cells

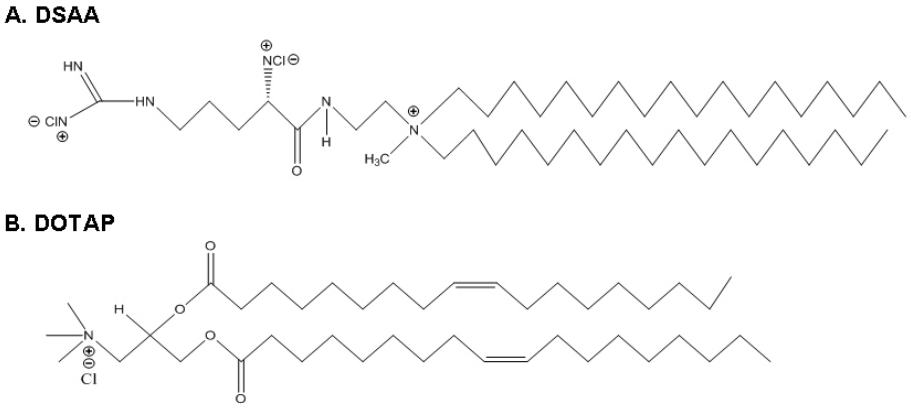

Figure 3.1 Chemical structure of DSAA (A) and DOTAP (B).

We used anisamide-targeted LPD nanoparticles containing DSAA as a carrier lipid to specifically deliver siRNA to the cultured B16F10 melanoma cells which express the sigma receptor. The structure of DSAA is shown in **Figure 3.1** The particle size of the nanoparticles was around 100 nm and the zeta potential was about 25 mV. To characterize

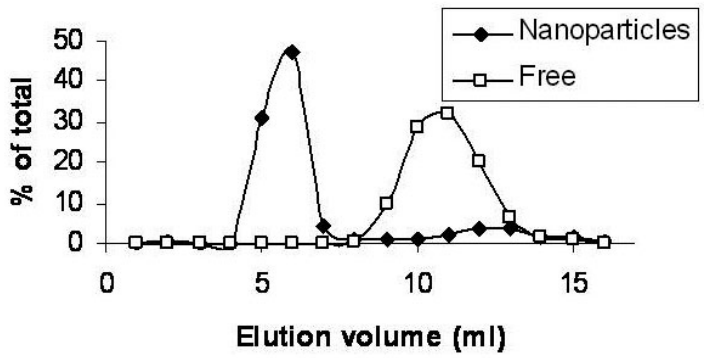

Figure 3.2 Sepharose CL 2B size exclusion chromatography of the nanoparticles. siRNA was labeled with FITC.

the new formulation, we used FITC labeled siRNA to prepare targeted nanoparticles using DSAA as the cationic lipid. The final formulation was fractionated by Sepharose CL 2B column chromatography. **Figure 3.2** indicates that the amount of siRNA loaded into the final formulation was about 85%.of the total siRNA. Since DSAA is new lipid, we compared the data collected with nanoparticles containing DSAA with those containing a previously used lipid, DOTAP. As shown in **Figure 3.3A**, confocal microscopy showed that nanoparticles containing DSAA could deliver cy-3 labeled siRNA into the cytoplasm of B16F10 cells more efficiently than those containing DOTAP. Furthermore, cy-3 siRNA uptake of the cells treated with the targeted nanoparticles DSAA AA+ was much more than that of cells treated with the non-targeted nanoparticles DSAA AA-. The results indicate that the nanoparticles containing DSAA could efficiently deliver siRNA into the tumor cells and the delivery was significantly enhanced by the presence of the targeting ligand (AA) on the nanoparticles.

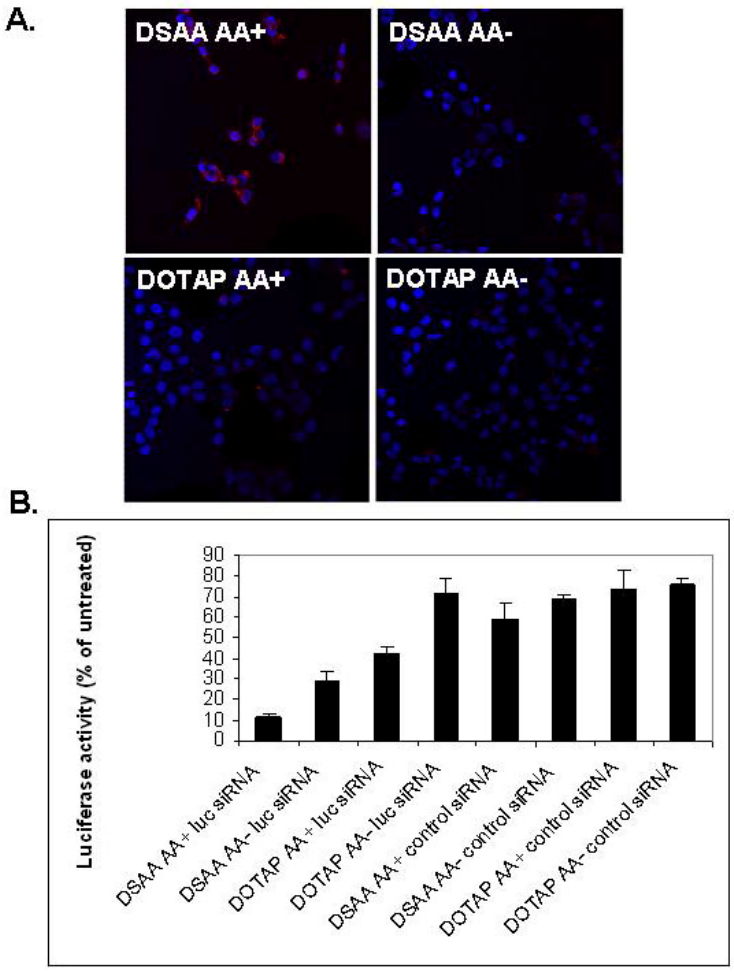

Figure 3.3 Intracellular uptake of siRNA and luciferase gene silencing in cultured melanoma cells. (**A**), fluorescence micrographs of B16F10 cells after treatment with 5'-cy3 labeled siRNA in the targeted nanoparticles (AA+) or the non-targeted nanoparticles (AA-) containing DSAA and DOTAP. (**B**), B16F10 cells were incubated with different formulations containing anti-luciferase siRNA. Luciferase activity in cells was measured after 24 h. Each value represents the mean ± S.D. (n = 3). Luc: luciferase.

3.3.2 Luciferase gene silencing *in vitro*

B16F10 cells stably transduced with the firefly luciferase gene were used to study in *vitro* gene silencing. Luciferase gene silencing effect of the nanoparticles containing DSAA was stronger than those containing DOTAP (**Figure 3.3B**). Furthermore, the silencing effect in the cells treated with the targeted nanoparticles was much higher than cells treated with the non-targeted nanoparticles, when DSAA was the carrier lipid. The result correlated very well with that of the intracellular siRNA uptake (**Figure 3.3A**).

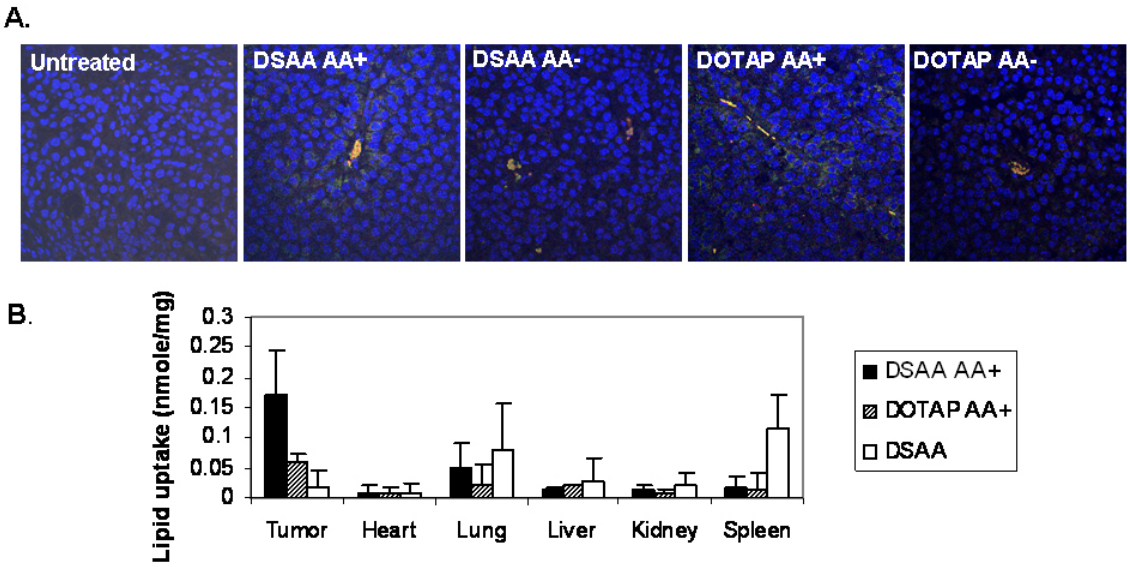

Figure 3.4 Tumor uptake of siRNA and lipid in different formulations. (**A**), fluorescence micrographs of cy3-siRNA (red) and NBD-cholesterol (green) in B16F10 tumor. Mice were injected with different formulations and sacrificed at 4 h. (**B**), tissue distribution of NBD-cholesterol in mice injected with different formulations. Data = mean $\pm$ S.D., n = 3. DSAA: non-PEGylated liposome containing DSAA and cholesterol (1:1 mole ratio).

3.3.3 Tissue distribution and intracellular uptake of siRNA and lipid

We further studied the siRNA and lipid distribution and bioavailability of major tissues in the B16F10 melanoma model in C57BL/6 mice. We used 10 mol% NBD-cholesterol labeled liposomes (green) and cy-3 labeled siRNA (red) to prepare PEGylated LPD and the final formulation was i.v. administered into the tumor bearing mice. As shown in **Figure 3.4A**, a clear overlap (yellow/orange) between NBD-cholesterol labeled liposomes and cy-3 labeled siRNA was observed, indicating intact nanoparticles were taken up by the tumor cells. The targeted nanoparticles containing DSAA or DOTAP (DSAA AA+ or DOTAP AA+) showed higher cytosolic delivery of cy-3 siRNA and NBD-cholesterol in the tumor tissue than the non-targeted nanoparticles (DSAA AA- or DOTAP AA-). Since the non-PEGylated liposomes containing DSAA/chol were a crucial component of the targeted nanoparticles (DSAA AA+), we compared the lipid (NBD-cholesterol) uptake of DSAA

AA+ with that of the non-PEGylated liposomes containing DSAA/chol. For quantitative results of lipid uptake (**Figure. 3.4B**), the targeted nanoparticles containing DSAA showed higher lipid delivery in the tumor tissue than the non-PEGylated liposomes containing DSAA, while other tissues showed lower uptake of lipid when treated with the targeted nanoparticles

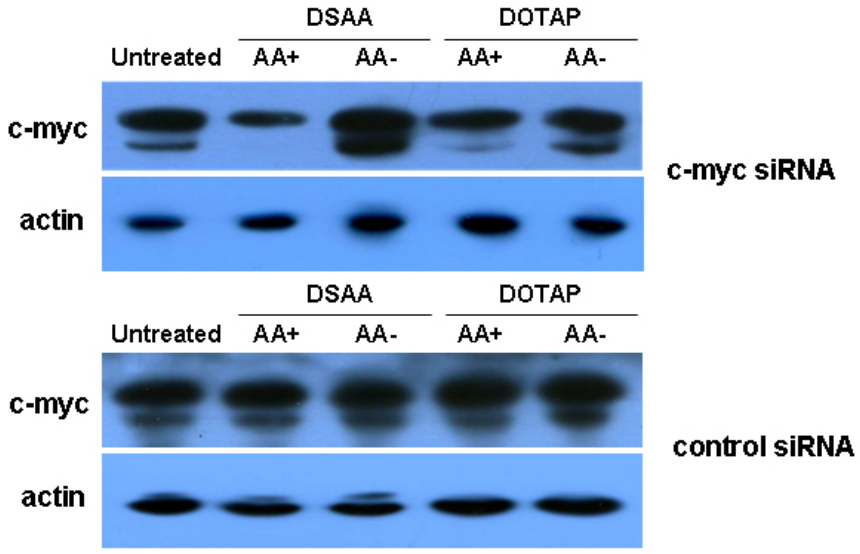

Figure 3.5 c-Myc expression in the tumor after treatment with siRNA in different formulations. Mice bearing B16F10 tumor were i.v. injected with siRNA formulated in different LPD nanoparticles. c-Myc expression was examined by western blot analysis.

containing DSAA than the non-PEGylated liposome containing DSAA. Taken together, these data indicated that the targeted nanoparticles containing DSAA could efficiently deliver siRNA and the carrier lipid to the tumor tissue and the intracellular delivery was ligand dependent.

3.3.4 c-Myc gene silencing *in vivo*

To examine the biological activities of siRNA *in vivo*, the c-myc level in the subcutaneous melanoma tumor was detected by western blotting (**Figure 3.5**). c-Myc in B16F10 tumor was silenced by c-Myc siRNA in the targeted nanoparticles DSAA AA+ and

DOTAP AA+. The c-Myc siRNA-containing DSAA AA- and DOTAP AA- and control siRNA showed no effect. The results indicated that the nanoparticle containing DSAA or DOTAP could systemically deliver siRNA into the tumor tissue and the delivery was specifically controlled by the targeting ligand (AA). The result correlated well with that of the intracellular siRNA uptake in the tumor tissue (**Figure 3.4A**).

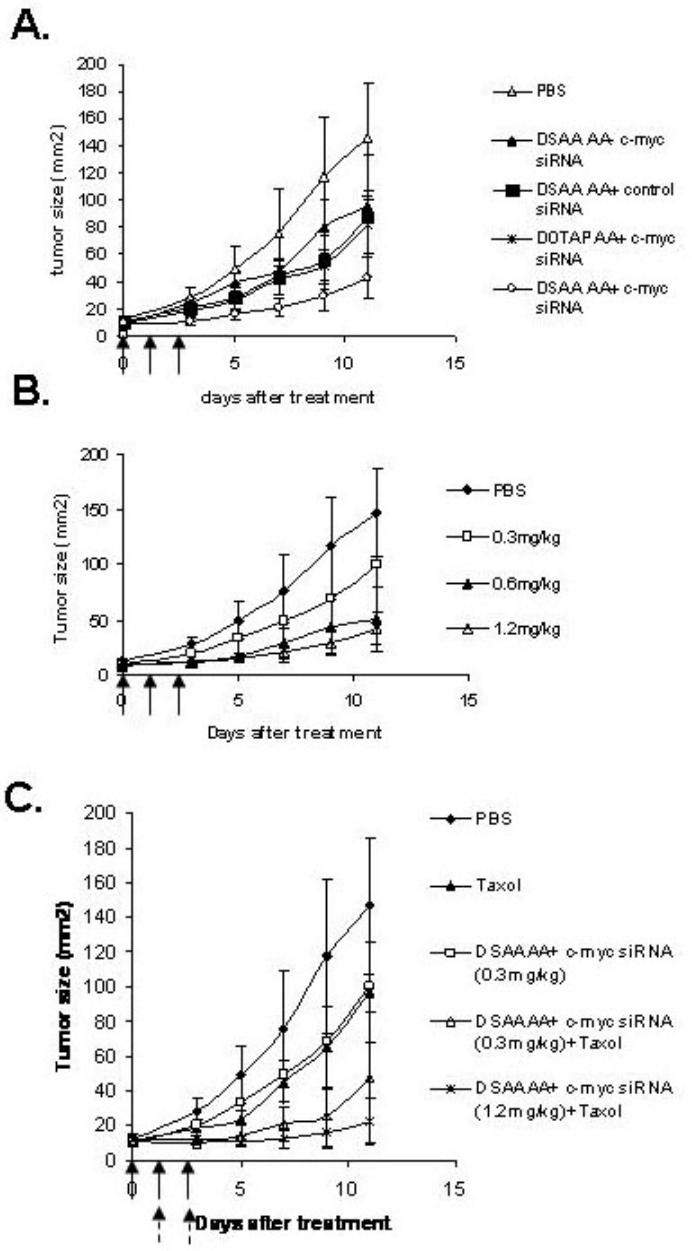

Figure 3.6 Tumor growth inhibition. (**A**), B16F10 tumor growth inhibition by siRNA in different formulations. (**B**), dose-dependent antitumor activity of c-myc siRNA formulated in DSAA AA+. (**C**), combination of c-myc siRNA formulated in the targeted DSAA nanoparticles and paclitaxel inhibited B16F10 tumor growth (20mg paclitaxel/kg). Solid arrows indicate the i.v. administrations of siRNA and dash-line arrows indicate the i.v. injections of paclitaxel. N= 4~7.

3.3.5 Tumor growth inhibition

Three injections of c-myc siRNA in DOTAP AA+ showed a partial inhibition of tumor growth ($P < 0.01$ at day 11) similar to that of c-myc siRNA in DSAA AA- and control

siRNA in DSAA AA+ (**Figure 3.6A**). A significant improvement in the tumor growth inhibition was observed with c-myc siRNA formulated in DSAA AA+ ($P < 0.0001$ at day 11), with an ED_{50} of 0.55mg/kg (**Figure 3.6B**). With additional paclitaxel treatment, which is a common first line chemotherapy agent for malignant melanoma, the therapeutic activity of c-myc siRNA formulated in DSAA AA+ showed further improvement (**Figure 3.6C**). Tumor growth was completely inhibited with the combination therapy for 1 week after the last dosing (**Figure 3.6C**).

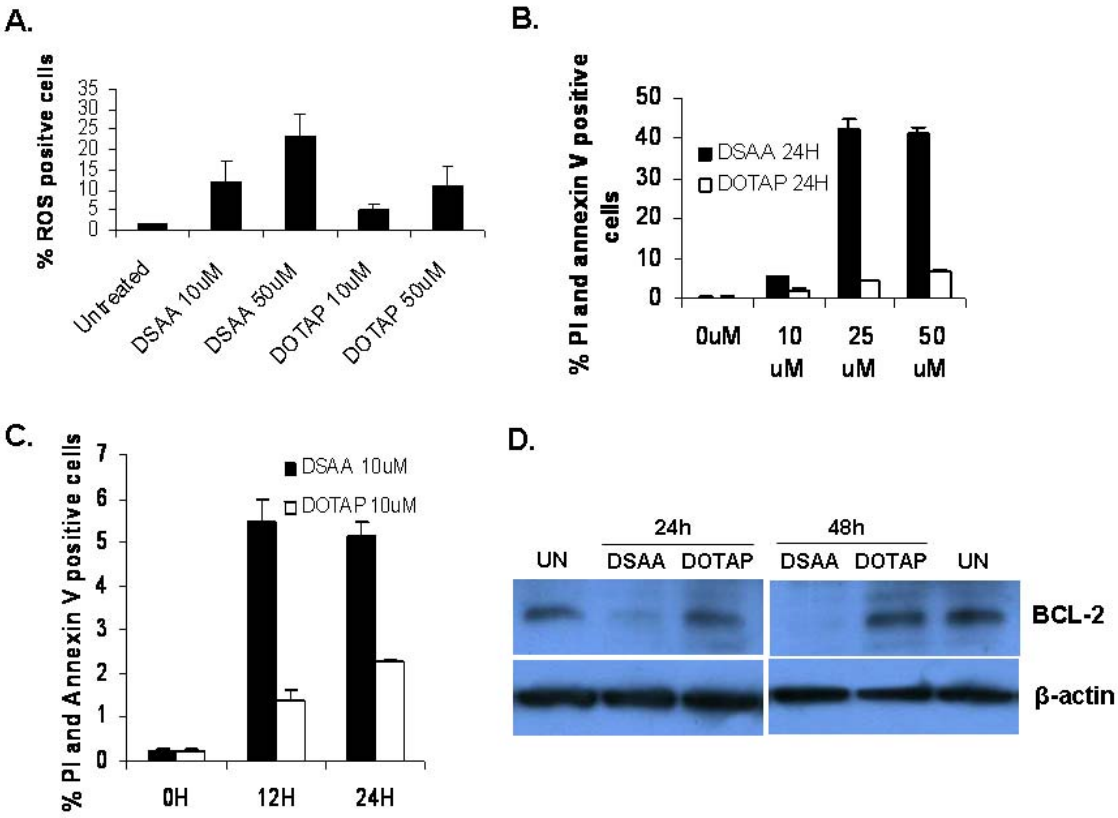

Figure 3.7. ROS generation and apoptosis induction and by liposome containing DSAA or DOTAP in mouse melanoma B16F10 cells. (A**)** dose-dependent ROS generation by DSAA or DOTAP after 1 h incubation with different concentrations of DSAA or DOTAP. The ROS content of cells was analyzed by flow cytometry. N=3, **P*<0.05. (B) and (C), dose- and time-dependent apoptosis induction by DSAA or DOTAP in B16F10 cells, respectively. (D), Bcl-2 expression in H460 cells after incubation with 50 μM DSAA and DOTAP for 24 and 48 h.

Since DSAA played an important role in the uptake and the anti-cancer activity of siRNA delivered to the tumor cells, we decided to study the biological functions of DSAA in some detail. We first investigated the ROS activation in the B16F10 cells since it plays an important role as an apoptosis inducer. B16F10 cells were treated with DOTAP/chol or DSAA/chol liposomes at different doses, and the cellular ROS content was measured by using dichlorofluorescin diacetate (DCFH-DA) and flow cytometry. As shown in **Figure 3.7**, DSAA could more efficiently generate ROS in B16F10 cells than DOTAP after one h of

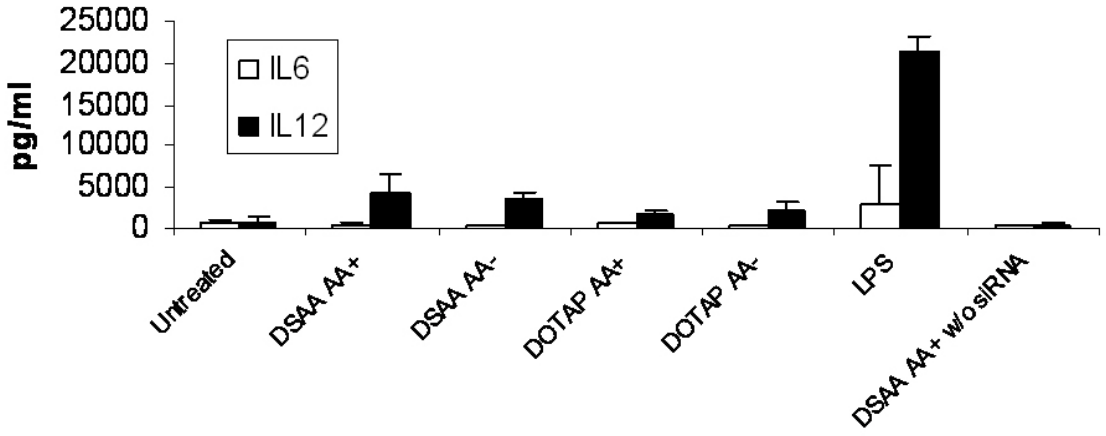

Figure 3.8 Serum cytokine levels of C57BL/6 mice treated with siRNA against c-myc in different formulations. Data = mean ±SD, *n* = 3~4.

treatment and the ROS induction was elevated in a dose-dependent manner. There was a statistically significant difference in the apoptosis induction between DSAA and DOTAP at concentrations of 10, 25 and 50 μM after 24 h incubation based on flow cytometry assay using propidium iodide (PI) and annexin V staining (**Figure 3.7B and C**). Since it has been report that ROS inducing apoptosis was regulated by the ubiquitination of Bcl-2 family proteins (144), we further studied the Bcl-2 protein expression after treatment of DSAA or DOTAP liposomes for different time periods in B16F10 cells. As shown in **Figure 3.7D**,

50μM DSAA could decrease Bcl-2 expression at 24 and 48 h after treatment. However, Bcl-2 expression remained unchanged after the treatment with DOTAP. These results suggest that ROS induced by DSAA may lead to apoptosis via Bcl-2 down-regulation. Thus, silencing c-myc by siRNA and ROS induction and the associated Bcl-2 down-regulation by DSAA may work together to impair the growth of a melanoma tumor.

3.3.6 Immunotoxicity

The proinflammatory cytokine (IL-6 and IL-12) levels in the serum were examined for evaluation of immunotoxicity induced by our formulations in C57BL/6 mice (**Figure 3.8**). c-Myc siRNA formulated in different formulations (DSAA AA+, DSAA AA-, DOTAP AA+ and DOTAP AA-) induced a significant production of IL-12, while IL-6 was not induced by the formulations. Empty nanoparticle showed very mild immunotoxicity. When treated with LPS (1mg/kg), both inflammatory cytokines were induced to high levels. The data suggested that the immunotoxicity of c-myc siRNA in DSAA AA+ was similar to DOTAP AA+. Since DSAA significantly enhanced the anti-cancer activity, but not the immunotoxicity, of c-myc siRNA, it is a valuable formulation lipid for nanoparticles for the siRNA delivery against the melanoma

3.4 DISCUSSION

Previous studies showed that a mixture of siRNAs against c-myc, MDM2 and VEGF had a tumor inhibition effect on the B16F10 melanoma lung metastasis model (40). In this study, we have improved the formulation by introducing a novel cationic lipid DSAA. Anisamide-targeted LPD nanoparticles containing DSAA effectively delivered siRNA to subcutaneous melanoma tumors, and induced elevated apoptosis and tumor growth inhibition.

Furthermore, c-myc siRNA so delivered also sensitized the tumor cells to paclitaxel, a commonly used chemotherapeutic agent for malignant melanoma.

c-Myc oncoprotein, as a general transcription factor, regulates various key cellular processes such as cancer onset and maintenance in human tumors. Genetic aberrations of c-myc promote tumorigenesis in various forms of cancer, leading to about 70,000 cancer deaths per year in the U.S. (145). In melanoma, c-myc expression and activation are also essential for cancer cell proliferation (139). Down-regulation of c-myc protein induces apoptosis in melanoma cells and sensitizes the tumor cells to anti-cancer drugs (146, 147). It has also been demonstrated that over-expression of myc oncoprotein inhibits apoptosis triggered by paclitaxel in human melanoma (148). Data presented in **Figure 3.5** clearly indicate that c-myc oncogene in the murine melanoma model could be effectively down-regulated by using a systemic delivery vehicle carrying siRNA against c-myc. Such down-regulation brought tumor growth inhibition as predicted (**Figure 3.6**). The potency of the new anti-melanoma treatment, as shown by the relatively low ED_{50} (0.55 mg/kg for siRNA), compares favorably with other siRNA mediated therapies for cancer (149). The therapeutic activity could be further enhanced by combining it with a commonly used first line chemotherapy agent, i.e. paclitaxel.

A critical element for the success of the nanoparticle formulation is the new cationic lipid DSAA. Our data (**Figure 3.7D**) showed that the expression of Bcl-2 was down-regulated in B16F10 melanoma cells after the treatment of DSAA. The reduction of Bcl-2 may be related to the induction of ROS in B16F10 cells by DSAA (**Figure 3.7A**). Bcl-2 is an anti-apoptosis protein and over-expressed in various cancer cells. Down-regulation of Bcl-2 renders the cancer cell more sensitive to cell death triggered by chemotherapeutic agent or

radiation and leads to inhibition of tumor growth (150, 151). Chemotherapeutic drugs that promote down-regulation of Bcl-2 trigger strong apoptotic activity in B16F10 cells (152). c-Myc and Bcl-2 cooperate to suppress p53 functions in mediating chemotherapy-induced apoptosis (153, 154). Thus, it is not surprising that the combination of siRNA against c-myc and DSAA down-regulating Bcl-2 synergistically impaired the growth of the melanoma tumor and sensitized the tumor cells to paclitaxel. The combination therapy may also be considered for patients who developed drug-resistance in tumors with over-expressed c-myc. The possible mechanisms of the combination strategy using siRNA against c-myc and DSAA are shown in **Figure 3.9.** DSAA induced ROS, triggered apoptosis and down-regulated anti-apoptotic protein Bcl-2 which prevents the release of cytochrome c from mitochondria. C-

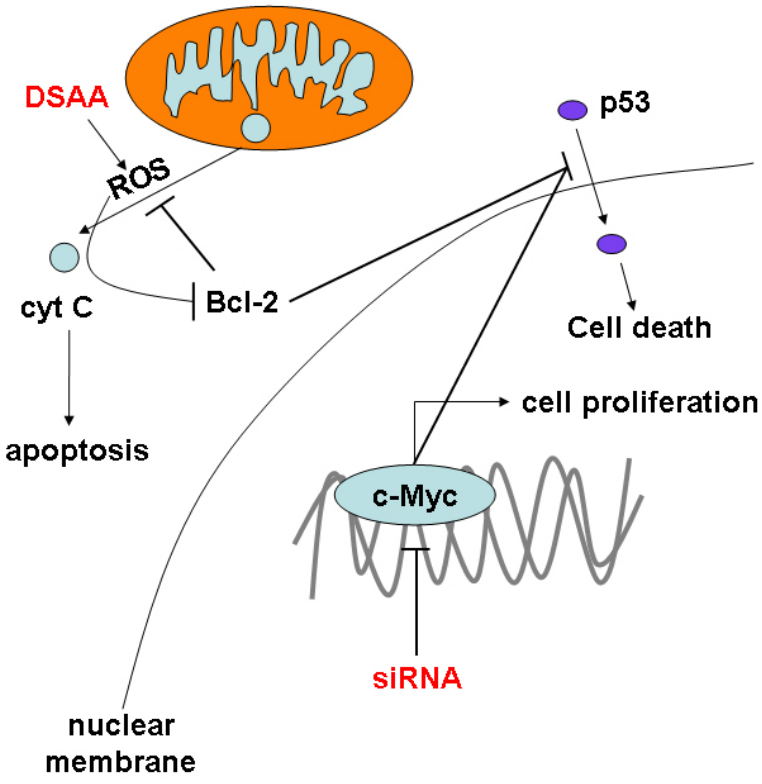

Figure 3.9 Schematic illustration of possible mechanisms of the combination strategy using c-myc siRNA and the cationic lipid DSAA. Cyt c: cytochrome c.

Myc protein silencing by siRNA inhibited cell proliferation and sensitized melanoma cells to chemotherapy drugs. siRNA against c-myc and DSAA may cooperate to activate nuclear translocation of p53 in mediating chemotherapy-induced apoptotic cell death in melanoma cells.

DSAA, a guanidinium containing cationic lipid, induced ROS and triggered apoptosis in B16F10 melanoma cells in a dose- and time-dependent manner (**Figure 3.7B and C**). ROS has important functions affecting cell growth, death, development and survival (155). Induction of ROS can initiate a lethal signal transduction resulting in damaged cellular integrity and apoptosis (156-159). We suspected that the guanidinium residue was playing a critical role in the induction of ROS in the cells and the generation of ROS collaborated in a synergistic manner with c-myc siRNA to inhibit tumor growth. The activity of DOTAP in inducing ROS is very limited (**Figure. 3.7A**), hence no effect in enhancing the tumor growth inhibition activity of c-myc silencing (**Figure. 3.6A**).

However, c-myc also plays a key role for cell proliferation, cell growth, differentiation, and cell death in the normal cells (160). In this study, we have used a targeted nanoparticle formulation (DSAA AA+) that can specifically deliver c-myc siRNA into the tumor tissue (**Figure 3.4A**). Furthermore, the enhanced uptake of lipid into the tumor also appeared to be ligand dependent. The formulation was thus not very immunotoxic as shown in **Figure 3.8**.

In summary, c-Myc siRNA formulated in the targeted nanoparticle containing DSAA could effectively impair tumor growth in the B16F10 melanoma model. The formulation shows great promise to be an effective therapeutic agent, perhaps used together with some traditional chemotherapies such as paclitaxel, for malignant melanoma.

4.0 NANOPARTICLES TARGETED WITH NGR MOTIF DELIVER C-MYC SIRNA AND DOXORUBICIN FOR ANTICANCER THERAPY

We have designed a PEGylated LPD nanoparticle for systemic, specific and efficient delivery of small interfering RNA (siRNA) into solid tumors in mice by modification with NGR (aspargine–glycine–arginine) peptide, targeting aminopeptidase N (CD13) expressed in the tumor cells or tumor vascular endothelium. LPD-PEG-NGR efficiently delivered siRNA to the cytoplasm and down-regulated the target gene in the HT-1080 cells but not CD13-negative HT-29 cells, whereas nanoparticles containing a control peptide, LPD-PEG-ARA, showed only little siRNA uptake and gene silencing activity. LPD-PEG-NGR efficiently delivered siRNA into the cytoplasm of HT-1080 xenograft tumor 4 h after intravenous injection. Three daily injections (1.2 mg/kg) of c-myc siRNA formulated in the LPD-PEG-NGR effectively suppressed c-myc expression and triggered cellular apoptosis in the tumor, resulting in a partial tumor growth inhibition. When doxorubicin (Dox) and siRNA were co-formulated in LPD-PEG-NGR, an enhanced therapeutic effect was observed.

4.1 INTRODUCTION

c-Myc oncogene is over-expressed and activated in various human tumors. It promotes cell growth, transformation and angiogenesis which play important roles in the progression and metastasis of tumor (161). Down-regulation of c-myc with antisense oligonucleotides inhibits tumor growth both *in vitro* and *in vivo* and sensitizes cancer cells to

chemotherapy (162, 163), possibly by induction of p53 and inhibition of Bcl-2 proteins which trigger cell apoptosis [3].

Surgical resection is a common primary cancer treatment. Radiation and chemotherapeutic agents such as Dox may improve treatment response and survival. However, resistance to chemotherapy and radiation often occurs and leads to poor prognosis. Delivery of siRNA against an oncogene or a drug resistant gene is a new strategy to increase the therapeutic armament (164-166). Dox, one of the most effective anticancer agents, is efficacious against various neoplasms such as acute lymphoblastic and myeloblastic leukemia, malignant lymphoma, soft tissue and bone sarcoma, breast, ovarian, prostate, bladder, gastric, and bronchogenic carcinoma (167). However, the associated cardiotoxicity caused by free radicals generated by Dox has prompted the development of a targeted delivery vehicle to tumor cells (168).

We have successfully developed a core/shell type of nanoparticle formulation, called LPD, to specifically deliver siRNA to tumor cells *in vivo* (25, 40, 169). Dox contains flat aromatic rings which intercalate into the DNA strands (170). Since dsDNA is a component of the LPD nanoparticle, we have decided to use the DNA as a carrier for Dox. We hypothesized that Dox may form a physical complex with the DNA inside the nanoparticles through non-covalent intercalation, which does not change the property of Dox or siRNA in the LPD nanoparticles. This novel system may provide a platform for efficient and specific co-delivery of siRNA and the DNA binding chemotherapy drug for cancer treatment.

In this study, we have designed the LPD nanoparticles armed with NGR, a peptide motif targeting CD13 (171) which is up-regulated in angiogenic tumor vasculature and various cancer cells such as HT-1080 human fibrosarcoma cells. CD13 is a multifunctional

protein involved in cancer angiogenesis, invasion, and metastasis (172). NGR-containing peptides have been successfully used to deliver cytotoxic drugs such as Dox, apoptotic peptides, and cytokines such as tumor necrosis factor (TNF) to the tumor or tumor vasculature and enhance the antitumor activity of the cargo (171, 173-178).

In the present study, we have developed LPD nanoparticles modified with PEGylated NGR for targeted co-delivery of siRNA and Dox *in vitro* and *in vivo*. We have shown increasing cellular uptake of siRNA, profound down-regulation of the target gene, enhanced apoptosis of the tumor cells and improved tumor growth inhibition effect triggered by LPD-PEG-NGR containing c-myc siRNA. These results indicate that the suppression of c-myc protein by NGR-targeted siRNA therapy and the co-delivery of c-myc siRNA and Dox could provide an efficient strategy for cancer treatment.

4.2 MATERIALS AND METHODS

4.2.1 Materials

DOTAP and cholesterol were purchased from Avanti Polar Lipids, Inc. (Alabaster, AL). Protamine sulfate (fraction X from salmon) and calf thymus DNA (for hybridization, phenol-chloroform extracted and ethanol precipitated) were purchased from Sigma-Aldrich (St. Louis, MO). Dox was purchased from IFFECT CHEMPHAR (HK). Synthetic 19-nt RNAs with 3' dTdT overhangs on both sequences were purchased from Dharmacon (Lafayette, CO). For quantitative studies, cy3 was conjugated to 5' sense sequence. 5'-cy3 and 5'-FITC labeled siRNA sequence was also obtained from Dharmacon. The sequence of c-myc siRNA was 5'-AACGUUAGCUUCACCAACAUU-3' and control siRNA with sequence 5'-AATTCTCCGAACGTGTCACGT-3' was obtained from Dharmacon. DSPE-PEG-NGR (GNGRGGVRSSSRTPSDKYC), a peptide ligand conjugated to a PEG chain

tethered to a phospholipid (**Figure 4.1A**), and DSPE-PEG-ARA (GARAGGVRSSSRTPSDKYC), a similar conjugate but containing the control peptide ARA, were supplied by Ambrilia (179). These conjugates were used to modify the surface of the nanoparticles, as described (100), to obtain LPD-PEG-NGR and LPD-PEG-ARA containing siRNA.

4.2.2 Cell culture

HT-1080 and HT-29 cells were obtained from American Type Culture Collection. HT-1080 cells were maintained in MEM Alpha Media (GibcoBRL) supplemented with 10% fetal bovine serum (Invitrogen, Carlsbad, CA), 100 U/ml penicillin, and 100 μg/ml streptomycin (Invitrogen). HT-29 cells were maintained in McCoy's 5A Medium Modified Medium (cellgro) supplemented with 10% fetal bovine serum (Invitrogen, Carlsbad, CA), 100 U/ml penicillin, and 100 μg/ml streptomycin (Invitrogen). To study the siRNA uptake, HT-1080 cells were chosen as the CD-13 receptor positive human tumor cell lines and H-29 cells as receptor negative control cell lines [17].

4.2.3 Preparation of PEGylated LPD Formulations

LPD were prepared according to the previously method with slight modifications (100). Briefly, cationic liposomes composed of DOTAP and cholesterol (1:1 molar ratio) were prepared by thin film hydration followed by membrane extrusion to reduce the particle size. To prepare LPD, 18 μL of protamine (2 mg/mL), 140 μL of deionized water, and 24 μL of a mixture of siRNA and calf thymus DNA (2 mg/mL) were mixed and kept at room temperature for 10 min before adding 120 μL of cationic liposome (10mM). LPD stand at room temperature for 10 min before the addition of DSPE-PEG. LPD was then mixed with

37.8 μL of DSPE-PEG-NGR or DSPE-PEG-ARA (17 mg/mL) and kept at 50-60 ºC for 10 min.

4.2.4 Cellular Uptake Study

Human HT-1080 and HT-29 cells, originally obtained from ATCC, (1×10^5 per well) were seeded in 12-well plates (Corning Inc., Corning, NY) 12 h before experiments. Cells were treated with different formulations at a concentration of 250 nM for 5'-cy3-labeled siRNA or 1.5 μM Dox in serum containing medium at 37 °C for 4 h. Cells were washed twice with PBS, counterstained with DAPI and imaged using a Leica SP2 confocal microscope. Dox uptake of HT-1080 and HT-29 cells was also measured by flow cytometry. Briefly, cells were treated with different formulations at a concentration of 1.5 μM Dox in serum containing medium at 37 °C for 1 h. Cells were harvested and resuspended at a concentration of 1×10^6 cells/mL. Cells were washed with PBS and analyzed immediately by flow cytometry.

4.2.5 Gene silencing study

Sterile round cover slips (1 cm × 1 cm) were placed into each well in 24-well plates. HT-1080 cells (5×10^4 cells/0.5 ml/well) were then seeded into each well overnight. Cells were treated with different formulations at a concentration of 250 nM for c-myc siRNA in 10% FBS containing medium at 37 °C for 24 h. Cells were washed three times with PBS and fixed with cold acetone/methanol 1:1 for 10 min. Cells were incubated with anti c-myc antibody (Santa Cruz Biotechnology, Inc.) at 1:50 dilution for 1 h. After washing with PBS, immunostaining was carried out by using a kit (DakoCytomation Envision + Dual Link System-HRP (DAB+), DakoCytomation, Carpinteria, CA) following the vendor's protocol. For *in vivo* study, HT-1080 tumor bearing mice (tumor size ~1 cm^2) were i.v. injected with

siRNA in different formulations (1.2 mg siRNA/kg, one injection per day for 3 days). A day after the third injection, tumors were collected, paraffin embedded and sectioned. Some sections were analyzed for TUNEL assay (see below). Sections of 7 ¼ μm thick were immunostained with primary antibodies and visualized by using kits from DakoCytomation. Samples were imaged by using a Nikon Microphot SA microscope.

4.2.6 Western blot analysis

Cells were lysed in lysis buffer CelLytic M Cell Lysis Reagent, (Sigma) for 30 min on ice and the supernatant was collected after centrifugation at 12,000 rpm. Cell lysate were separated on a 10% acrylamide gel and transferred to a PVDF membrane. Membranes were blocked for 1 h in 5% skim milk and then incubated with polyclonal antibody against c-myc (Santa Cruz Biotechnology, Inc.) overnight. Membranes were washed in PBST (PBS with 0.1% Tween-20) three times and then incubated for 1 h with secondary antibody. Membranes were washed four times and then developed by an enhanced chemiluminescence system according to the manufacturer's instructions (PerkinElmer). For *in vivo* study, HT-1080 tumor bearing mice (tumor size ~1 cm^2) were i.v. injected with siRNA in different formulations (1.2 mg siRNA/kg, one injection per day for 3 days). A day after the third injection, mice were killed and tumor samples were collected. Total protein (40 μg) isolated from the tumors was loaded on a polyacrylamide gel, electrophoresed, blotted as described above.

4.2.7 Assessment of Apoptosis by TUNEL Staining

Paraffin sections of HT-1080 tumor were stained by using TACS^{TM} TdT Kit (R&D Systems, Minneapolis, MN) according to the manufacturer's recommendation. The apoptotic

cells were counted in four randomly selected visual fields for each treatment. The apoptotic index was calculated as the ratio of apoptotic nuclei to total nuclei.

4.2.8 Tumor uptake study

Mice with tumor size of ~1 cm^2 were i.v. injected with cy3-labeled siRNA (1.2 mg/kg) or Dox (1.2mg/kg) in different formulations. Four h later, mice were killed and tissues were collected, fixed in 10% formalin and embedded in paraffin. Tumor tissues were sectioned (7 ¼ μm thick) and imaged using a Leica SP2 confocal microscope.

4.2.9 Tissue distribution study

Mice with tumor size of ~1 cm^2 were i.v. injected with FITC-labeled siRNA or Dox in different formulations (1.2 mg/kg). Four h later, mice were killed and tissues were collected and homogenized in lysis buffer and incubated at room temperature for 30 min. The supernatant was collected after centrifugation at 14,000 rpm for 10 min and 50 μl supernatant was transferred to a black 96-well plate (Corning, Corning, NY). The fluorescence intensity of the sample was measured by a plate reader (Bioscan, Washington, DC) at excitation wavelength 485 nm and emission wavelength 535 nm. siRNA and Dox concentration in each sample was calculated from a standard curve.

4.2.10 Tumor growth inhibition study

HT-1080 tumor bearing mice (size 16–25 mm^2) were i.v. injected with different formulations containing siRNA (1.2 mg/kg) or Dox (0.3 mg/kg) once per day for 3 days. Tumor size in the treated mice was measured after treatment.

4.2.11 Statistical analysis

All statistical analyses were performed by student *t*-test. Data were considered statistically significant when *p* value was less than 0.05.

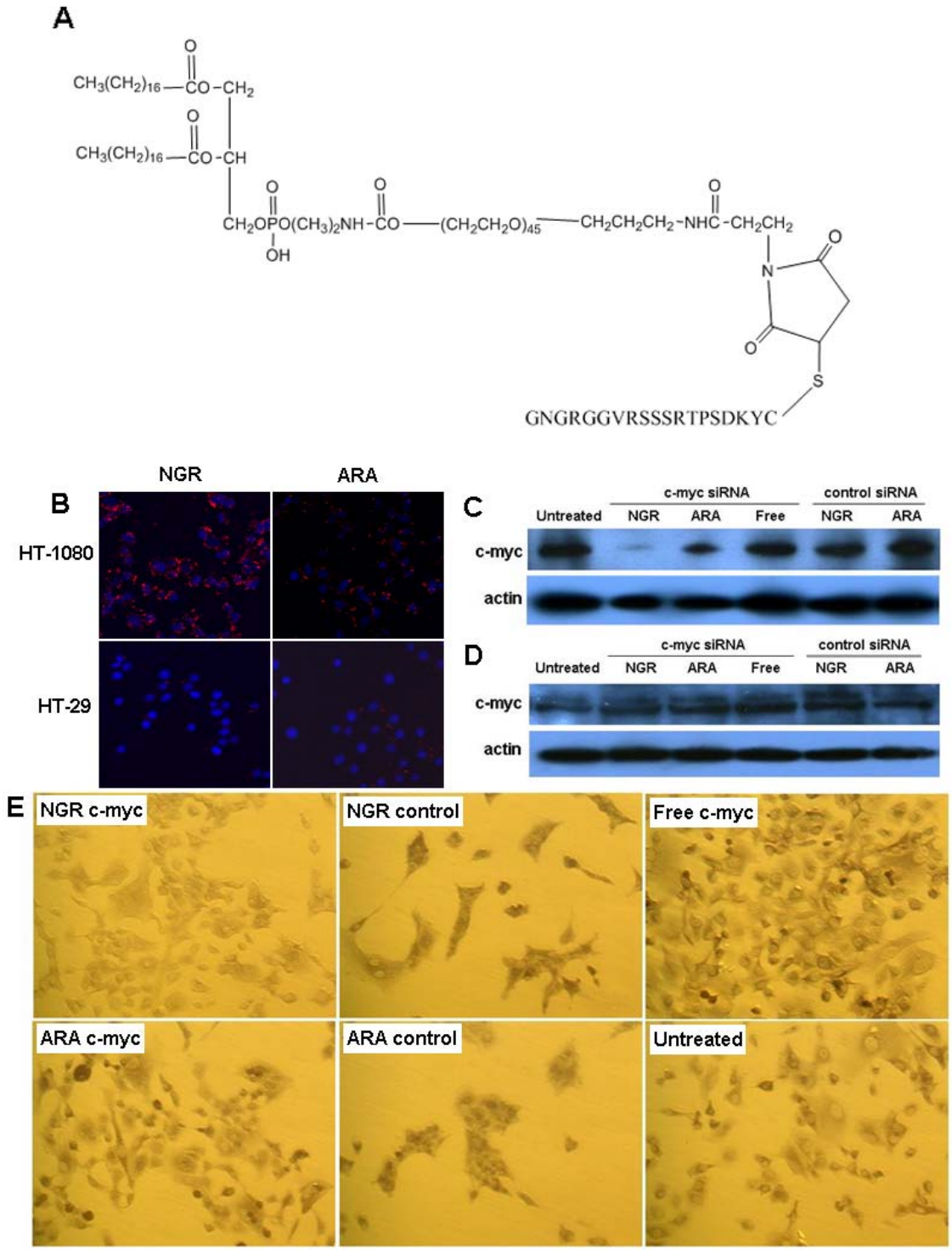

Figure 4.1 Intracellular uptake of siRNA and c-myc expression inhibited by siRNA formulation *in vitro*. (**A**) the structure of DSPE-PEG-NGR. (**B**) fluorescence photographs of HT-1080 and HT-29 cells after treatment with 5' Cy3 labeled siRNA against an irrelevant target in LPD-PEG-NGR and LPD-PEG-ARA for 4 h. Western blot analysis of c-myc and β-actin in HT-1080 cells (**C**) and HT-29 (**D**) after treatment with 250nM siRNA in different formulations for 24 h. (**E**) immunocytochemical staining of c-myc after treatment with 250nM siRNA in different formulations for 24 h.

4.3 RESULTS

4.3.1 Uptake of siRNA *in vitro*

The average size of the LPD-PEG-NGR nanoparticles was 197±1 nm and the zeta potential was 30.5±0.6 mV. As shown in **Figure 4.1B**, the uptake of fluorescently labeled siRNA was much greater in HT-1080 cells treated with LPD-PEG-NGR than cells treated with LPD-PEG-ARA. It indicates that NGR ligand increased the delivery efficiency of the nanoparticles for CD13 expressing cells, HT-1080. The CD13-negative cell line HT-29 (**Figure 4.1B**) did not show fluorescence, suggesting that uptake of siRNA is related to CD13 expression.

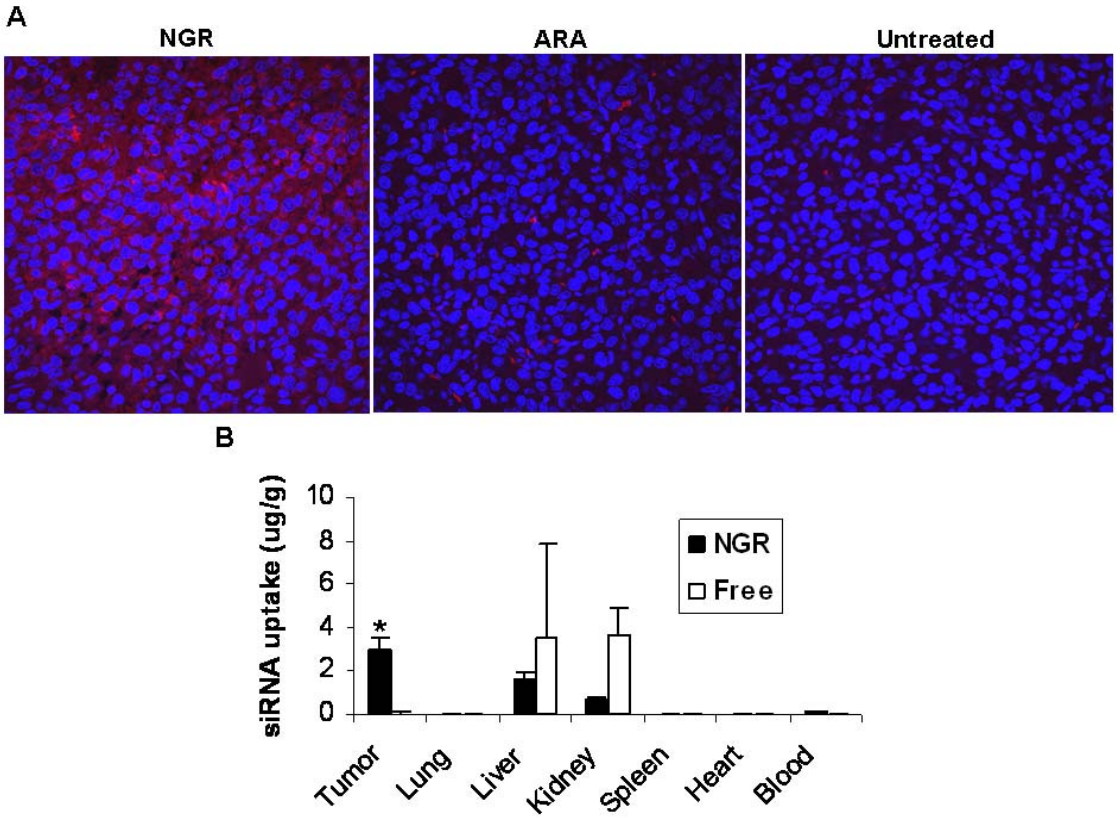

Figure 4.2 Tumor uptake of siRNA in different formulations. (**A**) fluorescence signal of cy3 labeled siRNA in HT-1080 tumor observed by confocal microscopy. (**B**) tissue distribution of FITC-siRNA in different formulations. Data = mean ±SD, n = 3. * indicates $P<0.05$ compared with free siRNA. NGR: LPD-PEG-NGR. ARA: LPD-PEG-ARA. c-Myc: c-Myc siRNA. Control: control siRNA.

c-Myc gene silencing *in vitro*

To further demonstrate the biological activity of the formulation, siRNA against human c-myc was delivered by either LPD-PEG-NGR or LPD-PEG-ARA. Its effect on c-myc levels was determined by immunostaining and western blot analysis (**Figure 4.1C-E**). The c-myc protein expression of HT-1080 cells treated with c-myc siRNA-containing LPD-PEG-NGR was significantly inhibited (**Figure 4.1C,E**). However, anti c-myc siRNA-containing LPD-PEG-ARA could only slightly down-regulate c-myc. The CD13-negative cell line HT-29 (**Figure 4.1D,E**) did not show silencing activity. The data indicates that siRNA could effectively suppress c-myc expression and the silencing activity was ligand dependent.

4.3.2 Uptake of siRNA *in vivo*

We studied the cy3-siRNA uptake of HT-1080 tumor tissue in the tumor-bearing mice 4 h after i.v. injections using confocal microscopy. As shown in **Figure 4.2A**, the intracellular fluorescence signals were hardly detected in the tumor tissues collected from the mice treated with LPD-PEG-ARA. The LPD-PEG-NGR showed strong cytosolic delivery of cy3-siRNA in the tumor tissue. The distribution of cy3-siRNA in the tumor was heterogeneous. These results indicate that the LPD-PEG-NGR can efficiently deliver siRNA to the tumor tissue and the intracellular delivery is targeting peptide dependent. In other organs (**Figure 4.2B**), the liver and the kidney showed stronger uptake of free siRNA than siRNA formulated in the targeted nanoparticles, whereas the targeted nanoparticles showed stronger siRNA delivery in the tumor tissue than free siRNA. The uptake of siRNA formulated in the targeted nanoparticles was under the detection limit in the heart, the spleen, and the lung.

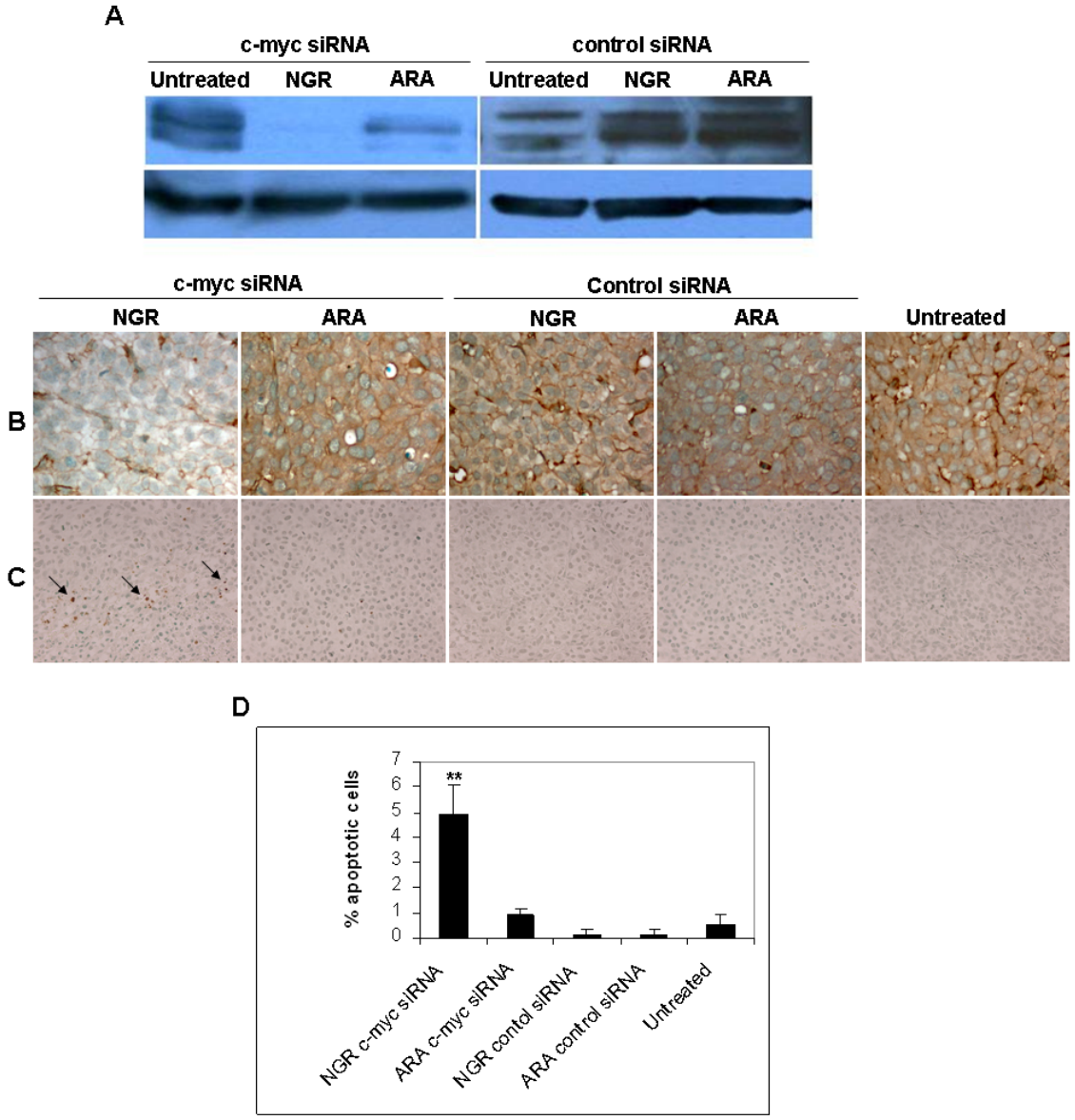

Figure 4.3 c-Myc expression and apoptosis induction in HT-1080 xenograft tumor. (**A**) western blot analysis of c-myc in the HT-1080 xenograft tumor after treatment with different formulations. c-Myc expression (**B**) and TUNEL staining (**C**) in HT-1080 tumor cells after treated with siRNA with different formulation in vivo. (**D**) quantitative analysis of TUNEL positive staining in the tumors treated with different formulations. N=3~5. ** indicates $P < 0.001$.

4.3.3 c-Myc gene silencing and apoptosis induction

To examine the biological activities of siRNA in vivo, c-myc level in the tumor was assayed by western blot analysis and immunostaining (**Figure 4.3A, B**). c-Myc expression in HT-1080 tumor was silenced by siRNA delivered with LPD-PEG-NGR. The LPD-PEG-

ARA showed only a partial effect, whereas the control siRNA showed no effect. We also stained for the apoptotic markers in the HT-1080 tumor (**Figure 4.3C**). **Figure 4.3C and 3D** indicate that about 5 % of HT-1080 cells treated with c-myc siRNA containing LPD-PEG-NGR underwent apoptosis as detected by the TUNEL staining. This value was significantly higher than the ones treated with c-myc siRNA formulated in LPD-PEG-ARA, or control siRNA formulated in either LPD-PEG-NGR or LPD-PEG-ARA. The results indicate that c-myc siRNA formulated with LPD-PEG-NGR can promote cell death in the HT-1080 tumor and the apoptosis effect was targeting peptide dependent.

4.3.4 Tumor growth inhibition by siRNA nanoparticles

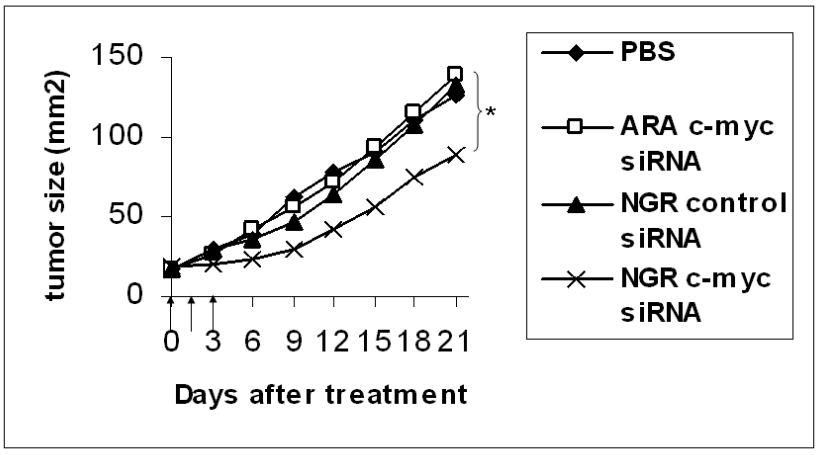

Figure 4.4 HT-1080 xenograft tumor growth inhibition by siRNA in different formulations. Solid arrows indicate the intravenous administrations of siRNA (1.2 mg/kg). Data = mean, n = 5–7. SD of the data points is not shown for clarity. * indicates $P < 0.05$.

Three injections of c-myc siRNA in LPD-PEG-NGR showed a partial inhibition of tumor growth ($P < 0.05$ at day 21) (**Figure 4.4**). Other control groups treated with c-myc siRNA formulated in LPD-PEG-ARA, control siRNA formulated in LPD-PEG-NGR had no therapeutic effect. The results indicate that c-myc siRNA formulated with LPD-PEG-NGR can inhibit the growth of HT-1080 tumor and the tumor growth inhibition effect was

targeting peptide dependent. The LPD-PEG-NGR nanoparticles efficiently delivered of siRNA to the solid tumor and almost totally silenced the target gene, c-myc, throughout the entire HT-1080 tumor. Since only partial apoptosis and growth inhibition of the tumor was observed, we hypothesized that it was due to the existence of alternative mechanisms of proliferation or some anti-apoptosis events in the tumor. To enhance the therapeutic activity of LPD-PEG-NGR nanoparticles containing c-myc siRNA, we co-delivered siRNA and Dox to the tumor cells. Dox has a unique property to bind with dsDNA by base intercalation (170). Since dsDNA is a component of the LPD nanoparticles, we have decided to use DNA as a carrier for Dox. We hypothesized that Dox will form a physical complex with DNA inside the LPD nanoparticles by non-covalent intercalation, which will not change the property of Dox or siRNA in the LPD nanoparticles.

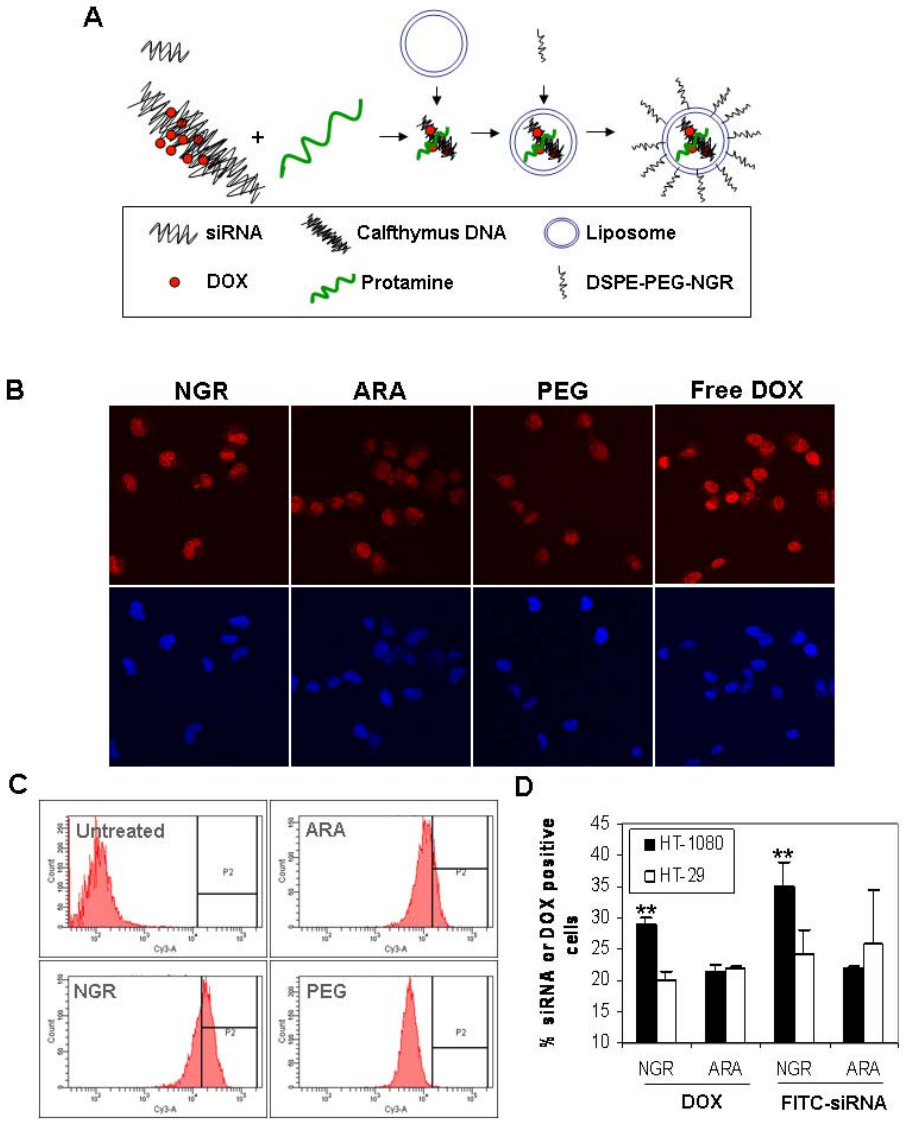

Figure 4.5 Intracellular uptake of DOX *in vitro.* (**A**) illustration of preparation of LPD-PEG-NGR containing siRNA and DOX. (**B**) fluorescence photographs of HT-1080 and HT-29 cells after treatment with DOX in LPD-PEG-NGR (NGR), LPD-PEG-ARA (ARA) and LPD-PEG (PEG) for 1 h. Quantitative measurement of DOX uptake in HT-1080 cells by flow cytometry (**C**). Uptake of siRNA and DOX by HT-1080 and HT-29 cells were compared (**D**). cells were treated with different formulations containing DOX and FITC-siRNA for 1 h and analyzed for fluorescence by flow cytometry. Data = mean ± SD, n = 3. ** indicates $P < 0.001$.

4.3.5 Characterization of the nanoparticles containing siRNA and Dox

In this study, we have explored a novel strategy for specifically co-delivery of siRNA and Dox to the tumor by using DNA-Dox physical complex. The preparation of LPD-PEG-

NGR containing Dox is shown in **Figure 4.5A**. **Figure 4.6** showed that the fluorescence of Dox was quenched upon its intercalation into DNA, whereas the fluorescence was enhanced when the cationic liposomes were added. The average size of the LPD-PEG-NGR nanoparticles containing Dox was 188±29 nm and the zeta potential was 27.2±1.0 mV. The resulting nanoparticles efficiently delivered Dox to the HT-1080 cells as much as the free Dox (**Figure 4.5B**). Dox was found in the nuclei of the cells. Dox uptake was further

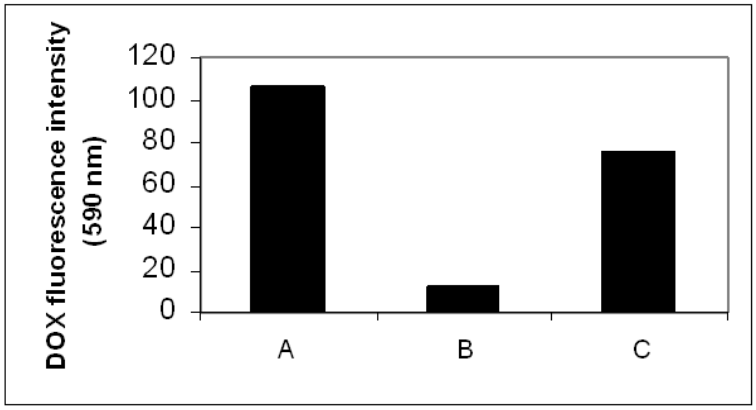

Figure 4.6 DOX fluorescence intensity during the nanoparticle self-assembly. (A) fluorescence of free DOX. **(B)** after the addition of calf thymus DNA and siRNA. Addition of protamine did not change the fluorescence, i.e. same as **(B)**. **(C)** addition of DOTAP/chol liposomes. Dox : DNA : siRNA : protamine = 1:1:1:1.5 (wt ratio).

compared among different nanoparticle formulations by using flow cytometry. FITC labeled siRNA was included in the nanoparticles for comparison. As can be seen in **Figure 4.5D**, both siRNA and Dox were taken up by CD13 positive HT-1080 cells more than the CD13 negative HT-29 cells. However, the enhanced uptake was only seen with formulations targeted with NGR. Thus, peptide targeted LPD nanoparticles showed potential to delivery both siRNA and Dox to tumor cells in a target specific manner.

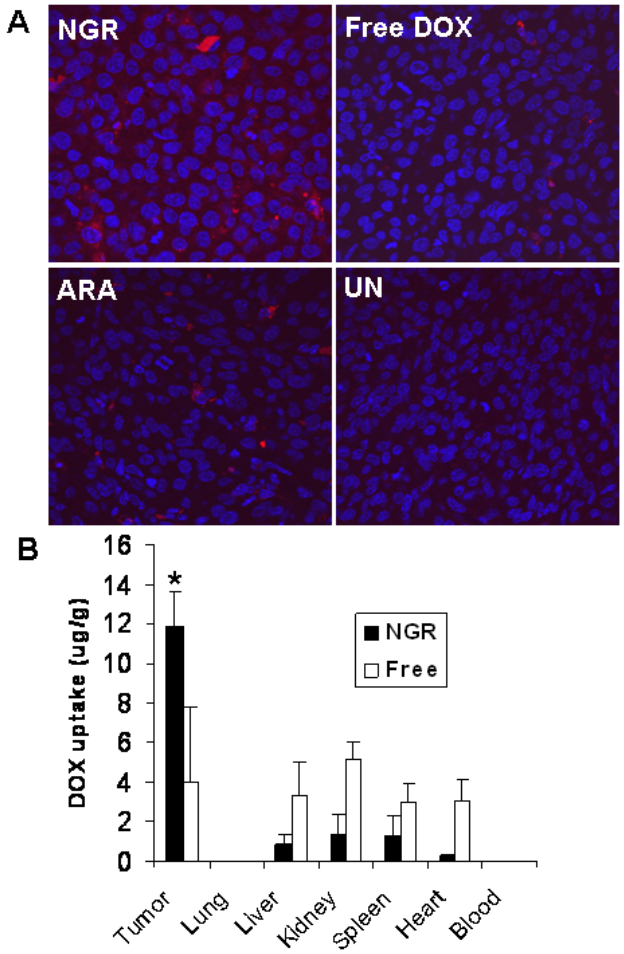

Figure 4.7 Tumor uptake of DOX in different formulations. (**A**) fluorescence signal of DOX in HT-1080 tumor observed by confocal microscopy. (**B**) tissue distribution of DOX in different formulations. Data = mean ± SD, n = 3. * indicates $P<0.05$ compared with free DOX.

4.3.6 Uptake of Dox *in vivo*

We studied the Dox uptake of HT-1080 tumor tissue in the tumor-bearing mice 4 h after i.v. injection using confocal microscopy. As shown in **Figure 4.7A**, the LPD-PEG-NGR showed stronger cytosolic delivery of cy3-siRNA in the tumor tissue than LPD-PEG-ARA and free Dox. The distribution of Dox in the tumor was heterogeneous. These results indicate that the LPD-PEG-NGR can efficiently deliver Dox to the tumor tissue and the intracellular delivery is targeting peptide dependent. In the quantitative analysis (**Figure 4.7B**), liver, kidney, heart and spleen showed stronger uptake of free Dox than Dox formulated in the

targeted nanoparticles, whereas the targeted nanoparticles showed stronger Dox delivery in the tumor tissue than free Dox.

4.3.7 Tumor growth inhibition by nanoparticles containing siRNA and DOX

Three injections of c-myc siRNA in LPD-PEG-NGR showed a partial inhibition of tumor growth ($P < 0.05$ at day 21) (**Figure 4.5 and 4.8**). The control group treated with free Dox at a dose of 0.3mg/kg had no therapeutic effect (**Figure 4.8**). The admixture of free Dox and c-myc siRNA in LPD-PEG-NGR induced similar tumor growth inhibition as c-myc siRNA in LPD-PEG-NGR. A significant improvement in tumor growth inhibition was observed when treated with Dox and c-myc siRNA co-formulated in LPD-PEG-NGR. The results indicate that Dox and c-myc siRNA co-delivered by targeted nanoparticles can synergistically inhibit tumor growth and enhance the therapeutic effect.

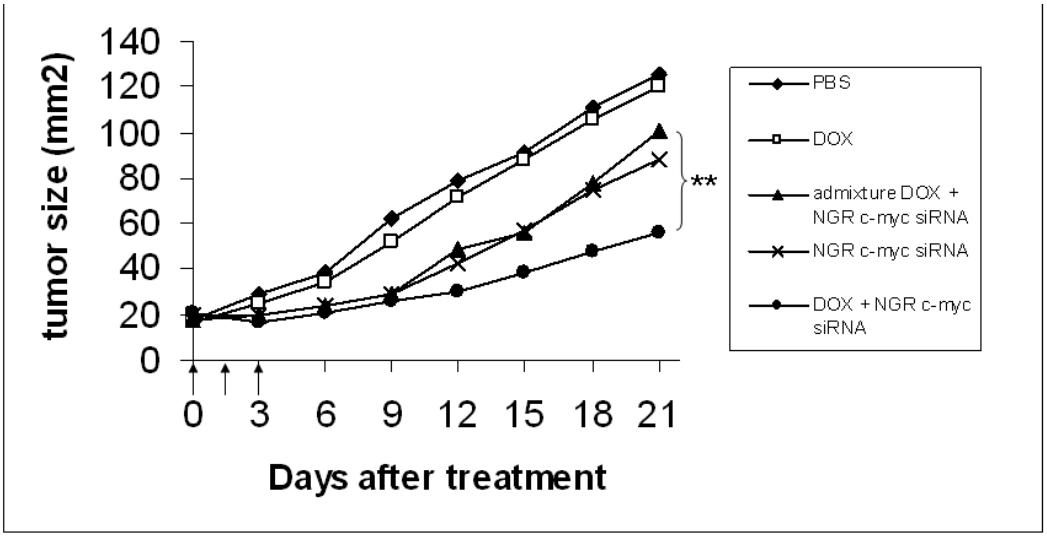

Figure 4.8 HT-1080 xenograft tumor growth inhibition by siRNA and DOX in different formulations. Solid arrows indicate the intravenous administrations of siRNA (1.2 mg/kg) and DOX (0.3 mg/kg). Data = mean, $n = 5–7$. SD of the data points is not shown for clarity. ** indicates $P < 0.01$.

4.4 DISCUSSION

c-Myc gene is a key in cancer onset and maintenance in various human tumors. The genetic alterations of c-myc are related to approximately 70,000 U.S. cancer deaths per year. Over-expression and activation of c-myc induces various forms of cancer. However, expression of the c-myc is also essential for proliferation and regulation in normal mammalian cells. The aim of this study is to design a targeted nanoparticle formulation that can specifically deliver c-myc siRNA into the tumor site, down-regulate c-myc expression in the tumor and achieve therapeutic cures. Our formulation can also help understand the function and mechanism of c-myc in tumor development.

Our results demonstrate that inhibition of c-myc protein expression by siRNA could induce apoptosis in HT-1080 tumors and significantly suppress tumor growth of HT-1080 cells in nude mice (**Figure 4.3** and **4.4**). Through co-delivery of Dox and siRNA in the LPD formulation, siRNA against c-myc sensitized HT-1080 cells to Dox chemotherapy (**Figure 4.8**). The combination strategy may be effective to overcome the drug resistance of cancer cells which over-express c-myc gene. Therefore, the new formulation may serve as a new strategy for cancer therapy.

There are two major issues with siRNA based approaches in cancer therapy: 1. poor selectivity in delivery, i.e., inadequate siRNA uptake by the tumor and nonspecific siRNA uptake by normal tissues, and 2. unfavorable pharmacokinetics, i.e., rapid clearance of free siRNA in the blood. LPD-PEG-NGR is a PEGylated LPD containing siRNA or Dox, or both, coated with a tumor targeting peptide containing the NGR motif. We have demonstrated that the nanoparticles can protect siRNA from degradation in the systemic circulation in our previous study (25). In this study, we have shown that it can deliver siRNA and Dox into the

tumor site, increase the accumulation of siRNA and Dox in the tumor tissues (**Figure** 4.**2** and 4.**7**), down-regulate the target gene (Figure 3) and improved tumor growth inhibition effect (**Figure** 4.**5** and 4.**8**). Furthermore, it has been reported that NGR motif can also target the tumor blood vessels (180). Our results also demonstrate that LPD-PEG-NGR can specifically and efficiently deliver the fluorescence labeled siRNA into the HUVEC endothelial cells. By using siRNA against angiogenesis, our delivery system could serve as a carrier to deliver therapeutic siRNA into tumor vascular endothelial cells and disrupt tumor vasculature. LPD-PEG-NGR containing therapeutic siRNA could serve as a novel anti-cancer agent for a wide variety of tumors.

In **Figure 4.5D**, NGR targeted LPD nanoparticles deliver more siRNA and Dox to HT-1080 tumor cells than to HT-29 tumor cells. However, the nonspecific uptake of Dox (**Figure 4.5C** and **4.5D**) may be due to the poor entrapment of Dox in the LPD nanoparticles. The data in **Figure 4.6** suggest that when the cationic liposomes interacted with the negatively charged DNA/protamine complex, there was a substantial leakage of Dox from the nanoparticle associated DNA. Indeed, Dox encapsulation in the final LPD nanoparticles was only about 20%. It implies that addition of cationic liposome may decrease the entrapment efficiency. The positive charge of the C-3′ amine of Dox is required to stabilize the intercalation into DNA via charge interaction with the negative charge of the DNA phosphate backbone (181). Cationic lipid may directly compete with the Dox for interaction with calf thymus DNA and dislodge Dox from the DNA. However, the small amount of Dox entrapped in the LPD-PEG-NGR induced a significantly increased tumor uptake (**Figure 4.7**) in the HT-1080 tumor model. A significant improvement in therapeutic effect was also achieved by the small amount of Dox entrapped in the targeted nanoparticle (**Figure 4.7**).

Free, un-entrapped Dox was rapidly cleared from the blood circulation after i.v. administration and rarely up-taken in the tumor tissue. If the interaction of DNA with cationic liposomes, but not with protamine, was the cause of the Dox leakage, we will attempt to modify the nanoparticle formulation to enhance entrapment efficacy in our future study.

The tumor homing peptide (NGR) modified nanoparticle provides an enhancement of drug potency and may potentially be a therapeutic agent against drug resistant tumors when combined with siRNA against drug resistant genes such as p-glycoprotein.

5.0 NANOPARTICLES DELIVERING SIRNA AND DOXORUBICIN OVERCOME DRUG RESISTANCE IN CANCER

Multi-drug resistant cells are new targets for cancer therapy as they display drug resistance by over-expression of multiple drug resistance (MDR) transporters which can efflux chemotherapy drug molecules. In this study, we have used a multi-functional anionic LPD-II nanoparticle for efficient systemic co-delivery of small interfering RNA (siRNA) against c-myc and doxorubicin (Dox), into P-gp-positive NCI/ADR-RES tumors in a xenograft model. c-myc siRNA delivered by the targeted nanoparticles significantly down-regulated both c-myc and P-gp expressions in the tumor, caused enhanced Dox uptake and sensitized tumor cells to Dox. Furthermore, the synergistic therapeutic effect of Dox and c-myc siRNA on apoptosis was caspase-3 dependent. Three daily intravenous injections of c-myc siRNA and Dox co-formulated in the targeted nanoparticles showed a significant improvement in tumor growth inhibition. This is the first report of systemic co-delivery of Dox and c-myc siRNA to a drug resistant tumor by using a multi-functional gene delivery system.

5.1 INTRODUCTION

The occurrence of drug resistance is a main impediment to the success of cancer chemotherapy. Cancer cells develop different ways to be resistant to chemotherapy drugs. Over-expression of drug transporter proteins, such as P-glycoprotein (P-gp) plays a key role to regulate drug resistance. Development of strategies to down-regulate the expression of P-

gp or inhibit P-gp function has been the major subject of cancer research. For example, one of the strategies to overcome MDR is to use carriers like nanoparticles to avoid P-gp mediated drug efflux. Only the drug presenting in the cell membrane can be effluxed out of the cancer cell. The drug delivered by nanoparticles is internalized in the cytoplasm or the lysosome and not pumped out by P-gp (182). Doxorubicin (Dox)-loaded liposomes are able to overcome MDR by increasing Dox uptake in the nuclei and extending retention in the nuclei of the MDR cells (183, 184).

Small interfering RNA (siRNA) is a promising novel approach of cancer therapy. It offers a new strategy to down-regulate the targeted oncogene for therapeutic intervention. c-Myc which is over-expressed and activated in various human tumors was selected as a target oncogene in this study. It stimulates cell growth, angiogenesis and transformation which are the keys of the occurrence of the tumor progression and metastasis (161). Suppression of c-myc protein with antisense oligonucleotides impeded tumor growth and sensitizes cancer cells to chemotherapy (162, 163). c-Myc also involves in the regulation of P-gp expression (185, 186). Therefore, c-myc siRNA can be a potential therapeutic agent that sensitizes MDR tumors to chemotherapeutic drugs such as Dox.

Systemically delivering siRNA to tumors remains a major hurdle in cancer gene therapy (142, 187). Major problems of siRNA delivery include poor cellular uptake, low stability and rapid clearance from the systemic circulation. We have developed a nanoparticle formulation, LPD to intravenously deliver siRNA to the solid tumor in high efficiency (25, 40, 59, 169). siRNA-containing LPD is coupled to a targeting moiety that targeted delivers the therapeutic siRNA into cancer cells via receptor specific endocytosis.

In the present study, we have further developed the multi-functional LPD-II nanoparticles, made with anionic lipids which co-deliver siRNA and Dox into the MDR tumor cells and trigger synergistic anti-cancer effect. We co-formulated siRNA and Dox in the LPD-II nanoparticles via Dox intercalation into the DNA in the nanoparticles. The nanoparticles were targeted specifically to the tumor cells by modification with anisamide (AA), a ligand of sigma receptor over-expressed in many human cancer cells. We hypothesized that c-myc siRNA delivered to the MDR cells will down-regulate both c-myc and P-gp and sensitize the tumor cells to the co-delivered Dox, resulting in an enhanced therapeutic activity of the nanomedicine. The experiments were carried out in a xenograft model of the MDR tumor.

5.2 MATERIALS AND METHODS

5.2.1 Materials

DOPA, DOPE and cholesterol were purchased from Avanti Polar Lipids, Inc. (Alabaster, AL). Protamine sulfate (fraction X from salmon) and calf thymus DNA were purchased from Sigma-Aldrich (St. Louis, MO). Dox was purchased from IFFECT CHEMPHAR (Hong Kong). Synthetic 19-nt RNAs with 3' UU overhangs on both sequences were purchased from Dharmacon (Lafayette, CO). For quantitative studies, FITC or cy5.5 was conjugated to 5' sense sequence. 5.5'-cy3 and 5'-FITC labeled siRNA sequence was also obtained from Dharmacon. The sequence of c-myc siRNA was 5'-AACGUUAGCUUCACCAACAUU-3' and control siRNA with sequence 5'-AATTCTCCGAACGTGTCACGT-3' was obtained from Dharmacon.

5.2.2 Cell culture

NCI/ADR-RES cells were a kindly gift of Russell Mumper, PhD (UNC, school of pharmacy). NCI/ADR-RES cells were maintained in DMEM high glucose with GlutaMAX (GibcoBRL) supplemented with 10% fetal bovine serum (Invitrogen, Carlsbad, CA), 100 U/ml penicillin, and 100 μg/ml streptomycin (Invitrogen).

5.2.3 Experimental animals

Female athymic nude mice of age 6–8 weeks were purchased from National Cancer Institute, Frederick, MD. All work performed on animals was in accordance with and permitted by the University of North Carolina Institutional Animal Care and Use committee.

5.2.4 Preparation of PEGylated LPD-II Formulations

LPD-II were prepared according to the previously method with slight modifications (188). Briefly, anionic liposomes composed of DOPA, DOPE and cholesterol (2:1:1 molar ratio) were prepared by thin film hydration followed by membrane extrusion to reduce the particle size. To prepare LPD-II, 48 μL of protamine (2 mg/mL), 60 μL of deionized water, and 24 μL of a mixture of siRNA and calf thymus DNA (2 mg/mL) were mixed and kept at room temperature for 10 min before adding 90 μL of cationic liposome (20 mM). LPD stand at room temperature for 10 min before the addition of DSPE-PEG. LPD was then mixed with 54 μL of DSPE-PEG or DSPE-PEG-AA (10 mg/mL) and kept at 50-60 ºC for 10 min for the attachment of the PEG chains to the surface membrane of the nanoparticles.

5.2.5 Transmission electron microscopy (TEM) image

TEM images of the LPD-II nanoparticles were acquired by the use of JEOL 100CX II TEM (JEOL, Japan). Briefly, 5 μl of LPD-II nanoparticles was dropped on to a 300 mesh carbon coated copper grid (Ted Pella, Inc., Redding, CA). Excess sample was removed by

blotting with a filter paper. The grid was air dried and viewed in TEM without staining. The scale bar was automatically shown in the image according to the magnification.

5.2.6 Cellular Uptake Study

NCI/ADR-RES cells (1×10^5 per well) were seeded in 12-well plates (Corning Inc., Corning, NY) 12 h before experiments. Cells were treated with different formulations at a concentration of 250 nM for 5'-FITC-labeled siRNA or 1.5 μM Dox in serum containing medium at 37 °C for 4 h. Cells were washed twice with PBS, counterstained with DAPI and imaged using a Leica SP2 confocal microscope. Dox and siRNA uptake of NCI/ADR-RES cells was also measured by flow cytometry. Briefly, cells were treated with different formulations at a concentration of 250 nM 5'-FITC-labeled siRNA or 1.5 μM Dox in serum containing medium at 37 °C for 1 h. Cells were harvested and resuspended at a concentration of 1×10^6 cells/mL. Cells were washed with PBS and analyzed for fluorescence by flow cytometry.

5.2.7 Gene silencing study

NCI/ADR-RES tumor bearing mice (tumor size ~1 cm^2) were i.v. injected with siRNA and Dox in different formulations (1.2 mg siRNA/kg, one injection per day for 2 days). A day after the third injection, tumors were collected, paraffin embedded and sectioned. Sections of 7 ¼ μm thick were immunostained with primary antibodies and visualized by using kits from DakoCytomation. Samples were imaged by using a Nikon Microphot SA microscope or Leica SP2 confocal microscope.

5.2.8 Quantitative RT-PCR

NCI/ADR-RES tumor bearing mice (tumor size ~1 cm^2) were i.v. injected with siRNA and Dox in different formulations (1.2 mg siRNA/kg, one injection per day for 2

days). A day after the third injection, mice were killed and tumor samples were collected. Total RNA were extracted with the RNeasy® Mini Kit (Qiagen, Valencia, CA) by following the manufacturer protocol. cDNA was then prepared in the presence of reverse transcriptase (Promega, Madison, WI). The mRNA levels were determined by an ABI PRISM HT7500 sequence detection system (Applied Biosystems, Foster City, CA) as described previously (189). The oligomer pairs used for the amplification of PCR products were AAGCCACAGCATACATCC (forward primer for c-myc), TTACGCACAAGAGTTCCG (reverse primer for c-myc), CACCACCAACTACTTAGC (forward primer for GADPH) and GTAGAGGCAGGAATGATG (reverse primer for GADPH).

5.2.9 Western blot analysis

NCI/ADR-RES tumor bearing mice (tumor size ~1 cm^2) were i.v. injected with siRNA and Dox in different formulations (1.2 mg siRNA/kg, one injection per day for 2 days). A day after the third injection, mice were killed and tumor samples were collected. Total protein (40 μg) isolated from the tumors was loaded on a polyacrylamide gel. Tumor lysate were separated on a 10% acrylamide gel and transferred to a PVDF membrane. Membranes were blocked for 1 h in 5% skim milk and then incubated with polyclonal antibody against c-myc (Santa Cruz Biotechnology, Inc.) overnight. Membranes were washed in PBST (PBS with 0.1% Tween-20) three times and then incubated for 1 h with the secondary antibody. Membranes were washed four times and then developed by an enhanced chemiluminescence system according to the manufacturer's instructions (PerkinElmer).

5.2.10 Tumor uptake study

Mice with tumor size of ~1 cm^2 were i.v. injected with cy5.5-labeled siRNA (1.2 mg/kg) and Dox (1.2mg/kg) in different formulations. Four h later, mice were killed and

tissues were collected, fixed in 10% formalin and embedded in paraffin. Tumor tissues were sectioned (7 ¼ μm thick) and imaged using a Leica SP2 confocal microscope.

5.2.11 Tumor growth inhibition study

NCI/ADR-RES tumor bearing mice (size 16–25 mm^2) were i.v. injected with different formulations containing siRNA (1.2 mg/kg) or Dox (1.2 mg/kg) once per day for 3 days. Tumor size in the treated mice was measured after treatment.

5.2.12 Statistical analysis

All statistical analyses were performed by student *t*-test. Data were considered statistically significant when *p* value was less than 0.05.

5.3 RESULTS

5.3.1 Preparation and characterization of the nanoparticles

We have developed LPD-II nanoparticles for delivering plasmid DNA into tumor cells (188). In this study, we further explored the potential of LPD-II for specifically co-delivery of siRNA and Dox to the tumor by using DNA-Dox physical complex. DNA, Dox and siRNA was first complexed with a slight excess protamine such that the condensed DNA nanoparticles are positively charged. The complex is then entrapped into anionic liposomes composed of DOPE/cholesterol/DOPA (1:1:2 mol/mol) *via* charge interaction. The solution was incubated at 50°C for 10 min with either DSPE-PEG or DSPE-PEG-AA micelles for surface modification of the LPD-II. **Figure 5.1A** showed that the fluorescence of Dox was quenched upon its intercalation into the DNA, and it was further quenched when the anionic

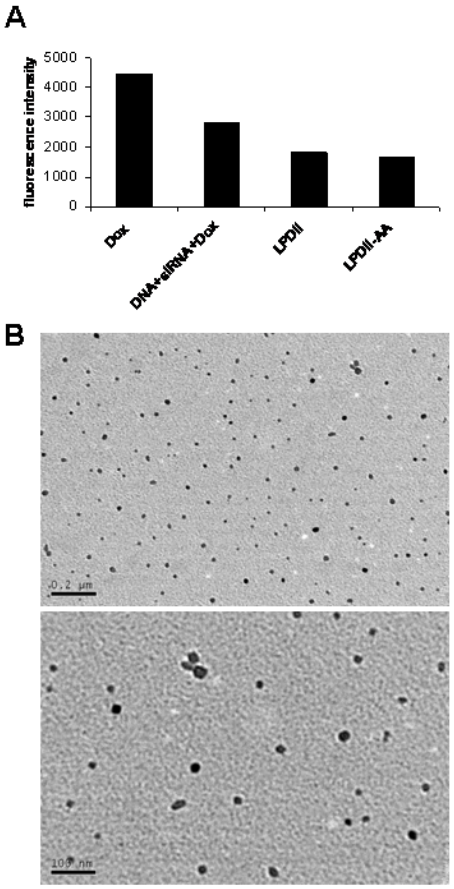

Figure 5.1 Characterization of LPD II nanoparticles. A, DOX fluorescence intensity during the nanoparticle self-assembly. B, TEM images of PEGylated LPD-II nanoparticles shown in two different magnifications.

liposomes were added. The average size of the nanoparticles containing Dox was 62.7 ± 13.3 nm measured by dynamic light scattering and the zeta potential was -19.4 ± 1.1 mV. TEM images of the PEGylated LPD-II nanoparticles are shown in **Figure 5.1B**. These nanoparticles are well-dispersed spheres with sizes ranging from 20 to 50 nm. The particle

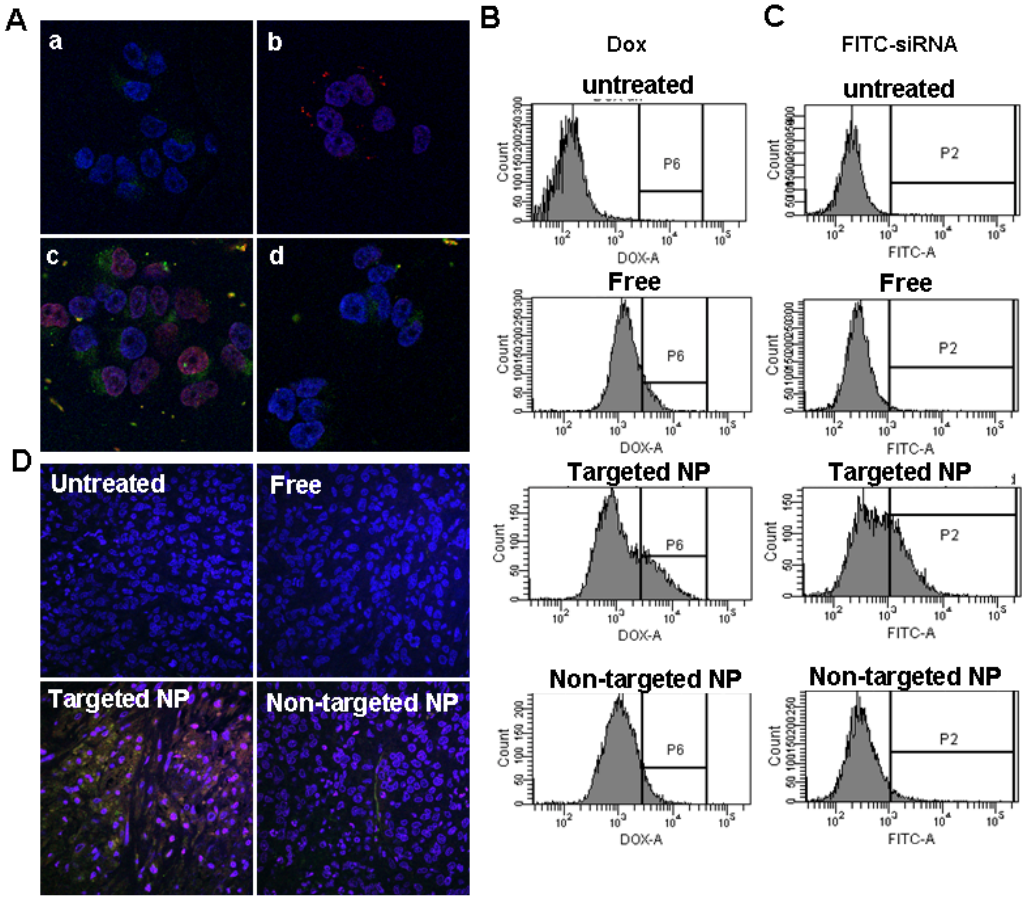

Figure 5.2 Intracellular uptake of siRNA and DOX *in vitro* and *in vivo* A, fluorescence photographs of NCI/ADR-RES cells after treatment with free siRNA (**a**), free Dox (**b**), siRNA and Dox in targeted nanoparticles (**c**) or non-targeted nanoparticles (**d**) for 1 h. Quantitative measurement of Dox (B) and siRNA (C) uptake in NCI/ADR-RES cells by flow cytometry. Cells were treated with different formulations containing Dox or FITC-siRNA for 1 h and analyzed for fluorescence by flow cytometry. D, tumor uptake of siRNA and Dox in different formulations. Fluorescence signal of Cy5.5 labeled siRNA and Dox in NCI/ADR-RES tumor was observed by confocal microscopy. NP: nanoparticle.

size revealed by TEM is usually smaller than that measured by light scattering, because the limiting membrane is not seen in TEM without negative staining.

5.3.2 Uptake of Dox and siRNA *in vitro*

As shown in the confocal micrographs in **Figure 5.2A,** the resulting nanoparticles efficiently delivered Dox (red) and FITC-labeled siRNA (green) to the NCI/ADR-RES cells. Dox was located in the nuclei of the cells and siRNA was found in the cytoplasm. The uptake of fluorescently labeled siRNA was much greater in the cells treated with targeted nanoparticles (LPD-PEG-AA) than the cells treated with non-targeted nanoparticles (LPD-PEG). It indicates that AA, a ligand for the sigma receptor, increased the delivery efficiency of the nanoparticles for NCI/ADR-RES cells. The uptake of fluorescently labeled siRNA was much greater in the cells treated with targeted nanoparticles than the cells treated with free Dox suggesting that the nanoparticles can overcome drug resistance in NCI/ADR-RES cells.

Dox and siRNA uptake was further compared among different nanoparticle formulations by using flow cytometry. As can be seen in **Figure 5.2B and C**, both siRNA and Dox delivered by targeted nanoparticles were taken up by NCI/ADR-RES cells more efficiently than those delivered by non-targeted nanoparticles or free drug. Thus, targeted LPD-II nanoparticles showed potential to delivery both siRNA and Dox to drug resistant tumor cells in a target specific manner.

5.3.3 Uptake of siRNA and Dox *in vivo*

We studied using confocal microscopy the cy5.5-siRNA (green) and Dox (red) uptake of NCI/ADR-RES tumor tissue in the tumor-bearing mice 4 h after i.v. injections. As shown in **Figure 5.2D**, the intracellular fluorescence signals were hardly detected in the tumor tissues collected from mice treated with non-targeted nanoparticles or free drug. The targeted nanoparticles showed strong cytosolic delivery of cy5.5-siRNA and nuclear delivery of Dox in the tumor tissue. Part of Dox co-localized with siRNA (yellow) in the cytoplasm of the

tumor cells. These results indicate that the targeted nanoparticles could efficiently deliver siRNA and Dox to the tumor tissue and the intracellularly delivery was dependent on the presence of the ligand on the nanoparticles.

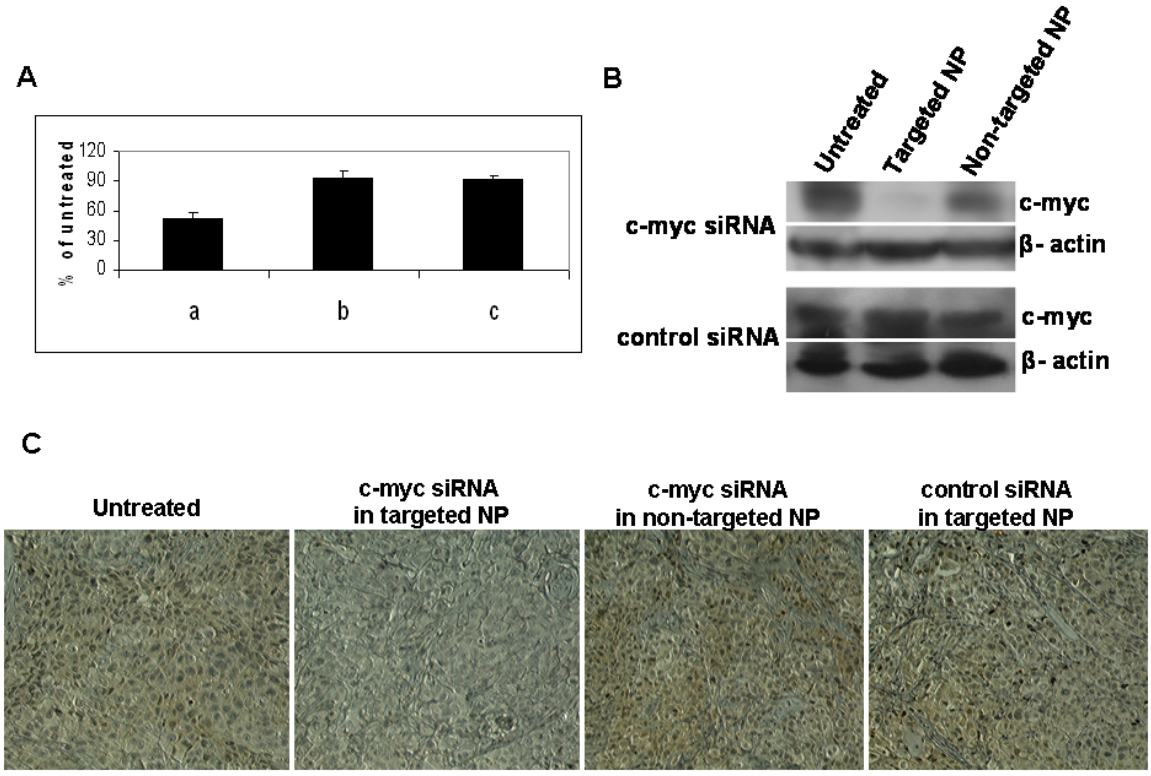

Figure 5.3 c-Myc expression in NCI/ADR-RES xenograft tumor. A**,** quantitative measurement of c-myc mRNA expression in the NCI/ADR-RES xenograft tumor using real time PCR. Western blot analysis (B) and immunostaining (C) of c-myc in the NCI/ADR-RES xenograft tumor after treatment with different formulations. **a**, c-myc siRNA and Dox co-formulated in targeted nanoparticles. **b**, c-myc siRNA and Dox in non-targeted nanoparticles. **c**, control siRNA and Dox in targeted nanoparticles.

5.3.4 c-Myc gene silencing

To address the activities of siRNA *in vivo*, c-myc level in the tumor was assessed by qRT-PCR, western blot analysis and immunostaining (**Figure 5.3**). Both c-myc mRNA and protein expressions of the NCI/ADR-RES tumor treated with c-myc siRNA and Dox-containing targeted nanoparticles were significantly inhibited (**Figure 5.3**). c-Myc expression in NCI/ADR-RES tumor was silenced by c-myc siRNA delivered with targeted

nanoparticles, whereas the non-targeted nanoparticles and the control siRNA showed no effect.

5.3.5 Effect of c-myc down-regulation on MDR transporter expression and drug resistance

To verify the regulatory effects of *c-myc* on the expression of MDR transporters [13], the protein level of MDR transporters were measured 72 h after transfection of the siRNA targeting c-myc. As shown in **Fig. 5.4A**, the MDR expression was significantly decreased in NCI/ADR-RES cells transfected with c-myc siRNA compared with those transfected with control siRNA. To address the MDR down-regulation *in vivo*, MDR level in the tumor was detected by immunostaining (**Figure 5.4C**). The MDR expression of the NCI/ADR-RES tumor treated with c-myc siRNA and Dox-containing targeted nanoparticles was significantly inhibited (**Figure 5.4C**). Non-targeted nanoparticles and the control siRNA showed no effect.

To elucidate whether the down-regulation of the c-myc expression could reverse drug resistance of NCI/ADR-RES cells, Dox uptake was further compared among cells transfected *in vitro* with the c-myc and control siRNAs by using flow cytometry. As shown in **Fig. 5.4B**, free Dox uptake was significantly increased in NCI/ADR-RES cells transfected with c-myc siRNA compared with those transfected with control siRNA. We further studied the Dox uptake of NCI/ADR-RES tumor tissue in the tumor-bearing mice 4 h after i.v. injections using confocal microscopy. Tumor bearing mice were given two daily injections of c-myc or control siRNA (1.2 mg/kg) formulated in the targeted nanoparticles. As shown in **Figure 5.4D**, free Dox uptake was higher in the tumor tissues collected from the mice treated with c-myc siRNA than the mice treated with control siRNA. The targeted nanoparticles

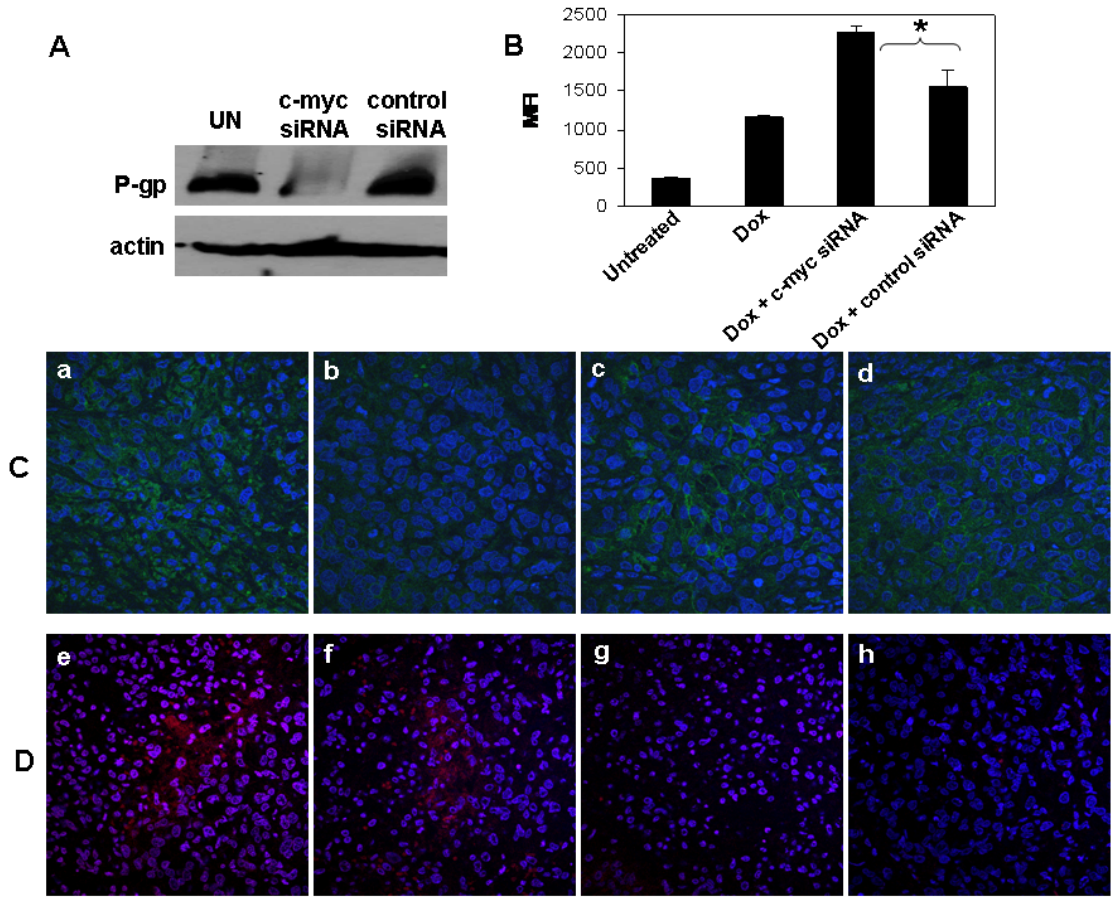

Figure 5.4 MDR expression in NCI/ADR-RES xenograft tumor. A, MDR expression in NCI/ADR-RES cells 72 h after transfection of siRNA with Lipofectamine *in vitro*. B, free Dox uptake in NCI/ADR-RES cells 72 h after transfection of siRNA with Lipofectamine. Cells were treated with free Dox for 30 min and analyzed for fluorescence by flow cytometry. C, MDR expression in NCI/ADR-RES tumors 24 h after dosing of different formulations (two daily intravenous administrations of 1.2 mg/kg siRNA formulated in nanoparticles). D, Tumor uptake of free Dox or Dox in the targeted nanoparticles 4 h after i.v. injection. Fluorescence signal of Dox in HT-1080 tumor was observed by confocal microscopy. Tumor bearing mice were given two daily injections of c-myc or control siRNA (1.2 mg/kg) formulated in the targeted nanoparticles. Free Dox or Dox formulated in the targeted nanoparticles was intravenous injected 24 h after the final treatment of siRNA. **a**, untreated. **b**, c-myc siRNA in targeted nanoparticles. **c**, c-myc siRNA in targeted nanoparticles. **d**, control siRNA in targeted nanoparticles. **e**, i.v administration of Dox in targeted nanoparticles 24 h after treatment of c-myc siRNA. **f**, i.v administration of Dox in targeted nanoparticles 24 h after treatment of control siRNA. **g**, i.v administration of free Dox 24 h after treatment of c-myc siRNA. **h**, i.v administration of free Dox 24 h after treatment of control siRNA. Data = mean ± SD, n = 3. * indicates $P < 0.01$. MFI: mean fluorescence intensity.

encapsulating Dox showed an increased cytosolic delivery of Dox on NCI/ADR-RES cells. Furthermore, the formulated Dox uptake was also slightly higher in the tumor tissues from

mice treated with c-myc siRNA than those treated with control siRNA. These results indicate that the uptakes of both free and formulated Dox were enhanced after treatment with c-myc siRNA in the targeted nanoparticles. These studies suggest that the down-regulation of c-myc expression could reverse drug resistance of NCI/ADR-RES cells through the regulation of MDR transporter expression.

5.3.6 Apoptosis induction and tumor growth inhibition by siRNA nanoparticles

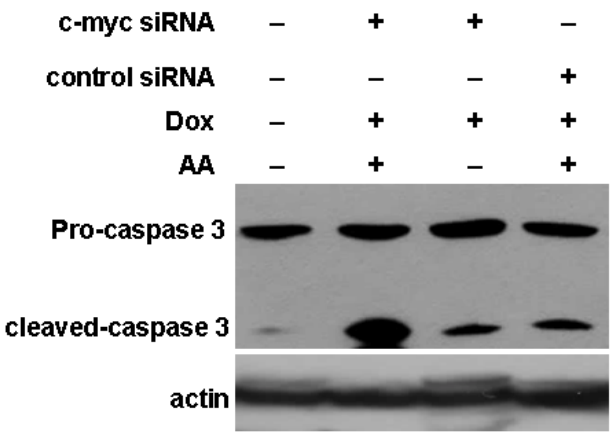

Figure 5.5 Apoptosis induction in NCI/ADR-RES xenograft tumor. Caspase 3 activation in NCI/ADR-RES tumors 24 h after dosing of different formulations (two daily intravenous administrations of 1.2 mg/kg siRNA and 1.2 mg/kg Dox co-formulated in the nanoparticles)

To examine the apoptosis induced by the nanoparticles in the tumors, the level of the active form of caspase-3 was detected by western blot analysis (**Figure 5.5**). Activation of caspase-3 is a common mechanism triggered by factors that induce apoptosis (190). As shown in **Figure 5.5,** active caspase-3 in the NCI/ADR-RES tumor from mice treated with targeted nanoparticles containing c-myc siRNA and Dox was significantly induced compared with those in the control groups. There was a slight increase of the active caspase-3 in the tumors from mice treated with non-targeted nanoparticles or targeted nanoparticles containing Dox and control siRNA compared with the untreated mice. The results indicate that c-myc siRNA and Dox formulated in the targeted nanoparticles could synergistically

promote apoptosis in the NCI/ADR-RES tumor and the cell killing effect was targeting ligand dependent.

To elucidate the synergistic effects of Dox and c-myc siRNA, tumor growth

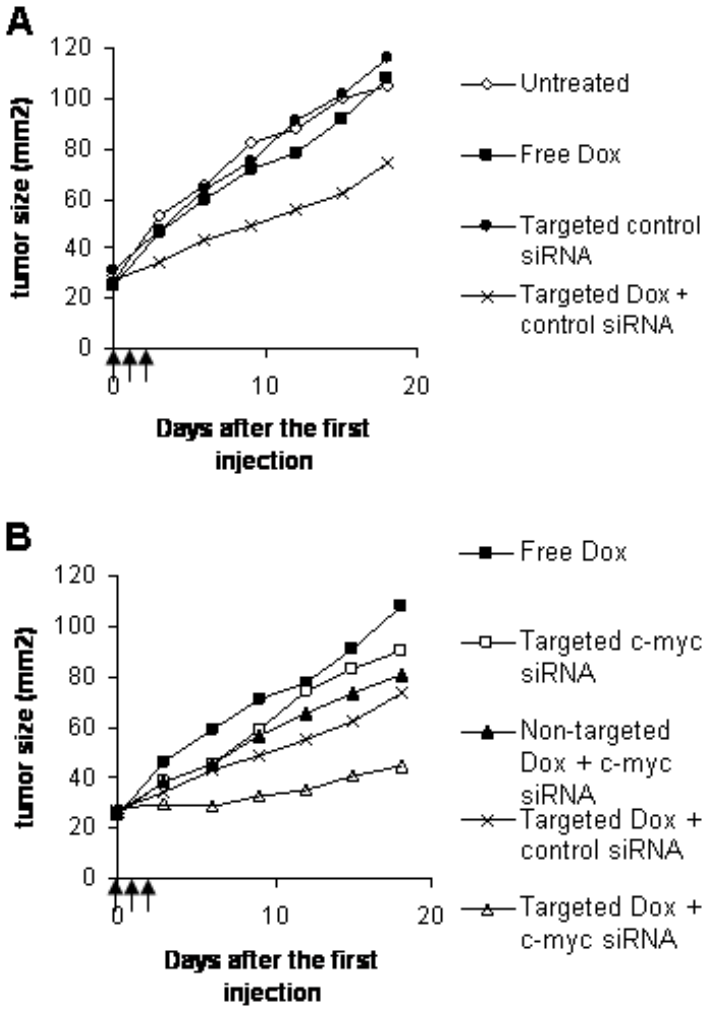

Figure 5.6 Growth inhibition of NCI/ADR-RES xenograft tumor by siRNA and Dox in different formulations. A, Comparison of anti-tumor efficacy of free Dox and Dox delivered by targeted nanoparticles. B, combination of c-myc siRNA and Dox co-formulated in different nanoparticles. Arrows indicate the intravenous administrations of siRNA (1.2 mg/kg) and Dox (1.2 mg/kg). Data = mean, n = 5–7. SDs of the data points are not shown for clarity.

inhibitory effects were examined *in vivo*. Three injections of control siRNA and Dox in the targeted nanoparticles showed a partial inhibition of tumor growth ($P < 0.05$ comparing with the untreated control at day 21) (**Figure 5.6A**). Other control groups treated with control

siRNA formulated in the targeted nanoparticles or free Dox had no therapeutic effect. The results indicate that Dox formulated in the targeted nanoparticles showed enhanced tumor inhibition effect.

Furthermore**,** three injections of c-myc siRNA in the targeted nanoparticles failed to show the therapeutic effect (**Figure 5.6B**). c-Myc siRNA and Dox in the non-targeted nanoparticles showed a partial inhibition of tumor growth ($P < 0.05$ at day 18) (**Figure 5.6B**). A significant tumor growth inhibition was observed when mice were treated with Dox and c-myc siRNA co-formulated in the targeted nanoparticles. Thus, targeted nanoparticles loaded with both Dox and c-myc siRNA could overcome P-gp-mediated drug resistance. Both therapeutic agents acted synergistically to inhibit tumor growth through caspase-3 activation and apoptosis induction.

5.4 Discussion

The occurrence of drug resistance is an important obstacle of cancer therapy. Drug transporter proteins, such as those in the MDR family, are over-expressed in most of drug resistant cancer cell lines and recurrent tumors in cancer patients. Dox is known as a MDR substrate and its reduced uptake and compromised therapeutic efficacy are related to MDR over-expression (191). In this study, our aim was to develop a multi-functional nanoparticle delivery system that can deliver therapeutic siRNA and Dox into the drug resistant tumors and achieve enhance therapeutic effect. The key components of the nanoparticles are a DNA-polycation condensed core coated with an anionic lipid membrane consisting of mainly DOPA. DSPE-PEG modified with AA, a targeting ligand, was also inserted to functionalize the nanoparticle surface. Protamine, an arginine-rich cationic peptide in the DNA-polycation condensed core of nanoparticles may also contribute to disrupting the endosomal membranes

and subsequent siRNA release (192). Recently, we have developed a multi-functional LPD nanoparticle formulation which co-delivers siRNA and Dox into the targeted tumor cells and triggers synergistic anti-cancer effect (193). However, our previously study suggested that when the cationic liposomes interacted with the negatively charged DNA/protamine complex, there was a substantial leakage of Dox from the nanoparticle associated DNA and Dox encapsulation in the final LPD nanoparticles was reduced. Comparing with the previously used LPD nanoparticles, the current LPD-II nanoparticles made with anionic lipids could carry more Dox in the formulation (**Figure 5.1A**).

Our studies demonstrated that siRNA and Dox co-formulated in the targeted nanoparticles showed enhanced cellular uptake of both siRNA and Dox and gene silencing activity in NCI/ADR-RES tumor cells *in vitro* and *in vivo*. A synergistic therapeutic activity was observed in NCI/ADR-RES tumor when treated with c-myc siRNA and Dox co-formulated in the targeted nanoparticles. The enhanced therapeutic effect was dependent on the AA ligand which is a substrate for the sigma receptor over-expressed in NCI/ADR-RES cells (data not shown) and many other cancer cells (111, 112).

Our approach to overcome cancer drug resistant is in two different strategies. First, we use a drug delivery vehicle to deliver Dox and to avoid P-gp -mediated drug efflux. As shown in **Figure 5.2**, targeted nanoparticles delivered more Dox to NCI/ADR-RES cells than non-targeted nanoparticles or free Dox. Dox entrapped in the targeted nanoparticles induced a significantly increased tumor uptake (**Figure 5.2**) in the NCI/ADR-RES tumor model. An enhanced therapeutic effect was achieved by the Dox formulated in the targeted nanoparticle (**Figure 5.5 and 5.6**). The LPD-II nanoparticles may affect drug uptake in MDR cells in three ways. First, the targeted nanoparticles enhance therapeutic efficacy against resistant

tumors by targeting drugs to tumor cells and increasing bioavailability of drugs at the tumor site. Second, the targeted nanoparticles avoid p-gp mediated drug efflux by using ligand dependent internalization. The internalized drugs which can not "see" the efflux transporter are not pumped out of the cells. Furthermore, the entrapped Dox may be maintained for a prolonged period of time in the circulation after i.v. administration and taken up more in the tumor tissue compared with the free Dox. The targeted nanoparticles which selectively deliver Dox to tumor cells can enhance both therapeutic efficacy and safety of the therapeutic agents.

The second strategy is to silence the MDR expression by siRNA. Instead of silencing the MDR itself, we chose to silence c-myc for two reasons. The first is that c-myc has been implicated to positively control MDR expression (186, 194, 195). Silencing c-myc may result in the down-regulation of MDR. The second is that c-myc is a well known oncogene, silencing of which may bring about a direct anticancer effect. In this study, we demonstrated that c-myc siRNA delivered by targeted nanoparticles significantly down-regulated both c-myc and MDR expressions in NCI/ADR-RES tumor, caused enhanced Dox uptake and sensitized drug resistant tumor cells to the co-delivered Dox. c-Myc, a transcription factor over-expressed in many human cancer cells, may activate MDR-1 transcription through the binding of the E-box motif (CACGTG) localized in the *MDR1* gene promoter (-272, -444) (196). Therefore, inhibition of c-myc expression by siRNA results in the down-regulation of the MDR expression.

To the best of our knowledge, this is the first pre-clinical study of systemic co-delivery of therapeutic siRNA and a chemotherapy drug to a drug resistant tumor by using a multi-functional gene delivery system. The nanoparticles used in the study also carried Dox.

Simultaneous delivery of both siRNA and a chemotherapeutic drug can be a powerful approach in cancer therapy, because siRNA can be chosen to inhibit the survival or signaling pathways which trigger drug resistance in cancer cells. We believe our delivery system may provide a platform for development of therapy against other types of cancer resistance to chemotherapy as well.

6.0 NANOPARTICLES MODIFIED WITH SCFV DELIVER SIRNA AND MIRNA FOR CANCER THERAPY

Targeted delivery of RNA-based therapeutics for cancer therapy remains a challenge. We have developed a LPH (liposome-polycation-hyaluronic acid) nanoparticle formulation modified with tumor specific scFv (single chain variable fragment) for systemic delivery of small interfering RNA (siRNA) and microRNA (miRNA) into lung metastasis of murine B16F10 melanoma. The siRNAs delivered by the scFv targeted nanoparticles efficiently down-regulated the target genes (c-myc/MDM-2/VEGF) in the lung metastasis. Two daily i.v. injections of the combined siRNAs in the C4-targeted nanoparticles significantly reduced the tumor load in the lung. miRNA-34a (miR-34a) induced apoptosis and inhibited survivin expression and down-regulated MAPK pathway in B16F10 cells. miR-34a delivered by the C4-targeted nanoparticles significantly down-regulated the survivin expression in the metastatic tumor and reduced tumor load in the lung. When miR-34a and siRNAs were co-formulated in C4-targeted nanoparticles, an enhanced anti-cancer effect was observed.

6.1 INTRODUCTION

RNA-based therapeutics such as siRNA and miRNA provide a promising strategy to treat cancer by targeting the specific proteins involved in the mechanism of proliferation, invasion, anti-apoptosis, drug resistance and metastasis (197-199). Our previous study demonstrated that a combination of siRNAs against MDM2, c-myc, and VEGF co-formulated in the targeted nanoparticles significantly reduced the lung metastasis and

increased the survival time of the tumor-bearing animals (40). miR-34a, a potential tumor suppressor in many types of human cancer including melanoma, was selected as a therapeutic target in this study. miR-34a is commonly down-regulated in many human cancers (200). Multiple mechanisms are involved in the anti-cancer effect of miR-34a. For example, miR-34a inhibits the proliferation and migration and triggers apoptosis in some cancer cell lines via the activation of p53 and down-regulation of c-Met (201, 202). It also directly targets the mRNA encoding E2F3 and significantly suppresses the expression of E2F3 protein, a key regulator of cell cycle progression (203). The activity of survivin promoter is decreased after the treatment of miR-34a (200). Taken together, we hypothesize that miR-34a may serve as a suitable anti-cancer therapeutic agent.

The key to develop RNA-based therapeutics is to have effective strategies for the delivery of siRNA or miRNA *in vivo* (204). For example, modification of antisense RNA with a cholesteryl functionality results in enhanced stability in the serum, improved cellular uptake and inhibition of target miRNA (205). Our strategy is to develop a nanoparticle formulation to deliver siRNA *in vivo* (25, 40, 169). Recently, we further demonstrated LPH containing hyaluronic acid (HA), a FDA approved drug, could systemically deliver siRNA into the tumor with relatively low toxicity compared with the well established LPD formulation. However, the therapeutic effect of the LPH nanoparticles has not been tested yet.

In this study, we have modified LPH nanoparticles with C4 scFv, a tumor specific monoclonal antibody (Zhu et al., Mol Cancer Ther, in press) to effectively deliver siRNA and miRNA to B16F10 lung metastasis in a syngeneic murine model. As a targeting ligand, scFv shows high affinity and low antigenicity in previous studies (206, 207). We hypothesize that

C4 scFv will target the nanoparticles to the lung metastasis and deliver siRNA and miRNA, or both, to inhibit tumor growth. The hypothesis was tested by using a combination of three different siRNAs and miR-45a.

6.2 MATERIALS AND METHODS

6.2.1 Materials

DOTAP, cholesterol, DSPE-PEG_{2000} and DSPE- PEG_{2000}-maleimide (DSPE-PEG-mal) were purchased from Avanti Polar Lipids (Alabaster, AL). Protamine sulfate (fraction X from salmon) and hyaluronic acid sodium salt from *Streptococcus equi* were obtained from Sigma-Aldrich (St. Louis, MO). B16F10 cells, obtained from American Type Culture Collection, were widely used to establish an experimental lung metastasis model. The cells stably expressed GL3 firefly luciferase via retrovirus mediated gene transduction in Dr. Pilar Blancafort's laboratory at the University of North Carolina at Chapel Hill. The cells were maintained in Dulbecco's modified Eagle's medium (Invitrogen, Carlsbad, CA) supplemented with 10% fetal bovine serum (Invitrogen, Carlsbad, CA). Antibodies conjugated with horseradish peroxidase (HRP) (mouse monoclonal antibodies against mouse MDM2, c-myc and rabbit polyclonal antibodies against VEGF), primary antibodies (mouse monoclonal antibodies against p-ERK and β-actin and rabbit polyclonal antibodies against survivin and ERK), and secondary antibodies conjugated with HRP (goat anti-mouse IgG-HRP and goat anti-rabbit IgG-HRP) were purchased from Santa Cruz Biotechnologies (Santa Cruz, CA). Primary antibody against Melan A was purchased from Abcam. MDM2 siRNA (target sequence: 5'-GCUUCGGAACAAGAGACUC-3'), c-myc siRNA (target sequence: 5'-GAACAUCAUCAUCCAGGAC-3'), VEGF siRNA (target sequence: 5'-CGAUGAAGCCCUGGAGUGC-3'), control siRNA (target sequence: 5'-

AATTCTCCGAACGTGTCACGT-3'), miR-34a (mature microRNA sequence: 5'-UGGCAGUGUCUUAGCUGGUUGU-3') and control miRNA were purchased from Dharmacon (Lafayette, CO).

6.2.2 Experimental animals

Female C57BL/6 mice of ages 6–7 weeks (weights 16–18 g) were purchased from NCI. All experiments performed with animals were in accordance with and approved by the Institutional Animal Care and Use Committee at University of North Carolina. C57BL/6 mice were i.v, injected with 2×10^5 B16F10 cells to establish experimental lung metastasis.

6.2.3 Preparation of LPH nanoparticles modified with scFv

The procedure of the formulation preparation was described earlier (208). Briefly, cationic liposomes composed of DOTAP and cholesterol (1:1 molar ratio) were prepared by thin film hydration followed by membrane extrusion to reduce the particle size. To prepare LPH, 18 μL of protamine (2 mg/mL), 140 μL of deionized water, and 24 μL of a mixture of siRNA or miRNA and HA (2 mg/mL) were mixed and kept at room temperature for 10 min before adding 60 μL of cationic liposome (20mM). After 10 min at room temperature, LPH was mixed with 37.8 μL of DSPE-PEG-maleimide (10 mg/mL) and incubated at 50-60 ºC for 10 min. For scFv conjugation, thiolated scFv was incubated with LPH nanoparticles containing DSPE-PEG-mal for 2 h at room temperature and the unreacted maleimide groups were quenched by adding L-cystein.

6.2.4 Cellular Uptake Study

B16F10 cells were seeded in 12-well plates (Corning Inc., Corning, NY) 12 h before experiments. Cells were treated with different formulations at a concentration of 250 nM for

FITC-labeled siRNA in serum containing medium at 37 °C for 1 h. Cells were washed twice with PBS, counterstained with DAPI and imaged using a Leica SP2 confocal microscope.

6.2.5 Gene silencing study and apoptosis analysis *in vitro*

B16F10 cells were seeded into 6 well plates at a concentration of 2 X 10^5 per ml 24 h before transfection. The cells were further transfected with miR-34a or a control miRNA at a final concentration of 100 nM using Lipofectamine 2000 (Invitrogen) according to the manufacturer's recommendations. Cells were harvested for the western blot assay and the analysis of apoptosis 72 h after transfection. Apoptosis was analyzed by annexin V staining. Briefly, 1 × 10^5 cells were harvested 72 h after transfection and resuspended in 100 µl binding buffer containing 5 µl annexin V-FITC (BD Biosciences, California, USA) for 15 min at room temperature in the dark. The Annexin V positive cells were analyzed by flow cytometry.

6.2.6 Gene silencing study in lung metastasis

B16F10 metastasis-bearing mice were given i.v. injections of the combined siRNA or miRNA formulated in the nanoparticles on days 10 and 11. Twenty-four h after the second injection, the mice were sacrificed and the tumor-loaded lungs were collected for the immunostaining or western blot analysis. Expressions of MDM2, c-myc and VEGF in the sections were examined immunohistochemically using the antibodies from a kit [DakoCytomation Envision + Dual Link System-HRP (DAB+); DakoCytomation, Carpinteria, CA] in accordance with the product protocol. The slides were imaged by using a Nikon phase contrast light microscope. For western blotting, total protein (10 µg) isolated from the tumor-loaded lung was electrophoresed in a polyacrylamide/sodium dodecyl sulfate gel and and transferred to a PVDF membrane. The membrane was blocked with 5% nonfat

milk in phosphate-buffered saline for 1 h and then incubated overnight with primary antibody at 4 °C. After the membrane had been washed with PBST (0.1% Tween 20 in PBS) 5 times, it was further incubated with the HRP-conjugated secondary antibody for 1 h. The membrane was washed and developed with enhanced chemiluminescence using ECL plus (GE Health Care, Buckinghamshire, UK) followed by autoradiography.

6.2.7 *In vivo* tumor growth/metastasis inhibition study

B16F10 metastasis-bearing mice were i.v. injected with siRNA or miRNA in the nanoparticles on days 8 and 9. On day 19, the mice were sacrificed and the tumor-loaded lungs were collected. For quantification of the lung metastasis nodules, one lobe per lung was analyzed for luciferase activity. The lung lobe was homogenized in 0.2 ml of lysis buffer (0.05% Triton X-100 and 2 mM EDTA in 0.1 M Tris–HCl) followed by centrifugation at 13,000 rpm for 10 min. Ten μl of the supernatant was mixed with 90 μl of luciferase substrate (Luciferase Assay System; Promega, Madison, WI), and the luciferase activity was measured by a plate reader (Bioscan, Washington, DC). The collected lobe was further fixed in 10% formalin for hematoxylin and eosin staining.

6.2.8 Statistical analysis

All statistical analyses were performed by student *t*-test.

6.3 RESULTS

6.3.1 Delivery of siRNA by using C4 ScFv modified nanoparticles

The LPH nanoparticles were self-assembled by charge-charge interaction. A slight excess amount of HA and siRNA or miRNA was first complexed with protamine such that

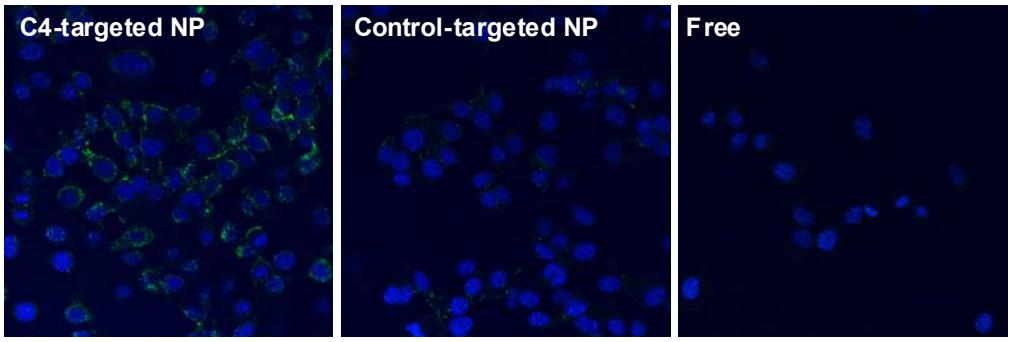

Figure 6.1 Intracellular uptake of siRNA *in vitro*. Fluorescence photographs of B16F10 cells after treatment with free siRNA or siRNA formulated in the C4-targeted or control-targeted nanoparticles for 1 h. Fluorescence signal of FITC-labeled siRNA in B16F10 cells was observed by the confocal microscopy.

the condensed cores were negatively charged. The complex was then encapsulated by cationic liposomes composed of DOTAP/cholesterol (1:1 mol/mol) *via* charge interaction. The nanoparticles were further PEGylated and modified with the tumor specific C4 scFv to increase the stability of the formulation in the blood circulation and selectively deliver the cargo into the tumor cells, respectively. The average size of the nanoparticles modified with C4 scFv was about 170 nm and the zeta potential was 10.9 ± 4.8 mV. As shown in **Figure 6.1**, the uptake of FITC-labeled siRNA was greater in B16F10 cells treated with C4-targeted nanoparticles than cells treated with control-targeted nanoparticles. The labeled siRNA appeared in the cytoplasm of the cells, but not in the nucleus. The result indicates that C4 scFv enhanced intracellular uptake of the nanoparticles for B16F10 cells.

6.3.2 *In vivo* gene silencing study

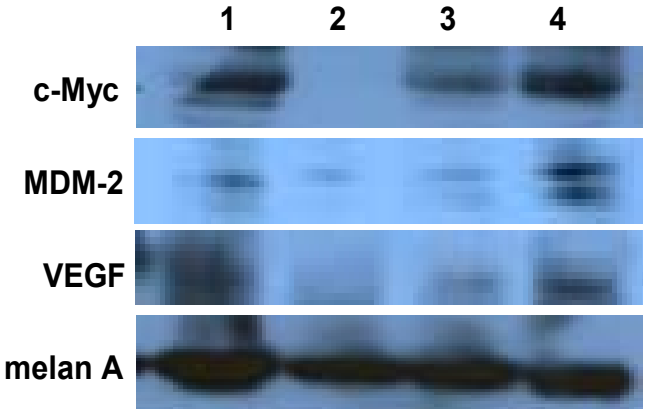

Figure 6.2 Protein expression in B16F10 tumor-bearing lung. Western blot analysis of c-myc, VEGF and MDM-2 in the lungs containing B16F10 metastasis nodules after i.v. injections of combined siRNAs in different formulations. Formulations: untreated control (1), combined siRNAs in the C4-targeted nanoparticles (2), combined siRNAs in the control-targeted nanoparticles (3), control siRNA in the C4-targeted nanoparticles (4).

To further investigate the biological activity of the nanoparticles *in vivo*, combined siRNAs against c-myc, MDM2 and VEGF (1:1:1 weight ratio) were delivered by either C4-targeted or control-targeted nanoparticles. The B16F10 lung metastasis-bearing mice were treated with different formulations on days 10 and 11 with two consecutive i.v. administrations (dose = 0.45 mg total siRNA/kg). The gene silencing activity was determined by western blot analysis (**Figure 6.2**) and immunostaining (**Figure 6.3**). As shown in the figures, the protein expression of c-myc, MDM2 and VEGR in the B16F10 lung metastasis was suppressed by the combined siRNAs delivered with C4-targeted nanoparticles. The control-targeted nanoparticles showed a partial gene silencing effect, whereas the control siRNA delivered by C4-targeted nanoparticles had no effect. The results indicate that the combined siRNAs formulated in the targeted nanoparticles modified with C4 scFv were able to simultaneously silence the expressions of the target oncogenes in the lung metastases.

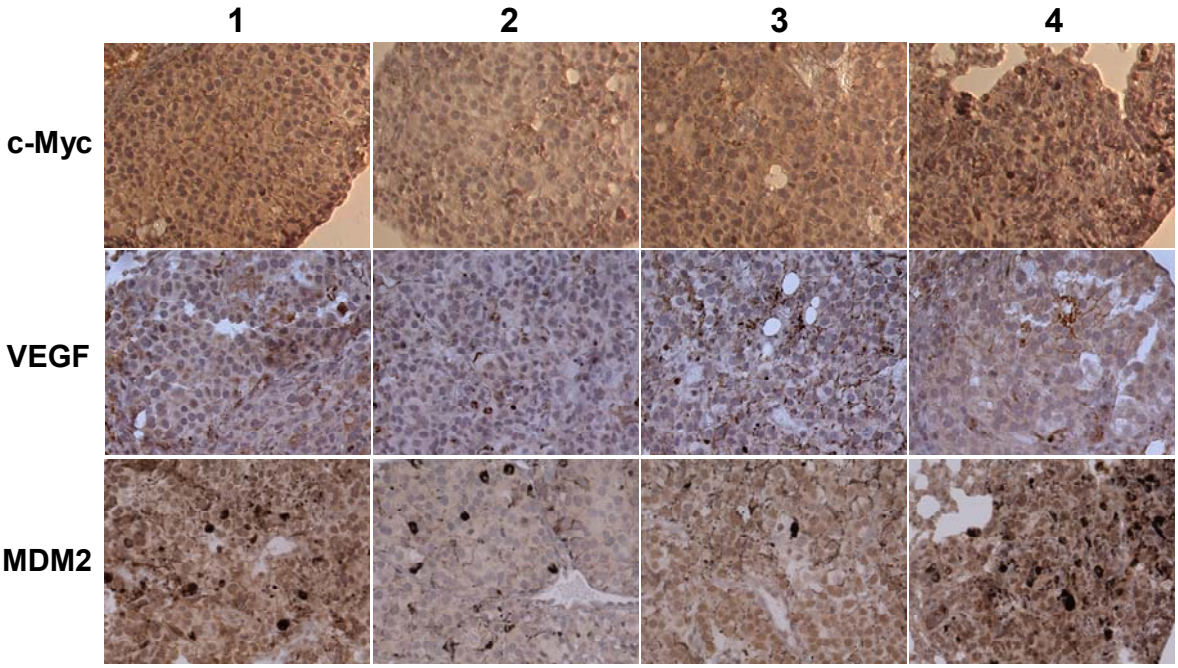

Figure 6.3 Immunostaining of the B16F10 tumor-bearing lung. Immunostaining of c-myc, VEGF and MDM-2 in the B16F10 metastatic nodules after i.v. injections of the combined siRNAs in different formulations. Formulations: untreated control (1), combined siRNAs in the C4-targeted nanoparticles (2), combined siRNAs in the control-targeted nanoparticles (3), control siRNA in the C4-targeted nanoparticles (4).

6.3.3 Tumor growth/metastasis inhibition by siRNA nanoparticles

To elucidate the therapeutic outcomes, the lung metastasis-bearing mice were treated with different formulations on days 8 and 9 with two consecutive i.v. administrations (dose = 0.45 mg total siRNA/kg). As shown in **Figure 6.4A**, the growth of the metastasis nodules in the lung was significantly inhibited when treated with the combined siRNAs formulated in the targeted nanoparticles modified with C4 scFv. Other control groups treated with the combined siRNAs formulated in the control-targeted nanoparticles and the control siRNA formulated in C4-targeted nanoparticles had no therapeutic effect. Furthermore, since B16F10 cells were stably transfected with firefly luciferase gene, the B16F10 lung metastases were further quantified by measuring the luciferase activity in the lung. As shown

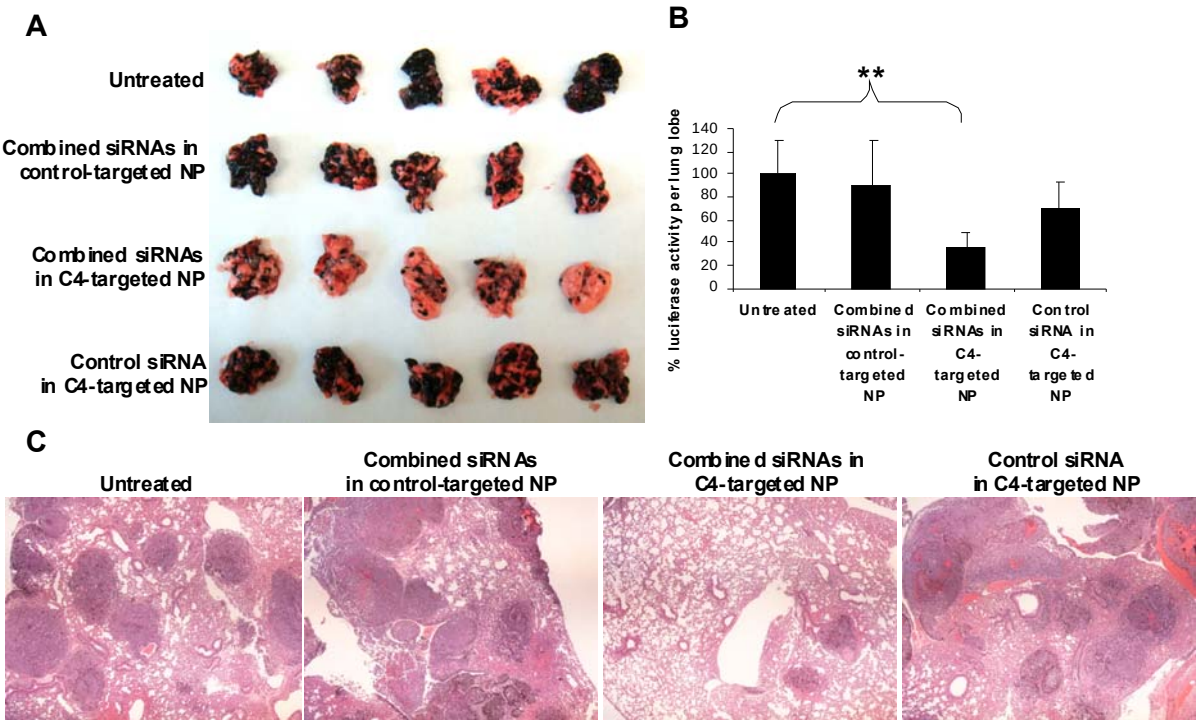

Figure 6.4 Tumor growth/metastasis inhibition by nanoparticles containing siRNA. A, images of the B16F10 tumor-bearing lung on day 19 after two consecutive i.v. injections of siRNAs in different formulations. **B**, luciferase activity in the tumor-bearing lung on day 19 after two consecutive i.v. injections on days 8 and 9 of siRNA in different formulations. $n = 5$. $^{**}P < 0.01$ as compared to the untreated group. **C**, photographs of the hematoxylin and eosin–stained tissue sections of B16F10 tumor-bearing lung on day 19 after two consecutive i.v. injections of siRNAs in different formulations. **NP**: Nanoparticles.

in **Figure 6.4B**, the combined siRNAs delivered by the C4-targeted nanoparticles suppressed the growth of the metastasis nodules; the tumor load decreased to about 30% of the untreated control ($P < 0.01$). Other control treatments showed no obvious therapeutic effect. The hematoxylin and eosin–stained tissue sections (**Figure 6.4C**) also showed a reduction in size and number of the metastasis nodules in the lung after treatment with the combined siRNAs formulated in the C4-targeted nanoparticles, whereas other control groups showed no

significant therapeutic effect. The results indicate that the combined siRNAs delivered by C4-targeted nanoparticles could inhibit the growth of B16F10 lung metastasis.

6.3.4 Apoptosis induction by miR-34a

We first determined whether transfection of miR-34a had any biological function on highly metastatic B16F10 cells. Annexin V staining was carried out to detect apoptosis 72 h after transfection. As shown in **Figure 6.5A**, apoptosis was significantly induced after the treatment with miR-34 compared with the control miRNA. This result suggested that miR-34a triggered cell death and might play a critical role in regulating the survival of B16F10 melanoma cells.

6.3.5 Down-regulation of survivin expression and MAPK signaling by miR-34a

Both survivin and MAPK signaling play important roles in melanoma development and progression and are regulated by miR-34a in some cancer cells (200, 209-212). To further test the specific regulation of survivin and MAPK signaling, B16F10 cells were transfected with miR-34a or a control miRNA. As shown in **Figure 6.5B**, western blot analysis showed that both survivin and p-ERK expressions were significantly down-regulated when B16F10 cells were treated with miR-34a, while the control miRNA had no effect. To further investigate the biological activity of miR-34a *in vivo*, miR-34a was delivered by either C4-targeted or control-targeted nanoparticles. The lung metastases-bearing mice were treated with different formulations on days 10 and 11 with two consecutive i.v. administrations (dose = 0.3 mg RNA/kg). The gene silencing activity was determined by western blot analysis. As shown in **Figure 6.5C**, the protein expression of survivin in the B16F10 lung metastasis was suppressed by miR-34a delivered with the C4-targeted nanoparticles. Neither the control-targeted nanoparticles containing miR-34a nor the control miRNA delivered by C4-targeted

nanoparticles showed any silencing effect. These results indicate that delivery of miR-34a inhibited the survivin expression and inactivated MAPK pathway, thus inducing apoptosis in the B16F10 melanoma.

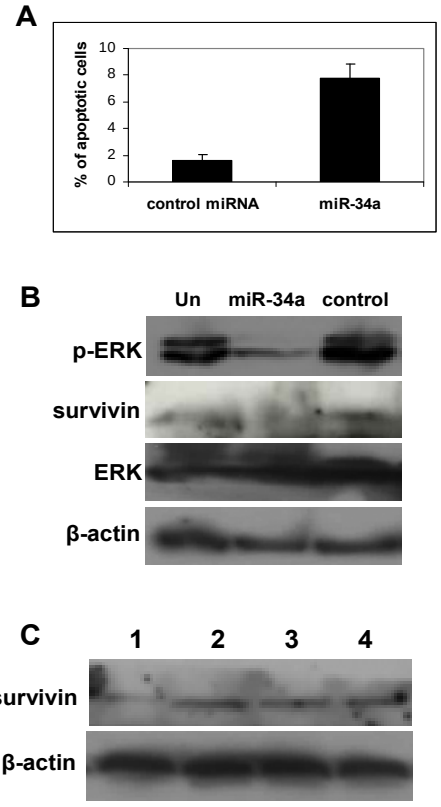

Figure 6.5 Apoptosis induction and target gene down-regulation by miR-34a. A, B16F10 cells treated with miR-34a or a control miRNA for 72 h and analyzed for annexin V staining by flow cytometry. **B**, survivin and pERK expression in B16F10 cells 72 h after transfection with miR-34a or a control miRNA. **C**, western blot analysis of survivin expression in lungs containing B16F10 metastatic nodules after i.v. injections of the miR-34a in different formulations. Formulations: miR-34a in the C4-targeted nanoparticles (1), miR-34a in the control-targeted nanoparticles (2), control miRNA in the C4-targeted nanoparticles (3) and untreated control (4).

6.3.6 Tumor growth/metastasis inhibition by nanoparticles containing siRNA and miRNA

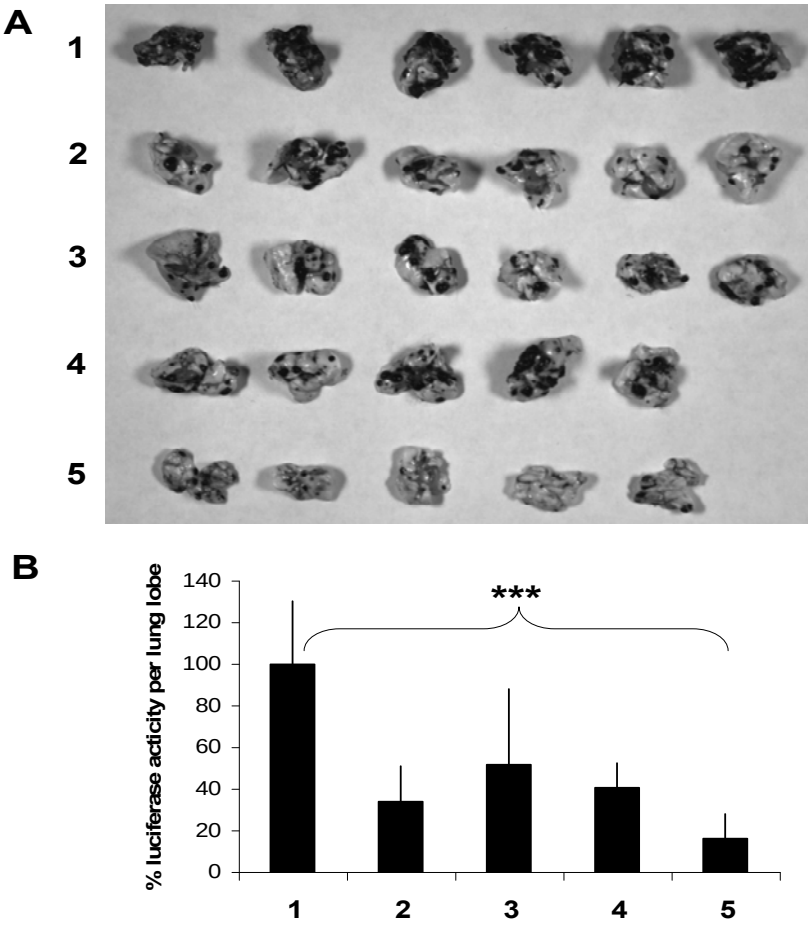

Figure 6.6 Tumor growth/metastasis inhibition by nanoparticles containing siRNA and miRNA A, images of the B16F10 tumor-bearing lungs on day 19 after two consecutive i.v. injections of siRNAs or miRNA in different formulations. **B**, luciferase activity in the tumor-bearing lungs on day 19 after two consecutive i.v. injections on days 8 and 9 of siRNAs and miRNA in different formulations. n = 5~6. *** indicates $P < 0.001$. Formulations: untreated control (1), combined siRNAs and control miRNA in the C4-targeted nanoparticles (2), control siRNA and miR-34a in the C4-targeted nanoparticles (3), combined siRNAs and miR-34a in the control-targeted nanoparticles (4) and combined siRNAs and miR-34a in the C4-targeted nanoparticles (5). Dose = 0.6 mg total RNA/kg. Combined siRNAs = c-myc:MDM-2:VEGF (1:1:1), siRNA:miRNA = 1:1, weight ratios.

To elucidate the therapeutic effect of the combination of siRNAs and miRNA, the lung metastasis-bearing mice were treated with different formulations on days 8 and 9 with two consecutive i.v. administrations (dose = 0.6 mg/kg, c-myc:MDM-2:VEGF:miR-34a = 1:1:1:3, weight ratio). As shown in **Figure 6.6A**, i.v. injections of siRNAs or miR-34a alone

in the C4-targeted nanoparticles showed a partial inhibition of the tumor load in the lung. The presence of the metastasis nodules was synergistically inhibited when treated with siRNAs and miR-34a co-formulated in the C4-targeted nanoparticles. siRNAs and miR-34a co-delivered by the control-targeted nanoparticles had a partial therapeutic effect. B16F10 lung metastasis was further quantified by measuring luciferase activity in the lung. As shown in **Figure 6.6B**, siRNAs and miRNA-34a co-delivered by the C4-targeted nanoparticles synergistically suppressed the growth of the metastasis tumor; the tumor load decreased to about 20% of the untreated control ($P < 0.001$). It was reduced to about 30% and 50% when treated with siRNAs and miR-34a alone, respectively ($P<0.01$). The results indicated that the combination of siRNAs and miR-34a co-delivered by C4-targeted nanoparticles could synergistically inhibit tumor growth and enhanced the therapeutic effect in B16F10 lung metastasis model.

6.4 DISCUSSION

RNA based therapeutics have recently been developed as a potential novel class of therapeutic agent to treat human diseases including cancer. RNA molecules such as siRNA and miRNA are highly effective therapies for cancer based on the ability to specifically silence the expression of cancer-related genes or to selectively regulate the pathways that are involved in the development and progression of malignancy. In this study, our delivery system provides an excellent platform to effectively, safely and selectively deliver RNA based therapeutics into the tumor.

Our study demonstrated that inhibition of c-myc, MDM-2 and VEGF protein expression by siRNA formulated with tumor specific scfv modified LPH nanoparticles significantly suppressed B16F10 metastatic tumor growth (**Figures 6.2, 6.3 and 6.4**).

Through co-delivery of miRNA and siRNA in the LPH formulation, the combination strategy is effective to trigger an enhanced therapeutic effect. To our knowledge, it is the first study of systemic delivery of miRNA for cancer therapy by using a targeted gene delivery system.

Many strategies were developed to treat cancer by targeting the cancer cells without affecting normal cells. Our results demonstrated that the formulation modified with tumor specific scFv is highly effective for delivery of siRNA or miRNA into the B16F10 lung metastasis. scFv has several advantages over the conventional monoclonal antibody or small molecule as a target moiety for drug/gene delivery to cancer. They include profound penetration into the tumor site, high specificity, strong affinity and low toxicity and weak induction of the unwanted immune response. Nanoparticles modified with C4 scFv may be internalized by the cells through receptor-mediated endocytosis. The cell-surface antigen associated with the B16F10 tumor to which C4 scFv targets was not characterized in this study. However, once identified, the tumor associated antigen could become a new target for cancer therapy.

miRNA, a potential therapeutic agent, regulates cellular behavior via specific targeting and down-regulating mRNAs by nearly perfect base-pairing (213). It has been reported that certain miRNAs are involved in the oncogenic and tumor suppressor networks and can potentially inhibit tumorigenesis (214). miR-34a was found to suppress tumor proliferation and migration and cause apoptosis in cancer cells by activating p53 and down-regulating c-Met and E2F3 (201-203). In this study, we found that miR-34a induced apoptosis, suppressed the survivin expression and inactivated MAPK pathway in B16F10 melanoma cells. Unlike other reports, we found the expression of c-Met was unaffected after

transfection of miR-34a (data not shown). The signaling molecules upstream of MAPK pathways which were down-regulated by miR-34a require further investigation.

7.0 SUMMARY

7.1 SUMMARY OF RESEARCH RESULTS AND FUTURE DIRECTIONS

In this study, our objective was to enhance the activity and expand the therapeutic applications of LPD nanoparticles for cancer therapy. First, the novel cationic lipids (DSGLA and DSAA) are developed to avoid the possible anti-apoptotic effect of DOTAP and deliver siRNA with high efficiency (**Chapter 2** and **3**). Our studies demonstrate that siRNA formulated in LPD prepared with an amino acid based cationic lipid containing a guanidine group showed enhanced cellular uptake, gene silencing activity and synergistic therapeutic activity with therapeutic siRNA in tumor cells *in vitro* and *in vivo*. The synergistic killing effect can be well controlled by attaching a targeting ligand to the nanoparticle formulation, which shows potential to be a safe and efficient siRNA based therapy for cancer.

We have also developed a LPD nanoparticle formulation modified with a peptide containing the NGR motif (**Chapter 4**). We have shown that the targeted nanoparticle formulation can specifically deliver c-myc siRNA into the tumor site, down-regulate c-myc expression in the tumor and improve therapeutic activity. Through co-delivery of Dox and siRNA in the LPD nanoparticles, siRNA against c-myc sensitized HT-1080 cells to Dox chemotherapy. The combination strategy has also been used to treat MDR tumors. We have further developed a multi-functional LPD-II nanoparticle formulation which co-delivers siRNA and Dox into the targeted MDR tumor cells and triggers anti-cancer effect (**Chapter**

5). Our studies demonstrated that siRNA and Dox co-formulated in the targeted nanoparticles showed enhanced cellular uptake of both siRNA and Dox and gene silencing activity in MDR tumor cells *in vitro* and *in vivo*. A synergistic therapeutic activity was observed in MDR tumor when treated with c-myc siRNA and Dox co-formulated in the targeted nanoparticles.

Furthermore, we use a foreign DNA, calf thymus DNA, to condense siRNA in the LPD nanoparticles. However, to avoid the unwanted immune responses and make the LPD formulation suitable for the clinical use, we have replaced calf thymus DNA with HA which has been approved by the US FDA. We have modified LPH nanoparticles with C4 scFv, a tumor specific monoclonal antibody (Zhu et al., Mol Cancer Ther, in press) to effectively deliver siRNA and miRNA to B16F10 lung metastasis in a syngeneic murine model. Therapeutic RNAs delivered with C4-targeted nanoparticles inhibit tumor growth in the B16F10 lung metastasis model. Overall, the combination therapy achieved by a single nanoparticle formulation provides a potential effective treatment for cancer.

Our future plan is to further apply the formulation to solve other problems of cancer therapy to enhance the antitumor effect and optimize the formulation to make it more suitable for clinical application. Recently, malignant-melanoma-initiating cells (MMIC) over-expressing ABCB5 P-glycoprotein (P-gp) were identified as novel cancer stem cells. MMIC, capable of self-renewal and differentiation, are required for growth of established tumors and are responsible for melanoma immune evasion (215, 216). Drug resistance is a major impediment to the successful treatment of melanoma as the MMICs which have the ability to efflux the commonly used chemotherapy drug Doxorubicin (Dox) through ABCB5-mediated transport [3]. We believe the key to successfully treating cancer is to attack cancer initiating

cells. Toward this end, siRNA can be a powerful tool to inhibit the survival or signaling pathways which trigger drug resistance in cancer initiating cells. We believe that our targeted multi-functional nanoparticles will be able to efficiently deliver chemotherapy drugs and therapeutic siRNAs into cancer initiating cells and lead to a profound therapeutic effect on malignant melanoma.

7.2 ENDING REMARKS

The work provides several formulations for RNA based cancer therapy. In addition, the ability to target tumor sites of the nanoparticles increased the therapeutic value of RNA therapeutics. The capacity to deliver siRNA or miRNA with the formulations will accelerate research on the function of these RNAs. The delivery systems make it possible to evaluate the functions of different therapeutic siRNAs or miRNAs both *in vivo* and *in vitro*. Such results would contribute to the basic cancer research and to the development of the potential therapeutic agents. Further progress will rely on a better understanding of the formulation itself and siRNA or miRNA function in the tumors. For example, the mechanism of endosomal escape of the LPD nanoparticles and the release of Dox from the multi-functional nanoparticles should be further studied.

APPENDIX A

YUNCHING CHEN'S PUBLICATION

Peer-reviewed Papers

- **Yunching Chen**, Xiaodong Zhu, Xiaoju Zhang, Bin Liu and Leaf Huang Nanoparticles modified with scFv Deliver siRNA and miRNA for Cancer Therapy (Mol Ther, revised)
- **Yunching Chen**, Jun Li and Leaf Huang. Nanoparticles Delivering siRNA and Doxorubicin Overcome Drug Resistance in Cancer (under review)
- **Yunching Chen**, Qi Yang, Surendar Reddy Bathula and Leaf Huang. Guanidinium Containing Cationic Lipid Delivers siRNA and Enhances Anticancer Effect in B16F10 Murine Melanoma Model. 2010 (Journal of Investigative Dermatology, revised)
- **Yunching Chen**, Jinzi Wu and Leaf Huang. Nanoparticles Targeted with Tumor Homing peptide Motif Deliver c-Myc siRNA And Doxorubicin for Targeted Anticancer Therapy.Mol Ther , 2010
- **Yunching Chen**, J.S., Qi Yang, Raffaella Fittipaldi, Surendar Reddy Bathula and Leaf Huang. Novel Cationic Lipid That Delivers and Enhances Therapeutic Activity of siRNA in Lung Cancer Cells. Molecular pharmaceutics, 2009
- Jun Li; **Yun-Ching Chen**; Yu-Cheng Tseng; Leaf Huang, Biodegradable Calcium Phosphate Nanoparticle with Lipid Coating for Systemic siRNA Delivery. Journal of Control Release 2009
- Shyh-Dar Li, **Yung-Ching Chen**, Michael J. Hackett and Leaf Huang. Targeted Delivery of siRNA by Self-assembled Nanoparticles. Mol Ther 16 (1): 163-169, 2008

Review Papers and Perspectives

- **Yunching Chen**.and Leaf Huang. Tumor-targeted delivery of siRNA by non-viral vector: safe and effective cancer therapy. Expert Opin Drug Deliv 5, (12), 1301-11.

Conference Abstracts

- **Yunching Chen**, Surendar Reddy Bathula and Leaf Huang. Novel Cationic Lipid That Delivers and Enhances Therapeutic Activity of siRNA in Melanoma Model. Chapel Hill Drug Conference, 2009
- **Yunching Chen**, J.S., Qi Yang, Raffaella Fittipaldi, Surendar Reddy Bathula and Leaf Huang. Novel Cationic Lipid That Targeted Delivers and Enhances Therapeutic Activity of siRNA in Cancer Cells. 7th Globalization of Pharmaceutics Education Network, Belgium, 2008
- **Yunching Chen**, J.S and Leaf Huang. Novel Cationic Lipid That Delivers and Enhances Therapeutic Activity of siRNA in Lung Cancer Cells. 11th Liposome Research Days Conference, Japan, 2008

BIBLIOGRAPHY

1. Napoli C, Lemieux C, Jorgensen R. Introduction of a Chimeric Chalcone Synthase Gene into Petunia Results in Reversible Co-Suppression of Homologous Genes in trans. Plant Cell 1990; 2: 279-89.

2. Ketzinel-Gilad M, Shaul Y, Galun E. RNA interference for antiviral therapy. J Gene Med 2006; 8: 933-50.

3. Fire A, Xu S, Montgomery MK, Kostas SA, Driver SE, Mello CC. Potent and specific genetic interference by double-stranded RNA in Caenorhabditis elegans. Nature 1998; 391: 806-11.

4. Zamore PD, Tuschl T, Sharp PA, Bartel DP. RNAi: double-stranded RNA directs the ATP-dependent cleavage of mRNA at 21 to 23 nucleotide intervals. Cell 2000; 101: 25-33.

5. Elbashir SM, Harborth J, Lendeckel W, Yalcin A, Weber K, Tuschl T. Duplexes of 21-nucleotide RNAs mediate RNA interference in cultured mammalian cells. Nature 2001; 411: 494-8.

6. Kim K, Lee YS, Harris D, Nakahara K, Carthew RW. The RNAi pathway initiated by Dicer-2 in Drosophila. Cold Spring Harb Symp Quant Biol 2006; 71: 39-44.

7. Li CX, Parker A, Menocal E, Xiang S, Borodyansky L, Fruehauf JH. Delivery of RNA interference. Cell Cycle 2006; 5: 2103-9.

8. Dave RS, Pomerantz RJ. RNA interference: on the road to an alternate therapeutic strategy! Rev Med Virol 2003; 13: 373-85.

9. Hoerter JA, Walter NG. Chemical modification resolves the asymmetry of siRNA strand degradation in human blood serum. RNA 2007; 13: 1887-93.

10. Butowski N, Chang SM. Small molecule and monoclonal antibody therapies in neurooncology. Cancer Control 2005; 12: 116-24.

11. Qi JH, Claesson-Welsh L. VEGF-induced activation of phosphoinositide 3-kinase is dependent on focal adhesion kinase. Exp Cell Res 2001; 263: 173-82.

12. Hadj-Slimane R, Lepelletier Y, Lopez N, Garbay C, Raynaud F. Short interfering RNA (siRNA), a novel therapeutic tool acting on angiogenesis. Biochimie 2007; 89: 1234-44.

13. Xie FY, Woodle MC, Lu PY. Harnessing in vivo siRNA delivery for drug discovery and therapeutic development. Drug Discov Today 2006; 11: 67-73.

14. Das B, Yeger H, Tsuchida R, et al. A hypoxia-driven vascular endothelial growth factor/Flt1 autocrine loop interacts with hypoxia-inducible factor-1alpha through mitogen-activated protein kinase/extracellular signal-regulated kinase 1/2 pathway in neuroblastoma. Cancer Res 2005; 65: 7267-75.

15. List AF, Glinsmann-Gibson B, Stadheim C, Meuillet EJ, Bellamy W, Powis G. Vascular endothelial growth factor receptor-1 and receptor-2 initiate a phosphatidylinositide 3-kinase-dependent clonogenic response in acute myeloid leukemia cells. Exp Hematol 2004; 32: 526-35.

16. Kou R, SenBanerjee S, Jain MK, Michel T. Differential regulation of vascular endothelial growth factor receptors (VEGFR) revealed by RNA interference: interactions of VEGFR-1 and VEGFR-2 in endothelial cell signaling. Biochemistry 2005; 44: 15064-73.

17. Huang DD. The potential of RNA interference-based therapies for viral infections. Curr HIV/AIDS Rep 2008; 5: 33-9.

18. Wieczorek M, Paczkowska A, Guzenda P, Majorek M, Bednarek AK, Lamparska-Przybysz M. Silencing of Wnt-1 by siRNA induces apoptosis of MCF-7 human breast cancer cells. Cancer Biol Ther 2008; 7: 268-74.

19. Rosell R, Cecere F, Cognetti F, et al. Future directions in the second-line treatment of non-small cell lung cancer. Semin Oncol 2006; 33: S45-51.

20. Guo J, Verma UN, Gaynor RB, Frenkel EP, Becerra CR. Enhanced chemosensitivity to irinotecan by RNA interference-mediated down-regulation of the nuclear factor-kappaB p65 subunit. Clin Cancer Res 2004; 10: 3333-41.

21. Guo J, Fu YC, Becerra CR. Dissecting role of regulatory factors in NF-kappaB pathway with siRNA. Acta Pharmacol Sin 2005; 26: 780-8.

22. Jones HE, Gee JM, Hutcheson IR, Knowlden JM, Barrow D, Nicholson RI. Growth factor receptor interplay and resistance in cancer. Endocr Relat Cancer 2006; 13 Suppl 1: S45-51.

23. Nicholson RI, Gee JM, Harper ME. EGFR and cancer prognosis. Eur J Cancer 2001; 37 Suppl 4: S9-15.

24. Scaltriti M, Baselga J. The epidermal growth factor receptor pathway: a model for targeted therapy. Clin Cancer Res 2006; 12: 5268-72.

25. Li SD, Chen YC, Hackett MJ, Huang L. Tumor-targeted delivery of siRNA by self-assembled nanoparticles. Mol Ther 2008; 16: 163-9.

26. Diehl KM, Grewal N, Ethier SP, Woods-Ignatoski KM. p38MAPK-activated AKT in HER-2 overexpressing human breast cancer cells acts as an EGF-independent survival signal. J Surg Res 2007; 142: 162-9.

27. Zhou BP, Liao Y, Xia W, Zou Y, Spohn B, Hung MC. HER-2/neu induces p53 ubiquitination via Akt-mediated MDM2 phosphorylation. Nat Cell Biol 2001; 3: 973-82.

28. Yoshizawa T, Hattori Y, Hakoshima M, Koga K, Maitani Y. Folate-linked lipid-based nanoparticles for synthetic siRNA delivery in KB tumor xenografts. Eur J Pharm Biopharm 2008.

29. Wang R, Lin F, Wang X, et al. The therapeutic potential of survivin promoter-driven siRNA on suppressing tumor growth and enhancing radiosensitivity of human cervical carcinoma cells via downregulating hTERT gene expression. Cancer Biol Ther 2007; 6: 1295-301.

30. Shen Y, Zhang YW, Zhang ZX, Miao ZH, Ding J. hTERT-targeted RNA interference inhibits tumorigenicity and motility of HCT116 cells. Cancer Biol Ther 2008; 7: 228-36.

31. Wang H, Nan L, Yu D, Agrawal S, Zhang R. Antisense anti-MDM2 oligonucleotides as a novel therapeutic approach to human breast cancer: in vitro and in vivo activities and mechanisms. Clin Cancer Res 2001; 7: 3613-24.

32. Martinez LA, Naguibneva I, Lehrmann H, et al. Synthetic small inhibiting RNAs: efficient tools to inactivate oncogenic mutations and restore p53 pathways. Proc Natl Acad Sci U S A 2002; 99: 14849-54.

33. Lawen A. Apoptosis-an introduction. Bioessays 2003; 25: 888-96.

34. Hao JH, Gu QL, Liu BY, et al. Inhibition of the proliferation of human gastric cancer cells SGC-7901 in vitro and in vivo using Bcl-2 siRNA. Chin Med J (Engl) 2007; 120: 2105-11.

35. Reed JC, Miyashita T, Takayama S, et al. BCL-2 family proteins: regulators of cell death involved in the pathogenesis of cancer and resistance to therapy. J Cell Biochem 1996; 60: 23-32.

36. Reinhold WC, Kouros-Mehr H, Kohn KW, et al. Apoptotic susceptibility of cancer cells selected for camptothecin resistance: gene expression profiling, functional analysis, and molecular interaction mapping. Cancer Res 2003; 63: 1000-11.

37. Herman JF, Mangala LS, Mehta K. Implications of increased tissue transglutaminase (TG2) expression in drug-resistant breast cancer (MCF-7) cells. Oncogene 2006; 25: 3049-58.

38. Riddick DS, Lee C, Ramji S, et al. Cancer chemotherapy and drug metabolism. Drug Metab Dispos 2005; 33: 1083-96.

39. Chen SM, Wang Y, Xiao BK, Tao ZZ. Effect of blocking VEGF, hTERT and Bcl-xl by multiple shRNA expression vectors on the human laryngeal squamous carcinoma xenograft in nude mice. Cancer Biol Ther 2007; 7.

40. Li SD, Chono S, Huang L. Efficient oncogene silencing and metastasis inhibition via systemic delivery of siRNA. Mol Ther 2008; 16: 942-6.

41. Chen AM, Zhang M, Wei D, et al. Co-delivery of doxorubicin and Bcl-2 siRNA by mesoporous silica nanoparticles enhances the efficacy of chemotherapy in multidrug-resistant cancer cells. Small 2009; 5: 2673-7.

42. Villares GJ, Zigler M, Wang H, et al. Targeting melanoma growth and metastasis with systemic delivery of liposome-incorporated protease-activated receptor-1 small interfering RNA. Cancer Res 2008; 68: 9078-86.

43. Scacheri PC, Rozenblatt-Rosen O, Caplen NJ, et al. Short interfering RNAs can induce unexpected and divergent changes in the levels of untargeted proteins in mammalian cells. Proc Natl Acad Sci U S A 2004; 101: 1892-7.

44. Pirollo KF, Chang EH. Targeted delivery of small interfering RNA: approaching effective cancer therapies. Cancer Res 2008; 68: 1247-50.

45. Grimm D, Pandey K, Kay MA. Adeno-associated virus vectors for short hairpin RNA expression. Methods Enzymol 2005; 392: 381-405.

46. Muruve DA. The innate immune response to adenovirus vectors. Hum Gene Ther 2004; 15: 1157-66.

47. Sato A, Choi SW, Hirai M, et al. Polymer brush-stabilized polyplex for a siRNA carrier with long circulatory half-life. J Control Release 2007; 122: 209-16.

48. Kakizawa Y, Furukawa S, Ishii A, Kataoka K. Organic-inorganic hybrid-nanocarrier of siRNA constructing through the self-assembly of calcium phosphate and PEG-based block aniomer. J Control Release 2006; 111: 368-70.

49. Vasir JK, Labhasetwar V. Polymeric nanoparticles for gene delivery. Expert Opin Drug Deliv 2006; 3: 325-44.

50. Bolcato-Bellemin AL, Bonnet ME, Creusat G, Erbacher P, Behr JP. Sticky overhangs enhance siRNA-mediated gene silencing. Proc Natl Acad Sci U S A 2007; 104: 16050-5.

51. Werth S, Urban-Klein B, Dai L, et al. A low molecular weight fraction of polyethylenimine (PEI) displays increased transfection efficiency of DNA and siRNA in fresh or lyophilized complexes. J Control Release 2006; 112: 257-70.

52. Lee JS, Green JJ, Love KT, Sunshine J, Langer R, Anderson DG. Gold, poly(beta-amino ester) nanoparticles for small interfering RNA delivery. Nano Lett 2009; 9: 2402-6.

53. Song WJ, Du JZ, Sun TM, Zhang PZ, Wang J. Gold Nanoparticles Capped with Polyethyleneimine for Enhanced siRNA Delivery. Small 2009.

54. Andersen MO, Howard KA, Paludan SR, Besenbacher F, Kjems J. Delivery of siRNA from lyophilized polymeric surfaces. Biomaterials 2008; 29: 506-12.

55. Rozema DB, Lewis DL, Wakefield DH, et al. Dynamic PolyConjugates for targeted in vivo delivery of siRNA to hepatocytes. Proc Natl Acad Sci U S A 2007; 104: 12982-7.

56. Novobrantseva TI, Akinc A, Borodovsky A, de Fougerolles A. Delivering silence: advancements in developing siRNA therapeutics. Curr Opin Drug Discov Devel 2008; 11: 217-24.

57. Halder J, Kamat AA, Landen CN, Jr., et al. Focal adhesion kinase targeting using in vivo short interfering RNA delivery in neutral liposomes for ovarian carcinoma therapy. Clin Cancer Res 2006; 12: 4916-24.

58. Merritt WM, Lin YG, Spannuth WA, et al. Effect of interleukin-8 gene silencing with liposome-encapsulated small interfering RNA on ovarian cancer cell growth. J Natl Cancer Inst 2008; 100: 359-72.

59. Li SD, Huang L. Surface-modified LPD nanoparticles for tumor targeting. Ann N Y Acad Sci 2006; 1082: 1-8.

60. Auguste DT, Furman K, Wong A, et al. Triggered release of siRNA from poly(ethylene glycol)-protected, pH-dependent liposomes. J Control Release 2008.

61. Yagi N, Manabe I, Tottori T, et al. A nanoparticle system specifically designed to deliver short interfering RNA inhibits tumor growth in vivo. Cancer Res 2009; 69: 6531-8.

62. de Wolf HK, Snel CJ, Verbaan FJ, Schiffelers RM, Hennink WE, Storm G. Effect of cationic carriers on the pharmacokinetics and tumor localization of nucleic acids after intravenous administration. Int J Pharm 2007; 331: 167-75.

63. Leng Q, Scaria P, Zhu J, Ambulos N, Campbell P, Mixson AJ. Highly branched HK peptides are effective carriers of siRNA. J Gene Med 2005; 7: 977-86.

64. Christian S, Pilch J, Akerman ME, Porkka K, Laakkonen P, Ruoslahti E. Nucleolin expressed at the cell surface is a marker of endothelial cells in angiogenic blood vessels. J Cell Biol 2003; 163: 871-8.

65. Derfus AM, Chen AA, Min DH, Ruoslahti E, Bhatia SN. Targeted quantum dot conjugates for siRNA delivery. Bioconjug Chem 2007; 18: 1391-6.

66. Shao K, Hou Q, Go ML, et al. Sulfatide-tenascin interaction mediates binding to the extracellular matrix and endocytic uptake of liposomes in glioma cells. Cell Mol Life Sci 2007; 64: 506-15.

67. Li J, Chen YC, Tseng YC, Mozumdar S, Huang L. Biodegradable calcium phosphate nanoparticle with lipid coating for systemic siRNA delivery. J Control Release; 142: 416-21.

68. Xia CF, Zhang Y, Boado RJ, Pardridge WM. Intravenous siRNA of brain cancer with receptor targeting and avidin-biotin technology. Pharm Res 2007; 24: 2309-16.

69. Pirollo KF, Rait A, Zhou Q, et al. Materializing the potential of small interfering RNA via a tumor-targeting nanodelivery system. Cancer Res 2007; 67: 2938-43.

70. Tietze N, Pelisek J, Philipp A, et al. Induction of Apoptosis in Murine Neuroblastoma by Systemic Delivery of Transferrin-Shielded siRNA Polyplexes for Downregulation of Ran. Oligonucleotides 2008; 18: 161-74.

71. Bartlett DW, Su H, Hildebrandt IJ, Weber WA, Davis ME. Impact of tumor-specific targeting on the biodistribution and efficacy of siRNA nanoparticles measured by multimodality in vivo imaging. Proc Natl Acad Sci U S A 2007; 104: 15549-54.

72. Cerchia L, Hamm J, Libri D, Tavitian B, de Franciscis V. Nucleic acid aptamers in cancer medicine. FEBS Lett 2002; 528: 12-6.

73. McNamara JO, 2nd, Andrechek ER, Wang Y, et al. Cell type-specific delivery of siRNAs with aptamer-siRNA chimeras. Nat Biotechnol 2006; 24: 1005-15.

74. Chono S, Li S-D, Huang L. An efficient and low immunostimulatory nanoparticle formulation for systemic siRNA delivery to the tumor. Journal of controlled release 2008.

75. Cho K, Wang X, Nie S, Chen ZG, Shin DM. Therapeutic nanoparticles for drug delivery in cancer. Clin Cancer Res 2008; 14: 1310-6.

76. Colin M, Maurice M, Trugnan G, et al. Cell delivery, intracellular trafficking and expression of an integrin-mediated gene transfer vector in tracheal epithelial cells. Gene Ther 2000; 7: 139-52.

77. WHO. Gender in lung cancer and smoking research. WHO 2004: 1-43.

78. Christopher ME, Wong JP. Recent developments in delivery of nucleic acid-based antiviral agents. Curr Pharm Des 2006; 12: 1995-2006.

79. Kawashita Y, Fujioka H, Ohtsuru A, et al. The efficacy and safety of gene transfer into the porcine liver in vivo by HVJ (Sendai virus) liposome. Transplantation 2005; 80: 1623-9.

80. Hou JQ, He J, Wang XL, Wen DG, Chen ZX. Effect of small interfering RNA targeting survivin gene on biological behaviour of bladder cancer. Chin Med J (Engl) 2006; 119: 1734-9.

81. Ohri SS, Vashishta A, Proctor M, Fusek M, Vetvicka V. Depletion of Procathepsin D Gene Expression by RNA Interference: A Potential Therapeutic Target for Breast Cancer. Cancer Biol Ther 2007; 6.

82. Qian H, Yu J, Li Y, et al. RNA interference against metastasis-associated gene 1 inhibited metastasis of B16F10 melanoma cell in C57BL/6 model. Biol Cell 2007.

83. Tong AW. Small RNAs and non-small cell lung cancer. Curr Mol Med 2006; 6: 339-49.

84. Nakanishi M, Noguchi A. Confocal and probe microscopy to study gene transfection mediated by cationic liposomes with a cationic cholesterol derivative. Adv Drug Deliv Rev 2001; 52: 197-207.

85. Lechardeur D, Lukacs GL. Intracellular barriers to non-viral gene transfer. Curr Gene Ther 2002; 2: 183-94.

86. Zuhorn IS, Hoekstra D. On the mechanism of cationic amphiphile-mediated transfection. To fuse or not to fuse: is that the question? J Membr Biol 2002; 189: 167-79.

87. Geusens B, Lambert J, De Smedt SC, Buyens K, Sanders NN, Van Gele M. Ultradeformable cationic liposomes for delivery of small interfering RNA (siRNA) into human primary melanocytes. J Control Release 2008.

88. Han SE, Kang H, Shim GY, et al. Novel cationic cholesterol derivative-based liposomes for serum-enhanced delivery of siRNA. Int J Pharm 2008; 353: 260-9.

89. Gaucheron J, Santaella C, Vierling P. Highly fluorinated lipospermines for gene transfer: synthesis and evaluation of their in vitro transfection efficiency. Bioconjug Chem 2001; 12: 114-28.

90. Sen J, Chaudhuri A. Design, syntheses, and transfection biology of novel non-cholesterol-based guanidinylated cationic lipids. J Med Chem 2005; 48: 812-20.

91. Bombelli C, Bordi F, Ferro S, et al. New Cationic Liposomes as Vehicles of m-Tetrahydroxyphenylchlorin in Photodynamic Therapy of Infectious Diseases. Mol Pharm 2008; 5: 672-9.

92. Obata Y, Suzuki D, Takeoka S. Evaluation of cationic assemblies constructed with amino acid based lipids for plasmid DNA delivery. Bioconjug Chem 2008; 19: 1055-63.

93. Bajaj A, Kondaiah P, Bhattacharya S. Gene transfection efficacies of novel cationic gemini lipids possessing aromatic backbone and oxyethylene spacers. Biomacromolecules 2008; 9: 991-9.

94. Bajaj A, Kondaiah P, Bhattacharya S. Synthesis and gene transfer activities of novel serum compatible cholesterol-based gemini lipids possessing oxyethylene-type spacers. Bioconjug Chem 2007; 18: 1537-46.

95. Kim HS, Moon J, Kim KS, et al. Gene-transferring efficiencies of novel diamino cationic lipids with varied hydrocarbon chains. Bioconjug Chem 2004; 15: 1095-101.

96. Vigneron JP, Oudrhiri N, Fauquet M, et al. Guanidinium-cholesterol cationic lipids: efficient vectors for the transfection of eukaryotic cells. Proc Natl Acad Sci U S A 1996; 93: 9682-6.

97. Li S, Rizzo MA, Bhattacharya S, Huang L. Characterization of cationic lipid-protamine-DNA (LPD) complexes for intravenous gene delivery. Gene Ther 1998; 5: 930-7.

98. Li SD, Huang L. Targeted delivery of antisense oligodeoxynucleotide and small interference RNA into lung cancer cells. Mol Pharm 2006; 3: 579-88.

99. Yan W, Chen W, Huang L. Mechanism of adjuvant activity of cationic liposome: phosphorylation of a MAP kinase, ERK and induction of chemokines. Mol Immunol 2007; 44: 3672-81.

100. Cui Z, Han SJ, Vangasseri DP, Huang L. Immunostimulation mechanism of LPD nanoparticle as a vaccine carrier. Mol Pharm 2005; 2: 22-8.

101. Ishida T, Iden DL, Allen TM. A combinatorial approach to producing sterically stabilized (Stealth) immunoliposomal drugs. FEBS Lett 1999; 460: 129-33.

102. Perouzel E, Jorgensen MR, Keller M, Miller AD. Synthesis and formulation of neoglycolipids for the functionalization of liposomes and lipoplexes. Bioconjug Chem 2003; 14: 884-98.

103. Eckert A, Bock BC, Tagscherer KE, et al. The PEA-15/PED protein protects glioblastoma cells from glucose deprivation-induced apoptosis via the ERK/MAP kinase pathway. Oncogene 2008; 27: 1155-66.

104. McCubrey JA, Steelman LS, Chappell WH, et al. Roles of the Raf/MEK/ERK pathway in cell growth, malignant transformation and drug resistance. Biochim Biophys Acta 2007; 1773: 1263-84.

105. Banerjee R, Tyagi P, Li S, Huang L. Anisamide-targeted stealth liposomes: a potent carrier for targeting doxorubicin to human prostate cancer cells. Int J Cancer 2004; 112: 693-700.

106. Daugas E, Susin SA, Zamzami N, et al. Mitochondrio-nuclear translocation of AIF in apoptosis and necrosis. FASEB J 2000; 14: 729-39.

107. Fehlberg S, Gregel CM, Goke A, Goke R. Bisphenol A diglycidyl ether-induced apoptosis involves Bax/Bid-dependent mitochondrial release of apoptosis-inducing factor (AIF), cytochrome c and Smac/DIABLO. Br J Pharmacol 2003; 139: 495-500.

108. Loeffler M, Daugas E, Susin SA, et al. Dominant cell death induction by extramitochondrially targeted apoptosis-inducing factor. FASEB J 2001; 15: 758-67.

109. Lorenzo HK, Susin SA, Penninger J, Kroemer G. Apoptosis inducing factor (AIF): a phylogenetically old, caspase-independent effector of cell death. Cell Death Differ 1999; 6: 516-24.

110. Modjtahedi N, Giordanetto F, Madeo F, Kroemer G. Apoptosis-inducing factor: vital and lethal. Trends Cell Biol 2006; 16: 264-72.

111. John CS, Bowen WD, Varma VM, McAfee JG, Moody TW. Sigma receptors are expressed in human non-small cell lung carcinoma. Life Sci 1995; 56: 2385-92.

112. Vilner BJ, John CS, Bowen WD. Sigma-1 and sigma-2 receptors are expressed in a wide variety of human and rodent tumor cell lines. Cancer Res 1995; 55: 408-13.

113. Matsumura Y, Maeda H. A new concept for macromolecular therapeutics in cancer chemotherapy: mechanism of tumoritropic accumulation of proteins and the antitumor agent smancs. Cancer Res 1986; 46: 6387-92.

114. Tanaka T, Shiramoto S, Miyashita M, Fujishima Y, Kaneo Y. Tumor targeting based on the effect of enhanced permeability and retention (EPR) and the mechanism of receptor-mediated endocytosis (RME). Int J Pharm 2004; 277: 39-61.

115. Klouz A, Said DB, Ferchichi H, et al. Protection of cellular and mitochondrial functions against liver ischemia by N-benzyl-N'-(2-hydroxy-3,4-dimethoxybenzyl)-piperazine (BHDP), a sigma1 ligand. Eur J Pharmacol 2008; 578: 292-9.

116. Pirollo KF, Chang EH. Does a targeting ligand influence nanoparticle tumor localization or uptake? Trends Biotechnol 2008; 26: 552-8.

117. Hiramatsu M. A role for guanidino compounds in the brain. Mol Cell Biochem 2003; 244: 57-62.

118. Yan W, Chen W, Huang L. Reactive oxygen species play a central role in the activity of cationic liposome based cancer vaccine. J Control Release 2008.

119. Liu WH, Cheng YC, Chang LS. ROS-mediated p38alpha MAPK activation and ERK inactivation responsible for upregulation of Fas and FasL and autocrine Fas-mediated cell death in Taiwan cobra phospholipase A(2)-treated U937 cells. J Cell Physiol 2009.

120. Giles GI. The redox regulation of thiol dependent signaling pathways in cancer. Curr Pharm Des 2006; 12: 4427-43.

121. Kim S, Lee TJ, Leem J, Choi KS, Park JW, Kwon TK. Sanguinarine-induced apoptosis: generation of ROS, down-regulation of Bcl-2, c-FLIP, and synergy with TRAIL. J Cell Biochem 2008; 104: 895-907.

122. Fleury C, Mignotte B, Vayssiere JL. Mitochondrial reactive oxygen species in cell death signaling. Biochimie 2002; 84: 131-41.

123. Zorov DB, Juhaszova M, Sollott SJ. Mitochondrial ROS-induced ROS release: an update and review. Biochim Biophys Acta 2006; 1757: 509-17.

124. Ivanov VN, Hei TK. Combined treatment with EGFR inhibitors and arsenite upregulated apoptosis in human EGFR-positive melanomas: a role of suppression of the PI3K-AKT pathway. Oncogene 2005; 24: 616-26.

125. Strong TV. Gene therapy for carcinoma of the breast: Genetic immunotherapy. Breast Cancer Res 2000; 2: 15-21.

126. Olie RA, Simoes-Wust AP, Baumann B, et al. A novel antisense oligonucleotide targeting survivin expression induces apoptosis and sensitizes lung cancer cells to chemotherapy. Cancer Res 2000; 60: 2805-9.

127. Pakunlu RI, Wang Y, Tsao W, Pozharov V, Cook TJ, Minko T. Enhancement of the efficacy of chemotherapy for lung cancer by simultaneous suppression of multidrug resistance and antiapoptotic cellular defense: novel multicomponent delivery system. Cancer Res 2004; 64: 6214-24.

128. Wu X, Deng Y, Wang G, Tao K. Combining siRNAs at two different sites in the EGFR to suppress its expression, induce apoptosis, and enhance 5-fluorouracil sensitivity of colon cancer cells. J Surg Res 2007; 138: 56-63.

129. Navolanic PM, Steelman LS, McCubrey JA. EGFR family signaling and its association with breast cancer development and resistance to chemotherapy (Review). Int J Oncol 2003; 22: 237-52.

130. Sulaimon SS, Kitchell BE. The basic biology of malignant melanoma: molecular mechanisms of disease progression and comparative aspects. J Vet Intern Med 2003; 17: 760-72.

131. Zhang XD, Wu JJ, Gillespie S, Borrow J, Hersey P. Human melanoma cells selected for resistance to apoptosis by prolonged exposure to tumor necrosis factor-related apoptosis-inducing ligand are more vulnerable to necrotic cell death induced by cisplatin. Clin Cancer Res 2006; 12: 1355-64.

132. Atallah E, Flaherty L. Treatment of metastatic malignant melanoma. Curr Treat Options Oncol 2005; 6: 185-93.

133. Hersey P. Apoptosis and melanoma: how new insights are effecting the development of new therapies for melanoma. Curr Opin Oncol 2006; 18: 189-96.

134. Tuma RS. Reactive oxygen species may have antitumor activity in metastatic melanoma. J Natl Cancer Inst 2008; 100: 11-2.

135. Tas F, Argon A, Camlica H, Topuz E. Temozolomide in combination with cisplatin in patients with metastatic melanoma: a phase II trial. Melanoma Res 2005; 15: 543-8.

136. Mathieu V, Le Mercier M, De Neve N, et al. Galectin-1 knockdown increases sensitivity to temozolomide in a B16F10 mouse metastatic melanoma model. J Invest Dermatol 2007; 127: 2399-410.

137. Nesbit CE, Tersak JM, Prochownik EV. MYC oncogenes and human neoplastic disease. Oncogene 1999; 18: 3004-16.

138. Dang CV, O'Donnell KA, Zeller KI, Nguyen T, Osthus RC, Li F. The c-Myc target gene network. Semin Cancer Biol 2006; 16: 253-64.

139. Mannava S, Grachtchouk V, Wheeler LJ, et al. Direct role of nucleotide metabolism in C-MYC-dependent proliferation of melanoma cells. Cell Cycle 2008; 7: 2392-400.

140. Zhuang D, Mannava S, Grachtchouk V, et al. C-MYC overexpression is required for continuous suppression of oncogene-induced senescence in melanoma cells. Oncogene 2008; 27: 6623-34.

141. Hong J, Zhao Y, Huang W. Blocking c-myc and stat3 by E. coli expressed and enzyme digested siRNA in mouse melanoma. Biochem Biophys Res Commun 2006; 348: 600-5.

142. Devi GR. siRNA-based approaches in cancer therapy. Cancer Gene Ther 2006; 13: 819-29.

143. Vannini I, Bonafe M, Tesei A, et al. Short interfering RNA directed against the SLUG gene increases cell death induction in human melanoma cell lines exposed to cisplatin and fotemustine. Cell Oncol 2007; 29: 279-87.

144. Li D, Ueta E, Kimura T, Yamamoto T, Osaki T. Reactive oxygen species (ROS) control the expression of Bcl-2 family proteins by regulating their phosphorylation and ubiquitination. Cancer Sci 2004; 95: 644-50.

145. Fest T, Mougey V, Dalstein V, et al. c-MYC overexpression in Ba/F3 cells simultaneously elicits genomic instability and apoptosis. Oncogene 2002; 21: 2981-90.

146. Bucci B, D'Agnano I, Amendola D, et al. Myc down-regulation sensitizes melanoma cells to radiotherapy by inhibiting MLH1 and MSH2 mismatch repair proteins. Clin Cancer Res 2005; 11: 2756-67.

147. Greco C, D'Agnano I, Vitelli G, et al. c-MYC deregulation is involved in melphalan resistance of multiple myeloma: role of PDGF-BB. Int J Immunopathol Pharmacol 2006; 19: 67-79.

148. Gatti G, Maresca G, Natoli M, et al. MYC prevents apoptosis and enhances endoreduplication induced by paclitaxel. PLoS One 2009; 4: e5442.

149. Sonoke S, Ueda T, Fujiwara K, et al. Tumor regression in mice by delivery of Bcl-2 small interfering RNA with pegylated cationic liposomes. Cancer Res 2008; 68: 8843-51.

150. Ciardiello F, Tortora G. Inhibition of bcl-2 as cancer therapy. Ann Oncol 2002; 13: 501-2.

151. Morris MJ, Cordon-Cardo C, Kelly WK, et al. Safety and biologic activity of intravenous BCL-2 antisense oligonucleotide (G3139) and taxane chemotherapy in patients with advanced cancer. Appl Immunohistochem Mol Morphol 2005; 13: 6-13.

152. Jun HS, Park T, Lee CK, et al. Capsaicin induced apoptosis of B16-F10 melanoma cells through down-regulation of Bcl-2. Food Chem Toxicol 2007; 45: 708-15.

153. Ryan JJ, Prochownik E, Gottlieb CA, et al. c-myc and bcl-2 modulate p53 function by altering p53 subcellular trafficking during the cell cycle. Proc Natl Acad Sci U S A 1994; 91: 5878-82.

154. Evans C, Morrison I, Heriot AG, et al. The correlation between colorectal cancer rates of proliferation and apoptosis and systemic cytokine levels; plus their influence upon survival. Br J Cancer 2006; 94: 1412-9.

155. Thannickal VJ, Fanburg BL. Reactive oxygen species in cell signaling. Am J Physiol Lung Cell Mol Physiol 2000; 279: L1005-28.

156. Cejas P, Casado E, Belda-Iniesta C, et al. Implications of oxidative stress and cell membrane lipid peroxidation in human cancer (Spain). Cancer Causes Control 2004; 15: 707-19.

157. Mates JM, Sanchez-Jimenez FM. Role of reactive oxygen species in apoptosis: implications for cancer therapy. Int J Biochem Cell Biol 2000; 32: 157-70.

158. Pelicano H, Carney D, Huang P. ROS stress in cancer cells and therapeutic implications. Drug Resist Updat 2004; 7: 97-110.

159. Lebedeva IV, Washington I, Sarkar D, et al. Strategy for reversing resistance to a single anticancer agent in human prostate and pancreatic carcinomas. Proc Natl Acad Sci U S A 2007; 104: 3484-9.

160. Wierstra I, Alves J. The c-myc promoter: still MysterY and challenge. Adv Cancer Res 2008; 99: 113-333.

161. Baudino TA, McKay C, Pendeville-Samain H, et al. c-Myc is essential for vasculogenesis and angiogenesis during development and tumor progression. Genes Dev 2002; 16: 2530-43.

162. Abaza MS, Al-Saffar A, Al-Sawan S, Al-Attiyah R. c-myc antisense oligonucleotides sensitize human colorectal cancer cells to chemotherapeutic drugs. Tumour Biol 2008; 29: 287-303.

163. Pastorino F, Brignole C, Marimpietri D, et al. Targeted liposomal c-myc antisense oligodeoxynucleotides induce apoptosis and inhibit tumor growth and metastases in human melanoma models. Clin Cancer Res 2003; 9: 4595-605.

164. Xia Z, Zhu Z, Zhang L, et al. Specific reversal of MDR1/P-gp-dependent multidrug resistance by RNA interference in colon cancer cells. Oncol Rep 2008; 20: 1433-9.

165. Yadav S, van Vlerken LE, Little SR, Amiji MM. Evaluations of combination MDR-1 gene silencing and paclitaxel administration in biodegradable polymeric nanoparticle formulations to overcome multidrug resistance in cancer cells. Cancer Chemother Pharmacol 2009; 63: 711-22.

166. Zhao P, Zhang Y, Sun M, He Y. Reversion of multidrug resistance in human glioma by RNA interference. Neurol Res 2008; 30: 562-6.

167. Bagalkot V, Farokhzad OC, Langer R, Jon S. An aptamer-doxorubicin physical conjugate as a novel targeted drug-delivery platform. Angew Chem Int Ed Engl 2006; 45: 8149-52.

168. Minotti G, Menna P, Salvatorelli E, Cairo G, Gianni L. Anthracyclines: molecular advances and pharmacologic developments in antitumor activity and cardiotoxicity. Pharmacol Rev 2004; 56: 185-229.

169. Chen Y, Sen J, Bathula SR, Yang Q, Fittipaldi R, Huang L. Novel cationic lipid that delivers siRNA and enhances therapeutic effect in lung cancer cells. Mol Pharm 2009; 6: 696-705.

170. Eckel R, Ros R, Ros A, Wilking SD, Sewald N, Anselmetti D. Identification of binding mechanisms in single molecule-DNA complexes. Biophys J 2003; 85: 1968-73.

171. Pasqualini R, Koivunen E, Kain R, et al. Aminopeptidase N is a receptor for tumor-homing peptides and a target for inhibiting angiogenesis. Cancer Res 2000; 60: 722-7.

172. Mina-Osorio P. The moonlighting enzyme CD13: old and new functions to target. Trends Mol Med 2008; 14: 361-71.

173. Arap W, Pasqualini R, Ruoslahti E. Cancer treatment by targeted drug delivery to tumor vasculature in a mouse model. Science 1998; 279: 377-80.

174. Curnis F, Sacchi A, Borgna L, Magni F, Gasparri A, Corti A. Enhancement of tumor necrosis factor alpha antitumor immunotherapeutic properties by targeted delivery to aminopeptidase N (CD13). Nat Biotechnol 2000; 18: 1185-90.

175. Ellerby HM, Arap W, Ellerby LM, et al. Anti-cancer activity of targeted pro-apoptotic peptides. Nat Med 1999; 5: 1032-8.

176. Garde SV, Forte AJ, Ge M, et al. Binding and internalization of NGR-peptide-targeted liposomal doxorubicin (TVT-DOX) in CD13-expressing cells and its antitumor effects. Anticancer Drugs 2007; 18: 1189-200.

177. Pastorino F, Brignole C, Di Paolo D, et al. Targeting liposomal chemotherapy via both tumor cell-specific and tumor vasculature-specific ligands potentiates therapeutic efficacy. Cancer Res 2006; 66: 10073-82.

178. Pastorino F, Brignole C, Marimpietri D, et al. Vascular damage and anti-angiogenic effects of tumor vessel-targeted liposomal chemotherapy. Cancer Res 2003; 63: 7400-9.

179. Corti A, Ponzoni M. Tumor vascular targeting with tumor necrosis factor alpha and chemotherapeutic drugs. Ann N Y Acad Sci 2004; 1028: 104-12.

180. Corti A, Curnis F, Arap W, Pasqualini R. The neovasculature homing motif NGR: more than meets the eye. Blood 2008; 112: 2628-35.

181. Priebe W, Van NT, Burke TG, Perez-Soler R. Removal of the basic center from doxorubicin partially overcomes multidrug resistance and decreases cardiotoxicity. Anticancer Drugs 1993; 4: 37-48.

182. Shah N, Chaudhari K, Dantuluri P, Murthy RS, Das S. Paclitaxel-loaded PLGA nanoparticles surface modified with transferrin and Pluronic((R))P85, an in vitro cell line and in vivo biodistribution studies on rat model. J Drug Target 2009; 17: 533-42.

183. Xu DH, Gao JQ, Liang WQ. Liposome-based intracellular kinetics of doxorubicin in K562/DOX cells. Pharmazie 2008; 63: 646-9.

184. Goren D, Horowitz AT, Tzemach D, Tarshish M, Zalipsky S, Gabizon A. Nuclear delivery of doxorubicin via folate-targeted liposomes with bypass of multidrug-resistance efflux pump. Clin Cancer Res 2000; 6: 1949-57.

185. He Y, Zhang J. [Study on the relationship between the abnormal expression of c-myc and multidrug resistance in KB cell lines]. Zhonghua Er Bi Yan Hou Ke Za Zhi 2000; 35: 454-6.

186. He Y, Zhang J, Yuan Y. The role of c-myc in regulating mdr1 gene expression in tumor cell line KB. Chin Med J (Engl) 2000; 113: 848-51.

187. Shen Y. Advances in the development of siRNA-based therapeutics for cancer. IDrugs 2008; 11: 572-8.

188. Lee RJ, Huang L. Folate-targeted, anionic liposome-entrapped polylysine-condensed DNA for tumor cell-specific gene transfer. J Biol Chem 1996; 271: 8481-7.

189. Song E, Zhu P, Lee SK, et al. Antibody mediated in vivo delivery of small interfering RNAs via cell-surface receptors. Nat Biotechnol 2005; 23: 709-17.

190. Janicke RU, Ng P, Sprengart ML, Porter AG. Caspase-3 is required for alpha-fodrin cleavage but dispensable for cleavage of other death substrates in apoptosis. J Biol Chem 1998; 273: 15540-5.

191. Puhlmann U, Ziemann C, Ruedell G, et al. Impact of the cyclooxygenase system on doxorubicin-induced functional multidrug resistance 1 overexpression and doxorubicin sensitivity in acute myeloid leukemic HL-60 cells. J Pharmacol Exp Ther 2005; 312: 346-54.

192. Zeng J, Wang S. Enhanced gene delivery to PC12 cells by a cationic polypeptide. Biomaterials 2005; 26: 679-86.

193. Chen Y, Wu JJ, Huang L. Nanoparticles Targeted with NGR Motif Deliver c-Myc siRNA And Doxorubicin for Anticancer Therapy

Mol Ther 2010.

194. Nakamura Y, Sato H, Motokura T. Development of multidrug resistance due to multiple factors including P-glycoprotein overexpression under K-selection after MYC and HRAS oncogene activation. Int J Cancer 2006; 118: 2448-54.

195. Banerjee S, Ganapathi R, Ghosh L, Yu CL. Down-regulation of ras and myc expression associated with mdr-1 overexpression in adriamycin-resistant tumor cells. Cell Mol Biol 1992; 38: 561-70.

196. Boumendjel A, Boutonnat J, Robert J. ABC Transporters and Multidrug Resistance 2009.

197. Castanotto D, Rossi JJ. The promises and pitfalls of RNA-interference-based therapeutics. Nature 2009; 457: 426-33.

198. Coburn GA, Cullen BR. siRNAs: a new wave of RNA-based therapeutics. J Antimicrob Chemother 2003; 51: 753-6.

199. Lu J, Getz G, Miska EA, et al. MicroRNA expression profiles classify human cancers. Nature 2005; 435: 834-8.

200. Gou D, Zhang H, Baviskar PS, Liu L. Primer extension-based method for the generation of a siRNA/miRNA expression vector. Physiol Genomics 2007; 31: 554-62.

201. Yan D, Zhou X, Chen X, et al. MicroRNA-34a inhibits uveal melanoma cell proliferation and migration through downregulation of c-Met. Invest Ophthalmol Vis Sci 2009; 50: 1559-65.

202. Li Y, Guessous F, Zhang Y, et al. MicroRNA-34a inhibits glioblastoma growth by targeting multiple oncogenes. Cancer Res 2009; 69: 7569-76.

203. Welch C, Chen Y, Stallings RL. MicroRNA-34a functions as a potential tumor suppressor by inducing apoptosis in neuroblastoma cells. Oncogene 2007; 26: 5017-22.

204. Hammond SM. MicroRNA therapeutics: a new niche for antisense nucleic acids. Trends Mol Med 2006; 12: 99-101.

205. Krutzfeldt J, Rajewsky N, Braich R, et al. Silencing of microRNAs in vivo with 'antagomirs'. Nature 2005; 438: 685-9.

206. Xia J, Bi H, Yao Q, Qu S, Zong Y. Construction of human ScFv phage display library against ovarian tumor. J Huazhong Univ Sci Technolog Med Sci 2006; 26: 497-9.

207. Tsantili P, Tzartos SJ, Mamalaki A. High affinity single-chain Fv antibody fragments protecting the human nicotinic acetylcholine receptor. J Neuroimmunol 1999; 94: 15-27.

208. Chono S, Li SD, Conwell CC, Huang L. An efficient and low immunostimulatory nanoparticle formulation for systemic siRNA delivery to the tumor. J Control Release 2008; 131: 64-9.

209. Chen Z, Liang K, Liu J, et al. Enhancement of survivin gene downregulation and cell apoptosis by a novel combination: liposome microbubbles and ultrasound exposure. Med Oncol 2009.

210. Takeuchi H, Morton DL, Elashoff D, Hoon DS. Survivin expression by metastatic melanoma predicts poor disease outcome in patients receiving adjuvant polyvalent vaccine. Int J Cancer 2005; 117: 1032-8.

211. Fecher LA, Amaravadi RK, Flaherty KT. The MAPK pathway in melanoma. Curr Opin Oncol 2008; 20: 183-9.

212. Li N, Fu H, Tie Y, et al. miR-34a inhibits migration and invasion by down-regulation of c-Met expression in human hepatocellular carcinoma cells. Cancer Lett 2009; 275: 44-53.

213. Tsuchiya S, Okuno Y, Tsujimoto G. MicroRNA: biogenetic and functional mechanisms and involvements in cell differentiation and cancer. J Pharmacol Sci 2006; 101: 267-70.

214. Ruvkun G. Clarifications on miRNA and cancer. Science 2006; 311: 36-7.

215. Schatton T, Murphy GF, Frank NY, et al. Identification of cells initiating human melanomas. Nature 2008; 451: 345-9.

216. Schatton T, Frank MH. Antitumor immunity and cancer stem cells. Ann N Y Acad Sci 2009; 1176: 154-69.